

Document downloaded from:

<http://hdl.handle.net/10251/84345>

This paper must be cited as:

Canet Perez, JV.; Dobón Alonso, A.; Tornero Feliciano, P. (2012). Non-Recognition-of-BTH4, an Arabidopsis Mediator Subunit Homolog, Is Necessary for Development and Response to Salicylic Acid. *Plant Cell*. 24(10):4220-4235. doi:0.1105/tpc.112.103028.



The final publication is available at

[http://doi.org/ 10.1105/tpc.112.103028](http://doi.org/10.1105/tpc.112.103028)

Copyright American Society of Plant Biologists

Additional Information

***Non-Recognition-of-BTH-4, an Arabidopsis Mediator subunit homolog, is necessary for development and response to salicylic acid.***

Juan Vicente Canet, Albor Dobón<sup>1</sup>, and Pablo Tornero<sup>\*</sup>

Instituto de Biología Molecular y Celular de Plantas (IBMCP); Universidad Politécnica de Valencia (UPV)-Consejo Superior de Investigaciones Científicas (CSIC); Ciudad Politécnica de la Innovación (CPI), Ed. 8E; C/ Ingeniero Fausto Elio s/n, 46022 Valencia, SPAIN.

<sup>\*</sup> Corresponding author, [ptornero@ibmcp.upv.es](mailto:ptornero@ibmcp.upv.es)

Phone: (+34)963879377 Fax (+34)963877859

IBMCP (UPV-CSIC) Avda. de los Naranjos s/n, 46022 Valencia (SPAIN)

The author responsible for distribution of materials integral to the findings presented in this article in accordance with the policy described in the Instructions for Authors ([www.plantcell.org](http://www.plantcell.org)) is: Pablo Tornero ([ptornero@ibmcp.upv.es](mailto:ptornero@ibmcp.upv.es)).

<sup>1</sup>Current address: Department of Crop Genetics, The John Innes Centre, Norwich Research Park, Norwich, NR4 7UH, UK.

Running title: Mediator and salicylic

Estimated length: 15.3 pages

## **Synopsis**

This work identifies *NRB4* (*Non-Recognition-of-BTH-4*), which acts in SA signaling in defense and development, finding that *NRB4* encodes a predicted subunit of the Mediator complex, which connects specific transcription factors to the general transcription machinery. *NRB4* functions downstream of *NPR1* (*Non-expresser-of-Pathogenesis-Related-1*) in SA signaling.

## **Abstract**

Salicylic acid (SA) signaling acts in defense and plant development. The only gene demonstrated to be required for the response to SA is Arabidopsis *NPR1* (*Non-expresser-of-Pathogenesis-Related-1*) and *npr1* mutants are insensitive to SA. By focusing on the effect of analogs of SA on plant development, we identified mutants in additional genes acting in the SA response. In this work, we describe a gene necessary for the SA response, *NRB4* (*Non-Recognition-of-BTH-4*). Three *nrb4* alleles recovered from the screen cause phenotypes similar to wild type in the tested conditions, except for SA-related phenotypes. Plants with *NRB4* null alleles express profound insensitivity to SA, even more than *npr1*. *NRB4* null mutants are also sterile and their growth is compromised. Plants carrying weaker *nrb4* alleles are also insensitive to SA, with some quantitative differences in some phenotypes, like systemic acquired resistance or pathogen growth restriction. When weak alleles are used, *NPR1* and *NRB4* mutations produce an additive phenotype, but we did not find evidence of a genetic interaction in F1, nor biochemical interaction in yeast or *in planta*. *NRB4* is predicted to be a subunit of Mediator, the ortholog of *MED15* in Arabidopsis. Mechanistically, *NRB4* functions downstream of *NPR1* to regulate the SA response.

## **Introduction**

Plants mount several types of resistance against different pathogens. Some types of defense consist of preexisting barriers, and others are inducible. The hormone salicylic acid (SA) is key for inducible defenses against biotrophic pathogens (reviewed by Vlot et al., 2009). Upon pathogen perception, SA biosynthesis is increased which induces the appropriate defense responses. In addition other hormones are involved in plant defense, including jasmonic acid (JA) and ethylene (ET), and there are complex interactions among hormone responses (reviewed by Robert-Seilaniantz et al., 2011). Although Methyl jasmonate (MeJA) is applied exogenously in the laboratory it has been shown that the active form is JA-Ile (reviewed by Browse, 2009). Broadly speaking, JA-Ile and ET act synergistically, but SA and JA-Ile negatively regulate each other.

A key player in the recognition of SA is *NPR1* (reviewed by Dong, 2004). Various genetic screens aiming to identify components of the SA response have exclusively found mutations in *NPR1* (Cao et al., 1994, Delaney et al., 1995, Glazebrook et al., 1996, and Shah et al., 1997), suggesting that it is the only gene responsible for the SA response, or the only one accessible through mutagenesis. A search for protein-protein interactions in yeast identified components that interact with NPR1, including *NIMINs* (*NIM1 –interacting protein-1*, Weigel et al., 2001) and *TGAs* (TGACG –motif-binding-factor, Zhang et al., 1999, and Després et al., 2000). NPR1 is sensitive to SA in yeast, activating the expression of genes in a stimulus dependent fashion (Maier et al., 2011), and it has been defined as a SA receptor, either binding to SA (Wu et al., 2012), or interacting with two paralogs, NPR3 and NPR4, which bind SA (Fu et al., 2012).

Benzothiadiazole (BTH) is an analog of SA and is used in the laboratory because it is not as phytotoxic as SA (Lawton et al., 1996). Repeated applications of BTH decrease the size and weight of treated plants (Canet et al., 2010a); this difference was used to screen for non recognition of BTH mutants (NRBs). The first complementation group derived from this screen, not surprisingly, was *NPR1* (Canet et al., 2010b). The next complementation group, *NRB4*, is the focus of this report.

As mentioned, SA is central to pathogen-induced responses, and many of these responses involve alterations in gene expression. Some of these changes in gene expression are regulated by DNA repair proteins (Song et al., 2011), identified as

suppressors of *npr1*, and by chromatin remodeling factors (Wang et al., 2010), identified as suppressors of the suppressors. There are also sets of transcription factors notably *TGAs* (Jakoby et al., 2002) and *WRKYs* (named after the conserved domain WRKYGQK, Eulgem et al., 2000) that act downstream of the SA response to regulate gene expression leading to defense. However, the mechanism by which these specific transcription factors sets interact with RNA Pol II remains unclear.

In yeast, the “Mediator” complex functions as a bridge between specific transcription factors and the core transcriptional machinery (Kelleher et al., 1990, and Flanagan et al., 1991). Mediator is a complex of *circa* 22 proteins, divided in four modules: head, middle, tail, and a detachable kinase domain. The tail module interacts with the specific transcription factors, and the head module interacts with RNA Pol II (Cai et al., 2009). The Mediator complex has been found in all eukaryotes tested (Chadick and Asturias, 2005) including in Arabidopsis (Backstrom et al., 2007). Indeed, several reports of Mediator subunits of Arabidopsis affecting a specific signaling process have appeared (reviewed by Kidd et al., 2011).

The plants with *nrb4* missense mutations we identified in the screen are only affected in SA response, not in other tested phenotypes; however, plants with null mutations in *NRB4* express severe defense and developmental phenotypes. *NRB4* is predicted to be a subunit of the Mediator complex located in the tail module, and in this work we show that the missense mutations are clustered in the KIX domain (named due to its interaction with the kinase inducible activation domain of CREB, Chrivia et al., 1993). Importantly, the orthologs in other species interact with different receptors and some of these receptors bind salicylates. From the phenotypes presented, we infer an essential role for *NRB4* in plants. This essential function could reflect a role for SA in normal development, as previously suggested (Vanacker et al., 2001).

## **Results**

### ***NRB4* is required for the SA response**

We previously performed a genetic screen for genes involved in the SA response; the first locus we found was *NPR1*, with 43 alleles (Canet et al., 2010b). The fourth locus (by number of alleles) from this screen was named *NRB4*, and the rest of loci will be described elsewhere. *NRB4* is defined by three alleles, which came from independent ethyl methanesulfonate (EMS) mutagenesis events. The plants with these alleles were almost as insensitive to BTH as *npr1-1* plants, at least in terms of diminished fresh weight when grown in the presence of BTH (Figure 1A). The *nrb4-1* plants had a less severe phenotype than the *nrb4-2* and *nrb4-3* plants (Figure 1A). The mutants were recessive (Figure 1A and Table S1) although in both *nrb4-2* and *nrb4-3*, F1s with Col-0 showed an effect on the SA response, as happens with the F1s with *npr1-1* (Figure 1A). There was no genetic interaction with *npr1* in the F1, and the F1s between the *nrb4* alleles were as insensitive to BTH as their parents (Figure 1A).

The screen and the quantification of the fresh weight were carried out with BTH. It was possible that these *nrb4* plants were impaired in response to BTH, but had no effect on the response to SA. To test this possibility, *nrb4* plants and controls were grown on MS plates with 500  $\mu$ M SA. *npr1* plants are unable to grow on these plates, likely because they are unable to detoxify SA (Cao et al., 1997). *nrb4-2* and *nrb4-3* plants behaved as *npr1-1*, and *nrb4-1* was intermediate between Col-0 and *npr1-1* (Figure 1B). This observation was quantified by measuring the amount of chlorophyll per plant for three different treatments (Figure 1C). The quantification corroborated the intermediate phenotype of *nrb4-1* plants, and showed no difference in chlorophyll in mock treatments. In fact, in the absence of treatment, there were no observable developmental phenotypes in the plants carrying any of the *nrb4* alleles; they were indistinguishable from Col-0 in our growth conditions.

The *nrb4* plants, like *npr1*, were also affected in SA-dependent defense (Figure 2). For example, inoculation with *Pseudomonas syringae* pv. *tomato* DC3000 (*Pto*) after SA and BTH treatments induced a strong resistance in Col-0, but not in *npr1-1* (Figure 2A). The *nrb4* plants showed some residual resistance, but the difference with respect to Col-0 was always considerable. PR1 is a Pathogenesis Related protein used as a marker for stress in plants (Wang et al., 2005), so we produced a PR1 immunoblot blot of plants

treated with *Pto* or BTH (Figure 2B). In both cases, strong accumulation of PR1 was observed only in Col-0. Therefore, even if SA and BTH induce a small amount of resistance in *nrb4* plants, this resistance does not result in the accumulation of PR1.

The similarities between *nrb4* and *npr1* plants extended beyond the initial characterization. When tested for enhanced disease susceptibility phenotypes (Glazebrook et al., 1996), *nrb4* plants were at least as susceptible as *npr1* (Figure 2C). Surprisingly, *nrb4-2* plants were wild type for pathogen-induced systemic acquired resistance (SAR), but the plants with the other two alleles, like all *npr1* plants, were SAR defective. (Figure 2D and Cao et al., 1994; Delaney et al., 1995). Since this was an important difference, this experiment was repeated several times, always with the same result. All *nrb4* and *npr1* plants showed similar effector-triggered immune (ETI) responses (Figure 2E and F) and responses to non-host pathogens (Figure 2G and H). Only in the case of RPS2-dependent ETI triggered by *Pto(avrRpt2)* we did observe a decrease in resistance in some plants; these paralleled the responses to *Pto* (Figure 2A, C, and D). Other pathogens tested included: *Pto(hrpC-)* (Deng et al., 1998) and *Plectosphaerella cucumerina* (Ton and Mauch-Mani, 2004). In these cases, the *nrb4* plants were not different from the wild type (Figure S1A and B, respectively).

Plants with *npr1* alleles differ in their response to MeJA induced resistance (Dobón et al., 2011). *nrb4* plants were wild type in their response to MeJA (Figure S1C) and also showed a wild type phenotype on MeJA plates (Figure S1D) and in growth of *Pto(cor-)*, (Mittal and Davis, 1995, Figure S1E).

*nrb4* and *npr1* plants shared most of the phenotypes related to SA-dependent defense and/or response to biotrophic pathogens. Thus, we addressed whether the corresponding genes act in the same pathway by constructing double mutant *nrb4 npr1-1*. These double mutant plants showed no additional change in fresh weight in response to BTH (Figure S2A). Therefore, another line was constructed with *npr1-70*, (a null allele with an intermediate response to BTH, Canet et al., 2010b), and *nrb4-1* since it was the weakest allele (Figure 1A). *nrb4-1 npr1-70* plants showed additive phenotypes, since these plants had a stronger phenotype than plants with either weak allele alone (Figure 3A). Similar results were obtained with respect to growth of *Pto* in response to SA and BTH treatment (Figure S2B).

This additive relationship implied that the genes were independent. Mechanistically this could be translated into several models. NPR1 functions in the nucleus (Kinkema et al., 2000 and Maier et al., 2011), and *NRB4* could affect its localization and, potentially, that of other proteins acting with NPR1. The trafficking of NPR1 can be manipulated with a transgenic line that over-expresses *NPR1* fused to the steroid hormone binding domain of the rat glucocorticoid receptor (*NPR1-HBD*, Kinkema et al., 2000). Upon application of the glucocorticoid dexamethasone (DEX), NPR1-HBD is forced to the nucleus, while in mock conditions it is excluded from the nucleus. The double *nrb4-2 NPR1-HBD* plant did not respond to BTH when DEX was applied (Figure 3B). Thus, the presence of NPR1 in the nucleus, in the presence of BTH, was not enough to trigger the response. An alternative explanation for these results could be that NRB4 is a chaperone, required for NPR1 stability. This explanation was ruled out with the help of a line that expressed NPR1 fused to GFP (Kinkema et al., 2000). In control conditions, NPR1-GFP was detected in the nucleus, (Figure S2C, compare with Figure 2A of Kinkema et al., 2000). The same localization was observed in this transgenic plant in an *nrb4-2* background (Figure S2D). Upon BTH application, NPR1-GFP was also detected in the nucleus, both in *NRB4* wild type and in *nrb4-2* backgrounds (Figure S2E and S2F, respectively). Therefore NPR1 was not only stable in *nrb4-2* plants but it is also localized in the nucleus. In spite of this wild type NPR1 behavior, this line did not respond to BTH (Figure S2G). Thus, NRB4 functions downstream of NPR1.

### **Cloning of NRB4 and phenotypes of null alleles**

Conventional mapping showed that *NRB4* is encoded by At1g15780, a gene labeled as “unknown” in TAIR (V9, Swarbreck et al., 2008). The predicted protein contains a KIX domain (Radhakrishnan et al., 1997) at the very beginning, and a glutamine rich region (Guo et al., 2007) in the middle (Figure 4A). The sequences of the three alleles revealed that each allele had a single point mutation in the KIX domain (Figure 4). The mutations were not extreme in terms of physiochemical distances (Grantham, 1974). In fact, the mutations introduced did not change the prediction of an alpha helix structure (Radhakrishnan et al., 1997). Therefore mutations that introduced small changes in the protein produced plants with a considerable change in phenotype.



Three independent T-DNA insertions in *NRB4* were found in the databases; two of them are in introns (*nrb4-4* and *nrb4-5*, Figure 4B). In the case of the third T-DNA we did not find any insertion (see Methods for details). One quarter of the progeny of plants heterozygous for *nrb4-4* (Table S1) were smaller in size and more chlorotic than wild type, while heterozygous plants were wild type (Figure 5A). The smaller plants were confirmed to be homozygous *nrb4-4* by PCR, and they grew very slowly in comparison with wild type plants (Figure 5A and S3A vs. S3B). *nrb4-4* plants did not seem to be affected in leaf anatomy (Figure S4), but we did observe differences in the trichomes. Wild type plants had trichomes with papillae on their surface and prominent cells at their base (Figure 5B), but *nrb4-4* plants lacked these two elements. Additionally, the arms of the trichomes were different, irregular and chaotically arranged (Figures 5C and S4F). Several types of staining showed no difference in cell death or callose deposition (Figure S5), but DAPI staining revealed differences in the nuclei (Kubista et al., 1987). *NPR1* and the SA response are necessary for appropriate DNA content in the nucleus, with *npr1-1* plants having more endoreplication than wild type (Vanacker et al., 2001). The point mutations in *nrb4* produced plants with normal endoreplication using this assay, but *nrb4-4* plants had the same or more DNA per cell than *npr1-1* (Figure S6A). Therefore, *NPR1* and *NRB4* share a role in controlling endoreplication of nuclear DNA.

When transferred to long day conditions to induce flowering, *nrb4-4* plants bolted, but did not produce any seeds (Figure 5D and S3). In most plants, there was no production of flowers at all, but in a few plants some flowers did appear (Figure S3D vs. S3E). These flowers did not have stamens, and the carpels did not completely enclose the ovules (Figure S3F). The growth habit of *nrb4-4* plants was normal until several days after bolting. Then several additional stems appeared, and afterwards a next generation of stems appeared in the previous stems in a pattern similar to a fractal (Figure 5D and S3C). Some plants kept growing up to 23 weeks, and when they died, they did not seem to be following the normal program of senescence.

The phenotypes of *nrb4-4* homozygous plants were reproduced by *nrb4-5* homozygous plants (Figure S6B). Similarly, the ratio of wild type vs. no response to BTH was 1:1 in all cases of F1s from heterozygous *nrb4-4* plants and any of the plants that were homozygous for an EMS allele (Table S1), while the plants with EMS alleles and the nulls were fully recessive (Figure 1A and Table S1). F1s between heterozygous *nrb4-4*

plants and heterozygous *nrb4-5* plants had a ratio of wild type vs. no response to BTH of 3:1 (Table S1). Therefore, the phenotypes observed in plants with the alleles *nrb4-4* and *nrb4-5* were caused only by the insertions of the T-DNAs in the *NRB4* gene, and one copy of the missense mutation was enough to complement the phenotypes of *nrb4-4* plants, besides the response to BTH.

The *nrb4-4* homozygous plants were easily distinguished at two or three weeks, and some experiments could be carried out or adapted to this circumstance. *nrb4-4* plants did not perceive BTH, either in terms of fresh weight (Figure 5E) or *Pto* growth (Figure 5F). The levels of symptoms in *nrb4-4* plants after inoculation with *Pto* indicated that these lines were more susceptible than any other genotype, but perhaps the growth of *Pto* was already reaching a maximum. This extra susceptibility could be quantified with a weak pathogen, *Pseudomonas syringae* pv. *maculicola* CR299 (*Pma* CR299, Ritter and Dangl, 1995). Thus, *Pma* CR299 was unable to grow in Col-0, *npr1-1*, or *nrb4-2*, but grew two log units (a hundred fold) in *nrb4-4* plants (Figure 5G).

Since plants with *nrb4-4* had an extreme susceptibility to pathogens, we wondered if they had also an extreme phenotype with SA. The responses to SA/BTH of the plants with null alleles were similar to the plants with EMS alleles (Figures 5E and F), so we searched for another phenotype. SA content was considered a promising one, since it increases in plants under biotic stress -like *Pto* inoculation- but it is also increased in *npr1* plants with respect to wild type. *nrb4-2* plants behaved like *npr1-1*, accumulating roughly the same SA amounts as the wild type in control conditions, and more than the wild type after *Pto* inoculation (Figure 5H). *nrb4-4* plants behaved differently, accumulating SA in both free and total form (free plus conjugated) in control conditions. Upon *Pto* inoculation, levels of both forms of SA were strongly increased (Figure 5H). It was possible to identify *nrb4-4* homozygous plants in vitro (Figure S6C) and to test their growth on plates with 500  $\mu$ M SA. Growth of these plants was severely affected on SA plates, while heterozygous or wild type siblings were largely unaffected by SA (Figure S6D).

### **NRB4 is an ortholog of MED15**

*NRB4* was co-immunoprecipitated in Arabidopsis with MED6 (Backstrom et al., 2007), a subunit of the Mediator Complex (reviewed by Taatjes, 2010). Due to its homology to

subunits of Mediator in other species, it was labeled MED15, and an *in silico* search shows that it is one of the three *MED15* loci in Arabidopsis (Mathur et al., 2011). The role of MED15 in plants may be divided among these three genes, since the expression of *NRB4* in yeast lacking a functional *GAL11/MED15* did not complement the mutant phenotypes (Figure S6E). MED15 belongs to the tail module of the Mediator, a module that interacts with specific transcription factors (Taatjes, 2010). Since *NRB4* is a subunit of the Mediator complex, and the Mediator complex is critical for global regulation of transcription (Boube et al., 2002), it seemed logical to test the behavior of other Mediator subunits in the SA response. The *Arabidopsis thaliana* genome encodes 51 additional potential Mediator complex-encoding genes (TAIR V9, Swarbreck et al., 2008), and we tested the plants with T-DNAs insertions available. Six genes had no insertion, 15 had one or more heterozygous insertions, and 30 had one or more homozygous insertions. These populations were tested in the same conditions that allowed the identification of *nrb4-4* homozygous plants, yet none of them produced a phenotype different from the wild type control (Table S2). Therefore, the role of *NRB4* in the SA response was unique among the Mediator subunits.

### **Molecular footprint of *nrb4***

The additional phenotypes of the plants with null alleles compared to the EMS alleles of *NRB4* were striking, but they did not point to any obvious process (e.g. auxins or light) that was be altered, besides the SA response. A transcriptomic analysis was performed in *nrb4-4* plants to identify possible physiological processes affected by the null mutation. Thus, RNAs from three biological replicates of *nrb4-2* plants and Col-0 three week old plants (without treatment or inoculation), plus *nrb4-4* of the same size (five weeks old) were isolated and hybridized to a commercial oligonucleotide microarray (see Methods). Interestingly, the molecular footprints of the two *nrb4* plants were quite different.

*nrb4-2* plants had a very small impact on transcription, with eight genes significantly downregulated, and only one upregulated (Supplemental Dataset 1A). By contrast, *nrb4-4* plants had 243 genes significantly downregulated, and 106 upregulated (Supplemental Dataset 1B). Among the genes upregulated, there were genes related to SA biosynthesis (*EDS5* and *SID2*) and to defense (e.g. *PR1*, *PR2*, and *PR3*), although the levels of induction of the defense genes were quite low in comparison to pathogen

inoculation of wild type plants (Supplemental Dataset 1). This induction, though significant, was not strong enough to detect PR1 protein by immunoblot (Figure S7A). The software package MapMan (Usadel et al., 2005) is able to identify groups of genes that are altered in one situation with respect to the control. In the case of *nrb4-2* plants, there were only two main groups (e.g. “signaling”) strongly altered ( $p < 0.001$ ), but in *nrb4-4* there were up to ten main groups strongly altered (Supplemental Dataset 1B), thus reflecting the severity of the pleiotropic phenotype of the mutant plants.

In spite of the main groups suggested by these and other analyses (see Methods), there was no evidence of specific processes being altered, other than SA and defense. Using the global footprint of the transcriptome, we searched for other mutants or treatments that could give us any hint about other processes regulated by *NRB4*. AtCAST is a software package that “enables the identification of unknown relations among experiments to uncover the underlying biological relationships” (Sasaki et al., 2011), and, with the default settings, AtCAST indicated a weak correlation (Spearman’s rank-order correlation coefficients) of the *nrb4-4* transcriptome with the transcriptome of plants overexpressing *ARR22* and *ARR21* (*Arabidopsis-response-regulators* Kiba et al., 2004, and Kiba et al., 2005, respectively). To put these correlations into perspective, several transcriptomic experiments were clustered with Cluster 3.0 (de Hoon et al., 2004 ; genes filtered for values  $>1$  with centroid linkage and hierarchical clustering) along the *nrb4-2* and *nrb4-4* transcriptome, and visualized with JavaTreeView (Saldanha, 2004) (Figure 6A). *nrb4-2* data was closer to *eds1* (Falk et al., 1999) and *NahG* (Lawton et al., 1995), two mutations that produced a decrease in defense, but *nrb4-4* data was closer to the treatments that induced defenses and to *ARR21* and *ARR22* overexpression. The correlations with *ARR21* and *ARR22* overexpressor plants, although not very strong, might indicate altered cytokinin signaling in *nrb4-4* plants. When the *nrb4* plants were grown in presence of trans-zeatin, there were no phenotypes of cytokinin insensitivity (Figure 6B), so even if the overexpression of genes involved in cytokinin signaling produced the data closest to *nrb4-4*, there was no visible cytokinin related phenotype caused by the *nrb4* alleles. The application of high amounts of cytokinins has been reported to induce SA biosynthesis and therefore defenses (Choi et al., 2010). There is also a negative regulation of cytokinins by SA, which may help to fine tune the amplitude of the defense output (Argueso et al., 2012). We did not detect any difference between the plants with EMS alleles of *nrb4* and the wild type in this

regard (Figure S7B), nor did the *nrb4-4* plants show cytokinin related phenotypes (Figure S7C). Therefore, there was no evidence for a role of *NRB4* in cytokinin response, or in any other specific process besides the SA response.

### ***NRB4* expression and localization**

*NRB4* expression is apparently unaltered by stimuli covered in the available microarray data (Hruz et al., 2008). We confirmed this by using RT-qPCR to measure the levels of *NRB4* after several treatments including *Pto* inoculation and chemical treatments (Figure 7A). There was a reproducible increase in *NRB4* expression after several treatments, but even in the best conditions (SA) it was quite low (1.46 fold induction). We did not detect any interaction between *NRB4* and *NPR1* (or its interactors), in yeast two hybrid assays, regardless of the presence of SA in the media (Figure S8). The EMS alleles did not produce a measurable instability in the mutated mRNA, but the *nrb4-4* mutation rendered the mRNA below the threshold of detection (Figure 7B). The expression of *NRB4* was unaltered in *npr1-1* plants (Figure 7B), and *NPR1* was detectable in *nrb4-2* at normal levels (Figure S9A).

Although the Mediator complex is described to act in the nucleus, *NRB4* did not contain any obvious nuclear localization signal. To determine the localization of the protein, we transiently over-expressed the *NRB4* cDNA fused to the *GFP* coding sequence at the 3' or 5' terminus in *N. benthamiana* (Figure 7C and D, respectively). In both cases, there was a strong localization in the nucleus, with *NRB4*-*GFP* accumulating also outside the nucleus. The nuclear localization did not change with the application of 350  $\mu$ M BTH (Figure S9B). The predicted size of *NRB4* was 146 kDa, well above the free diffusion limit into the nucleus of 50 kDa (Talcott and Moore, 1999).

These constructs were transformed into *nrb4* mutant *Arabidopsis*; none of the *GFP-NRB4* constructs complemented the *nrb4* mutants, but the *NRB4-GFP* plants complemented the EMS alleles with some variation when the response to BTH in terms of fresh weight was considered (Figure 8A). This variation was representative of the transgenic lines obtained regardless of the background. A version of *NRB4* containing the first 670 AA was also able to complement the mutations in some lines (Figure 8A), but the version of *NRB4* containing only the first 112 AA did not. In the complemented lines, *GFP* was not detectable by means of confocal microscopy or immunoblot (Figure

S10A). However, since there was detectable function, we also transformed the wild type Col-0 to study the effects of *NRB4* overexpression. In this experiment, *35S:NPR1* was included as a control, since it is more sensitive to SA (Cao et al., 1998). The transgenic lines that overexpressed both versions (1335 and 670 AA) of *NRB4* had an enhanced SA response as measured by fresh weight after BTH applications (Figure 8B). We additionally complemented the wild type restriction of *Pto* growth after SA or BTH application using these lines (Figure 8C, also checked for PR1 expression, Figure S10B). Note that the over-expression of *NRB4* did not produce a strong defense response under control conditions, but when SA or BTH was applied, there was an enhanced response to SA (Figure 8D). Therefore, the effect of *NRB4* was specific and limited to SA response.

## **Discussion**

### **A role for Mediator in SA response**

The Mediator complex interacts with RNA Pol II, but mutations in specific Mediator subunits typically impact specific phenotypes, rather than general transcription (reviewed by Taatjes, 2010). This observation has led to the hypothesis that the Mediator complex performs both general and specific roles to regulate gene expression (Taatjes, 2010). In plants, the Mediator complex is emerging as a crucial component of transcriptional regulation in response to specific signals (reviewed by Kidd et al., 2011). The components of the Mediator complex have been identified using biochemistry and genetics. Thus, the immunopurification of MED6 in Arabidopsis led to the identification of nineteen Mediator subunits, NRB4 among them (Backstrom et al., 2007). A null mutation in *SWP/MED14* produces sterile plants with reduced growth, small leaves, and an increase in endoreplication (Autran et al., 2002), similar to our observations with *nrb4-4* plants. The main difference in *swp/med14* mutants was the size of the cells; by contrast, in *nrb4-4* plants the size of cells was similar to wild type (Figure S4), and in *35S:NRB4*, the plants were macroscopically similar to wild type. In the case of *SWP*, both the knock out and the overexpressor produced plants and cells of smaller size than the wild type.

Mutations in *MED21* (Dhawan et al., 2009), *PFT1/MED25*, and *SETH10/MED8*, (Kidd et al., 2009) affect disease resistance against necrotrophic pathogens to different degrees. Specifically, null homozygous mutants in *MED21* have an embryo-lethal phenotype, and RNAi plants with low levels of *MED21* are more susceptible to necrotrophic pathogens (Dhawan et al., 2009). *PFT1* (*PHYTOCROME and FLOWERING TIME 1*) was first described as a gene required for the shade avoidance response and flowering (Cerdan and Chory, 2003). Once *PFT1* was identified as a Mediator subunit (Backstrom et al., 2007), a screen for similar phenotypes in the rest of subunits identified a mutant in *SETH10/MED8* as required for both wild type flowering time and resistance to necrotrophic pathogens (Kidd et al., 2009). Following this logic, we tested the available T-DNA insertions, but found no additional Mediator subunits with a measurable phenotype in SA response (Table S2).

It is striking that mutations in three subunits of Mediator cause defense phenotypes in response to necrotrophic pathogens that are related to JA-Ile response whereas

mutations in only one subunit, *NRB4*, cause a phenotype related to SA-dependent defense responses. A plausible explanation would be that *NRB4* is a negative regulator of JA-Ile, and its removal would increase JA-Ile response. Then, this increase in JA-Ile signaling could be observed as loss in SA signaling, since both signals crosstalk negatively (Robert-Seilaniantz et al., 2011). But we did not observe a specific phenotype related to JA-Ile in the plants with *nrb4* EMS alleles (MeJA plates, MeJA induced resistance, *P. cucumerina* infection, and growth of *Pto(cor-)*, Figure S1). In any case, in plants there are four subunits of Mediator involved in biotic stress. Plants with mutations in *MED25* are more sensitive to salt stress (Elfving et al., 2011), so there is clearly an over-representation of stress phenotypes in the described mutations of Mediator subunits.

*MED15* also plays a role in stress responses alongside its roles in other processes. *MED15* in *Drosophila* was identified in a mosaic screening where the effect of the mutation was limited to the wings (Terriente-Felix et al., 2010). Homozygous null mutations were lethal at embryogenesis, and the weak point mutations found were lethal at later stages (Terriente-Felix et al., 2010). *MDT-15* is the ortholog of *MED15* in *C. elegans*, and the knock down by RNAi of *MDT-15* produced multiple deleterious effects (reduced life span, sterility, etc., Taubert et al., 2006). A reduction in functional MDT-15 protein leads to animals being hypersensitive to xenobiotics, thus affecting selectively stress response related to ingestion (Taubert et al., 2008). *GAL11* is the ortholog of *MED15* in yeast, and the deletion of this gene is not lethal, but is essential for growth on nonfermentable carbon sources, for sporulation, and for mating (Mylin et al., 1991, and references herein). The deletion of *GAL11* renders yeast more sensitive to cycloheximide (Shahi et al., 2010). Using this phenotype, we introduced *NRB4* in yeast  $\Delta gal11$ , but it did not complement the growth in cycloheximide (Figure S6E). *NRB4* may not be the correct *MED15* ortholog, since an *in silico* analysis predicts that there are three *MED15s* in Arabidopsis (Mathur et al., 2011). The existence of more than one ortholog is not new in the Mediator complex in plants (Kidd et al., 2011) or other organisms (Bourbon et al., 2004). If *NRB4* is one of three *MED15* subunits of Arabidopsis, then its role in SA response is non-redundant, since the two null alleles of *NRB4* produced plants that did not respond to SA.



### **How specific is *NRB4*?**

Mediator is a complex required for the normal transcription of genes. In a high throughput screening for genes involved in any process, there could be a point when elements of the general transcriptional machinery would start to appear. Our data regarding *NRB4* do not fit this concept, but point towards a specific role for *NRB4* in the SA response. First, we did not see any noticeable phenotype in the plants with the three hypomorphic EMS alleles, besides the response to SA. It is true that the first selection was done with BTH, but in the case of *npr1*, different alleles diverge in their response to MeJA (Dobón et al., 2011). Second, the phenotypes of *nrb4-4* and *nrb4-5* plants, although dramatic, did not resemble mutants generally impaired in signaling (e.g. hormones and light). Third, the transcriptomes of both *nrb4-2* and *nrb4-4* plants were not indicative of perturbation of any specific process compared to untreated wild type plants (Supplemental Dataset 1). Fourth, *NRB4* has not been found in other screenings for hormone responses, and some have been carried out *en masse* in plate format. It is not a small protein (1335 AA), and it has a glutamine rich region. EMS is the most frequent mutagen used in Arabidopsis, and its effect in glutamine is introducing stop codons (two possible stop codons and one silent mutation, Martinez-Zapater and Salinas, 1998). Therefore, it is more likely to have stop codons introduced by EMS than the average coding sequence. Fifth, the overexpression of *NRB4* did not produce any noticeable phenotypes except an increase in response to SA (Figure 8). The specificity of *NRB4* should be localized in the KIX domain, since the three missense alleles were localized there. It is the more conserved domain, and half of the protein can be deleted without major loss of function (Figure 8).

### **A model of the SA response**

There are several genes that act downstream of NPR1. Among the genes found to be relevant in the SA response, there are several that are involved in DNA repair (Song et al., 2011) and chromatin remodeling (Wang et al., 2010) genes. Since these proteins play a role in forming a complex relevant for transcription (Durrant et al., 2007), perhaps *NRB4* is required for the proper function of these proteins.

We have shown that *NRB4* is necessary for the SA response, and the pivotal role of *NPR1* in this signaling has been abundantly reported (Maier et al., 2011, Wu et al.,

2012, and Fu et al., 2012). In spite of the importance of these genes in the response to SA, we did not detect any interaction between the genes or their proteins. The F1s between the mutant alleles were wild type (Figure 1A), no protein-protein interaction was detected in yeast or *in planta*, and the over-expression of *NPR1* in an *nrb4* mutant background did not restore the response to SA (Figures 3B and S2G). Such an effect could have occurred if the corresponding proteins worked together. As a consequence, with the necessary precautions for the evaluation of negative results, it seems that NRB4 and NPR1 act at different points in SA signaling, which also explains the phenotypes of the double mutants, both with strong and weak alleles (Figure 3A and S2A). A version of NPR1 tagged with GFP became localized in the nucleus, both in an *nrb4* and in a wild type background (Figure S2), but did not rescue the altered response to SA. Therefore, NRB4 does not play any role in the stability of NPR1 (i.e. it does not act as chaperone), the concentration of NPR1 in the nucleus is NRB4 independent, and NRB4 functions downstream of NPR1.

It is possible that NRB4 interacts with NPR1 only in special conditions. An interaction between NPR1 and SA has been detected only recently, since the SA-NPR1 complex is quite labile (Wu et al., 2012). Alternatively, the interaction could happen with a complex that would include SA, NPR1, NPR3 and/or NPR4 (Fu et al., 2012). There are ample precedents of MED15 interacting with a nuclear receptor. In yeast, GAL11/MED15 is necessary for the expression of genes required for growth in galactose media (Suzuki et al., 1988). But other functions include the use of fatty acids (see below) and the regulation of multidrug resistance (MDR). Thus,  $\Delta gal11$  yeast does not grow in media with small amounts of ethidium bromide (Mylin et al., 1991) or cycloheximide (Shahi et al., 2010), while the wild type grows unaffected. This pathway is the same used by *Candida glabrata* to pump ketoconazole out of the cell (Thakur et al., 2008). The mechanism is that Pdr1p and Pdr3p are xenobiotic nuclear receptors that bind GAL11 (specifically in the KIX domain) in a xenobiotic-dependent manner (Thakur et al., 2008). This is not a unique case, since in *C. elegans*, NHR-49 binds MDT-15/MED15 also in the KIX domain (Taubert et al., 2006). In this and other organisms, MED15 regulates the metabolism of fatty acids, with a proposed model that NHR-49 and other nuclear receptors are binding a hormone-like small molecule(s) present in the food (Taubert et al., 2006).

Although none of the previous examples involves a SA receptor, similar molecules have been found to participate in these pathways. Oaf1P is a yeast nuclear receptor that, upon binding fatty acids, interacts with GAL11, and activates the transcription of genes required for the use of fatty acids (Thakur et al., 2009). A similar function is carried out by NHR-49 in *C. elegans* (Taubert et al., 2006), and by PPAR $\alpha$  in vertebrates (Issemann and Green, 1990). These three receptors bind fatty acids, but also bind nonsteroidal anti-inflammatory drugs (NSAIDs), such as salicylates. Therefore, the orthologs of MED15 interact with receptors in the KIX domain that bind salicylates and fatty acids. There is a strong representation of proteins related to lipids among the Arabidopsis defense mutants (*eds1*, *pad4*, *sag101*, Wiermer et al., 2005; *dir1*, Maldonado et al., 2002; *ssi2*, Kachroo et al., 2003; *sfd1*, Nandi et al., 2004; etc.), so it is plausible that this connection is maintained in Arabidopsis. There are no genes in Arabidopsis with significant homology to *Oaf1P*, *NHR-49*, or *PPAR $\alpha$*  (Table S3), so it is possible that *NPR1*, *NPR3*, and *NPR4* have evolved independently from the aforementioned receptors.

There is a striking difference in phenotype between plants with the EMS mutations and the null mutations (Figure 5). The null mutants produce a stronger phenotype in defense than the EMS alleles, and a severe phenotype in development. The phenotype in defense is even stronger than that caused by the *npr1* alleles so far described (Canet et al., 2010b). *Psm* CR299 grows a hundred fold in *nrb4-4* plants, while it does not grow in the rest of genotypes (Figure 5G). More strikingly, SA itself is upregulated in *npr1* and *nrb4* plants, but in *nrb4-4* the levels reach a maximum. Interestingly, this implies that the metabolism of SA is partially independent of NRB4 and NPR1. It also implies that SA itself does not affect *Pto* directly, since the levels of SA in *nrb4-4* plants clearly exceed the levels of SA in wild type plants (Figure 5H). This increased phenotype caused by the null mutants could be explained if the EMS alleles were not completely devoid of function. The point mutations in the KIX domain do not impair *nrb4-1* metabolism of SA in plates (Figure 1B), or *nrb4-2* to develop SAR (Figure 2D). The *npr1* null alleles do not cause the same phenotype as the *nrb4* null alleles, perhaps because the rest of *NPR1* paralogs are able to compensate for its loss in the SA response (Canet et al., 2010b). The strong phenotype caused by the null *nrb4* in development could be due to additional signals that are lost in these mutants. However, so far we have found no indication of such signals.

SA plays an important role in different plant processes besides disease resistance (Rivas-San Vicente and Plasencia, 2011), and one possible explanation could be that the phenotypes of *nrb4* null plants are only due to a lack of response to SA, therefore supporting the postulated essential role of SA in normal plant development (Vanacker et al., 2001). Thus, *npr1-1* and *nrb4-4* plants showed increased endoreplication of the nuclear DNA (Figure S6A), reflecting a role of SA in this process. The available plants with less SA do not show any of the previous phenotypes (Vanacker et al., 2001), but several analysis show that these plants still have some SA (Rivas-San Vicente and Plasencia, 2011), and plants that lack several SA biosynthetic genes are not viable (Garcion et al., 2008).

## **Material and Methods**

### **Plant growth and inoculation**

*Arabidopsis thaliana* (L.) Heynh. was sown and grown as described (Canet et al., 2010a), in controlled environment rooms with days of 8 h at 21°C, 150  $\mu\text{mol m}^{-2} \text{s}^{-1}$  of light intensity and nights of 16 h at 19°C. The treatments, inoculations, and sampling started 30 minutes after the initiation of the artificial day to ensure reproducibility. The following genotypes were used: *npr1-1* (Cao et al., 1997), *35S:NPR1-HBD* and *35S:NPR1-GFP* (Kinkema et al., 2000), *rpm1* (Grant et al., 1995), *rps2* (Mindrinis et al., 1994), *nho1* (Lu et al., 2001), *arr1-3 arr10-5 arr12-1* (Argyros et al., 2008). *nrb4-4* was SAIL\_792\_F02 and *nrb4-5* was GABI\_955\_E02. The line in which we did not find any insertion was SALK\_106110C. *Pseudomonas syringae* pv. *tomato* DC3000 (*Pto*) was grown, inoculated and measured as described (Tornero and Dangl, 2001). Briefly, plants of 18 days were inoculated by spray with *Pto* at  $\text{OD}_{600}=0.1$  with 0.02% Silwet L-77 (Crompton Europe Ltd, Evesham, UK). Three days later, the amount of colony forming units (cfu) per plant was quantified and represented on a logarithmic scale. When inoculations of older plants were measured, a sample of known surface was taken, and the resulting unit was  $\text{Log}(\text{cfu}/\text{cm}^2)$ . Other strains used were *Pto(avrRpm1)* (Ritter and Dangl, 1996), and *Pto(avrRpt2)* (Debener et al., 1991). *P. syringae* pv. *tabaci*, and pv *phaseolicola* NPS3121 were obtained from Dr. Jeff Dangl (UNC, Chapel Hill, NC, USA). *P. syringae* pv *maculicola* CR299 has been described (Ritter and Dangl, 1995). Systemic Acquired Resistance was measured as reported (Macho et al., 2010), inoculating leaves with *Pto(avrRpm1)* or a mock treatment using a blunt syringe. For all the experiments, at least three independent treatments were performed (three independent sets of plants sown and treated on different dates). *Pto* was maintained as described (Ritter and Dangl, 1996).

### **Chemical treatments**

Primers and chemical products were purchased from SIGMA (St. Louis, MO, USA) unless otherwise stated. Benzothiadiazole (BTH, CGA 245704), in the form of commercial product (Bion® 50 WG, a gift from Syngenta Agro S.A. Spain) was prepared in water for each treatment and applied with a household sprayer. The response to BTH in terms of fresh weight was done as reported (Canet et al., 2010a). Briefly, plants were treated with mock or 350  $\mu\text{M}$  BTH four times over three weeks. Then, the fresh weight of the plants was recorded and expressed as the ratio between

BTH and mock treated plants. 100  $\mu\text{M}$  methyl jasmonate (MeJA, Duchefa, Haarlem, The Netherlands) was applied by spray with 0.1% DMSO and 0.02% Silwet L-77. Dexamethasone was applied at 2  $\mu\text{M}$ , diluted in water from a stock of 20 mM in EtOH. SA (in the form of sodium salicylate) was applied at 500  $\mu\text{M}$ . For the treatments with cytokinins, trans-zeatin at 5  $\mu\text{M}$  was used to imbibe pieces of wool rock (from a local gardening shop). Seeds were sown directly in the wool rock, and additional water was added to compensate for evaporation.

### **SA in plates and *in planta*.**

*Arabidopsis* seeds were surface-sterilized for 10 min in 70% ethanol and for 10 min in commercial bleach. Then, five washes were done with distilled water and the seeds were distributed on agar plates. The medium contains 0.5x Murashige and Skoog salts (Duchefa BV, Haarlem, the Netherlands), 0.6% (w/v) Phyto Agar (Duchefa), 2% (w/v) sucrose, with 0, 400 or 500  $\mu\text{M}$  SA (final concentration). The results were evaluated 14 days after transferring to growing conditions. The chlorophyll was extracted with ethanol for 2 hours at 65 °C, and quantified as described by Frye et al., 2001. Three replicates of 10 plants each per treatment and genotype were measured. For the measurement of SA *in planta*, three samples of c. 100 mg were frozen in liquid nitrogen. SA extraction was performed as described by (Huang et al., 2005 and Defraia et al., 2008).

### **Expression *in planta* and microscopy**

*NRB4* was cloned in pDONR221 (Invitrogen, Barcelona, Spain) from a RT-PCR product, and then transferred to pMDC43 (Curtis and Grossniklaus, 2003; *GFP-NRB4*) and pB7FWG2 (Karimi et al., 2002; *NRB4-GFP*) for expression *in planta*. *N. benthamiana* leaf tissue was mounted in water under a coverslip 4 days after infiltration with *Agrobacterium tumefaciens* containing the constructs. The *Arabidopsis* plants containing NPR1-GFP were three weeks old at the time of the pictures. A Leica TCS SL confocal laser scanning microscope (Leica, Heidelberg, Germany) using an HCX PL APO CS 40X/1.25 oil objective was used to study the subcellular localization of the fluorescence-tagged proteins. Green fluorescent protein was visualized by 488-nm excitation with an Ar laser, and its emissions were examined with a band-pass filter for 500 to 530 nm. The primers used are included as Supplemental Table S4. The SEM pictures were taken with a JSM-5410 scanning electron microscope (JEOL, Tokyo,

Japan) in the Electron Microscopy Service (Universidad Politécnica de Valencia, Spain).

### **Immunoblot and RT-qPCR**

Immunodetection of PR1 protein was carried out as described (Wang et al., 2005), using an Amersham ECL Plus Western Blotting Detection Reagents (GE HealthCare, Little Chalfont, UK). The second antibody was a 1:25000 dilution of Anti-Rabbit IgG HRP Conjugate (Promega, Madison, USA). Chemiluminescent signals were detected using a LA-3000 Luminescent Image Analyzer (Fujifilm Life Science, Stamford, CT, USA).

Total RNA was extracted with Trizol (Invitrogen), following the manufacturer's instructions. cDNA was synthesized with RevertAid™ First Strand cDNA Synthesis Kit (Fermentas, Madrid, Spain), and the quantitative PCR performed with LuminoCt Sybr Green qPCR Ready Mix (SIGMA) in a 7000 RT-PCR Systems machine (Applied Biosystems, Madrid, Spain), following the manufacturer's instructions. For each measurement, three biological replicates were done. The obtained values were referred to the geometric average of three reference genes (At3G18780, At1G49240, and At5G60390), as described (Vandesompele et al., 2002), and normalized, with mock treated Col-0 equal to one. The list of primers used is provided in Supplemental Table S4.

### **Microarrays and Software used**

RNA was isolated as described above and purified with “RNeasy Mini Kit” (Qiagen, Valencia, CA, USA). Array hybridization to an Arabidopsis GeneChip ATH1 (Affymetrix, Santa Clara, CA, USA) was performed following the manufacturer's recommendations. The hybridization was carried out in the “Sección de Chips de DNA-S.C.S.I.E.”, University of Valencia (Valencia, Spain). Three biological replicates of each genotype were hybridized, with no technical replicates (3 replicates of 3 genotypes, 9 microarrays). The original hybridization data files were submitted to the European Bioinformatics Institute (EMBL-EBI) ArrayExpress repository and the Accession number E-MEXP-3602 was assigned to this experiment. The analysis of the microarrays was accomplished with Robin 1.1.7 (Lohse et al., 2010). The “robust multi array averaging” normalization was used. Both mutants were compared with the wild type control and the p-value cutoff was set at 0.05, with the Benjamini & Hochberg p-value correction (Benjamini and Hochberg, 1995). After the p-value adjustment, a

nested F test was used to classify the comparisons as significant (Lohse et al., 2010). Then, the following software was used: MapMan, (Usadel et al., 2005), Sample Angler (<http://142.150.214.117>), AtCAST (Sasaki et al., 2011), Cluster 3.0 (de Hoon et al., 2004), and JavaTreeView (Saldanha, 2004). For the statistic analysis, we used Excel 2003 (Microsoft, Redmond, WA, USA) and Statgraphics 5.1 (Statpoint Technologies, Inc., Warrenton, VA, USA). The data analyzed corresponded with the following experiments: *eds1*, E-MEXP-546; *NahG*, E-GEOD-5727; *npr1-1*, E-GEOD-5745; *sid2*, and BTH, E-GEOD-9955; *PsES*, E-GEOD-5685; Mildew, E-GEOD-431; *ARR21*, GSE5699; and *ARR22*, GSE5698.

### **Accession Numbers**

Sequence data from this article can be found in the Arabidopsis Genome Initiative or GenBank/EMBL databases under the following accession numbers: NRB4, At1g15780; NPR1, At1g64280; ACT2, At3g18780; ACT8, At1g49240; and ELF, At5G60390.

### **Supplemental information**

The following materials are available in the online version of this article.

Supplemental Figure 1. Additional phenotypes of *nrb4* in defense.

Supplemental Figure 2. Epistasis of *NRB4* with *NPR1*.

Supplemental Figure 3. Additional pictures of *nrb4-4*.

Supplemental Figure 4. Additional pictures of Cryo-SEM.

Supplemental Figure 5. Stainings of *nrb4*.

Supplemental Figure 6. Characterization of *nrb4* null alleles.

Supplemental Figure 7. Phenotypes from the transcriptomic analysis

Supplemental Figure 8. Yeast n-hybrid interactions.

Supplemental Figure 9. Expression of *NPR1* and *NBR4*.

Supplemental Figure 10. Characterization of *NRB4* complementation.

Supplemental Table 1. Evaluation of segregations.

Supplemental Table 2. Evaluation of phenotypes in T-DNA insertion lines.

Supplemental Table 3. Lack of homologs in Arabidopsis for several nuclear receptors.

Supplemental Table 4. Primers used.

Supplemental Dataset 1. Transcriptomic analysis.



### **Acknowledgments**

This work was supported by the “Ministerio de Economía y Competitividad” (MINECO) of Spain (grant BIO201018896 to PT, a JAE-CSIC Fellowship to JVC and a FPI-MINECO to AD) and “Generalitat Valenciana” of Spain (grant ACOMP/2012/105 to PT). We appreciate the opinions and generous help of Drs. Jeff Dangl and Pablo Vera with the manuscript, and the revision of Dr. Philippa Borrill. The authors declare that they have no conflicts of interest.

### **Author contributions**

JVC and AD performed the experiments, analyzed the data and revised the paper. PT designed the research, analyzed the data and wrote the paper.

### **Figure legends**

**Figure 1. SA related phenotypes of *nrb4* plants.** **A** Plants were treated with either mock or 350  $\mu$ M BTH four times over three weeks, their weights recorded, and the ratio between the BTH and mock treated plants calculated (15 plants in three groups of five). The ratio is expressed as percentage of fresh weight (%FW). **B** Plants were grown on MS plates supplied with 0, 400 and 500  $\mu$ M SA, the picture shows the 500  $\mu$ M SA plate at day 14. **C** The chlorophyll content of plants growing in the plates described in B was measured as an indication of the response to SA (30 plants in three groups of 10). The experiments were repeated three times with similar results, and the data represent the average, with the error bars plotting the standard deviation. The letters above the bars indicate different homogeneous groups with statistically significant differences (Fisher's LSD Test,  $P < 0.05$ ). In panel C the differences were evaluated between genotypes grown at either 400  $\mu$ M SA or 500  $\mu$ M SA (marked with the symbol prime).

**Figure 2. Pathogenic phenotypes of *nrb4* plants.** **A** 17-day-old plants were treated with either 500  $\mu$ M SA, 350  $\mu$ M BTH or a mock solution. One day later the plants were inoculated with *Pseudomonas syringae* pv. *tomato* isolate DC3000 (*Pto*) at an  $OD_{600}$  of 0.1. Three days after inoculation, the growth of *Pto* was evaluated as Logarithm of colony forming units (cfu) per plant. **B** PR1 immunoblot of the indicated genotypes three days after mock or a *Pto* inoculation (top), and one day after mock or 350  $\mu$ M BTH treatment (bottom). The genotypes are abbreviated as in A. The arrow indicates the position of PR1 (14 kDa). **C** 32-day-old plants were treated with *Pto* as in A. In these plants, only a sample of the surface area was measured, so the units are  $\text{Log}(\text{cfu}/\text{cm}^2)$ . **D** Three leaves of 30-day-old plants were hand infiltrated with either *Pto(avrRpm1)* or a mock solution. Two days later *Pto* was inoculated and its growth in systemic leaves measured as in C. SAR stands for Systemic Acquired Resistance. **E** *Pto(avrRpm1)* was inoculated in *nrb4* as in A. *rpm1* is included as a control. **F** Inoculations with *Pto(avrRpt2)*, with *rps2* added as a control. **G** *Pseudomonas syringae* pv. *phaseolicola* isolate NPS3121 was inoculated as in A, with *nho1* used as a control. **H** Inoculations with *Pseudomonas syringae* pv. *tabaci* was inoculated as in A, with *nho1* used as a control. The experiments were repeated three times with similar results, and the data represent the average, with the error bars plotting the standard deviation of 15 plants in three groups of five in the panels A, E, F, G, and H. In C and D, 12 samples of known size from three plants were taken in three groups of four. The letters above the

bars indicate different homogeneous groups with statistically significant differences (Fisher's LSD Test,  $P < 0.05$ ). Asterisks indicate statistically significant differences from the mock treatment ( $P < 0.05$  one asterisk,  $P < 0.01$  two) using the Student's t test (one tail).

**Figure 3. Epistasis of *NRB4* with *NPRI*.** **A** Three double mutants *nrb4-1 npr1-70* were tested as in Figure 1A. **B** *35S:NPRI-HBD (NPRIHBD)* in an *nrb4-2* background was tested with and without dexamethasone (DEX) for its response to BTH. The experiments were repeated three times with similar results, and the data represent the average, with the error bars plotting the standard deviation of 15 plants in three groups of five. The letters above the bars indicate different homogeneous groups with statistically significant differences (Fisher's LSD Test,  $P < 0.05$ ).

**Figure 4. Predicted structure of *NRB4*.** **A** Drawing of the predicted *NRB4* protein, showing the conserved KIX domain and the region rich in glutamine. **B** Magnification of the KIX domain, showing the introns (horizontal lines), the point mutations (arrows) and the T-DNA insertions (triangles) found in *NRB4* (At1g15780). The number above the mutation indicates the number of allele. Only a section of the *NRB4* gene is shown; the region shown corresponds to the grey rectangle in A. **C** Sequence of the first 100 AA of *NRB4*, indicating the point mutations.

**Figure 5. *nrb4-4* is a null allele.** **A** From left to right, wild type plant, *NRB4/nrb4-4* plants, and *nrb4-4* homozygous plants. Picture taken after six weeks in short day conditions. **B** Cryo-SEM pictures of wild type trichomes. The leaves sampled were approximately 7 mm and plants were five weeks old. **C** Cryo-SEM of *nrb4-4* trichomes, although plants were seven weeks old in order to sample leaves of roughly the same size. The length of the bar (bottom of the picture) is 100  $\mu\text{m}$ . **D** Picture of *nrb4-4* plants taken after 18 weeks (seven in short day, eleven in long day). **E** Plants were tested as in Figure 1A, but with one more week of growth and two more treatments. **F** Response of *nrb4-4* plants to SA and BTH in growth curves. The inoculations were done as in Figure 2C, except that the *nrb4-4* plants were seven weeks old. **G** *Pseudomonas syringae* pv. *maculicola* CR299 was inoculated and its growth measured as F. **H** The amount of SA (both free and total) was measured three days after a mock or a *Pto* inoculation. The experiments were repeated three times with similar results, and the data represent the

average, with the error bars plotting the standard deviation of 15 plants in three groups of five, except in the case of H, where three samples of 100 mg were taken. The letters above the bars indicate different homogeneous groups with statistically significant differences (Fisher's LSD Test,  $P < 0.05$ ). The differences in free SA and total SA (marked with the symbol prime) were evaluated between genotypes. Asterisks indicate statistically significant differences from the mock treatment ( $P < 0.05$  one asterisk,  $P < 0.01$  two) using the Student's t test (one tail).

**Figure 6. Transcriptome analysis of *nrb4* mutants.** **A** The transcriptomes of *nrb4-2*, *nrb4-4*, and Col-0 plants were determined, and then compared with different transcriptomic experiments by means of hierarchical clustering with Cluster 3.0 (de Hoon et al., 2004), and visualized as a dendrogram with JavaTreeView (Saldanha, 2004). The references of the experiments used are specified in the Methods section, and the parameters used were the default settings. **B** Growth response to cytokinins. Seeds of the indicated genotypes were grown in rock wool imbibed with 5  $\mu\text{M}$  trans-zeatin. This picture was taken after 21 days' growth. *arr1,10,12* stands for the triple mutant *arr1 arr10 arr12*, used as a control for lack of response to cytokinins.

**Figure 7. Expression of *NRB4* and subcellular localization.** **A** *NRB4* expression was measured one day after treatment with mock, 350  $\mu\text{M}$  BTH, 500  $\mu\text{M}$  SA, and 100  $\mu\text{M}$  Methyl jasmonate (MeJA), or three days after a *Pto* inoculation (RNA extracted and RT-qPCR from three independent samples of 100 mg each). The levels of expression are normalized to three reference genes and to the level of Col-0. **B** RNA was extracted from three-week-old plants (five weeks for *nrb4-4*), and transcript levels for *NRB4* were measured by RT-qPCR as in A. **C** *Agrobacterium tumefaciens* with the construct *35S:NRB4-GFP* was infiltrated into leaves of *Nicotiana benthamiana*, and the expression was detected by confocal microscopy four days later. **D** Similar to C with the construct *35S:GFP-NRB4*. The experiments were repeated three times with similar results, and the data represent the average, with the error bars plotting the standard deviation of three samples. The letters above the bars indicate different homogeneous groups with statistically significant differences (Fisher's LSD Test,  $P < 0.05$ ).

**Figure 8. Phenotypes of transgenic lines.** **A** Transgenic plants homozygous for the construct *35S:NRB4-GFP (NRB4F)* or for the equivalent construct with only the first

670 AA (*NRB4M*), were obtained in the mutant alleles. The panel shows the response to BTH in fresh weight of the mentioned lines tested as in Figure 1A. **B** The constructs described in A were transformed into Col-0, and their response to BTH in fresh weight recorded. The number indicates an independent line. **C** Response of the transgenic lines described in A to SA and BTH in growth curves, as described in Figure 2A. **D** Response of the transgenic lines described in B to SA and BTH in growth curves, as described in Figure 2A. The experiments were repeated three times with similar results, and the data represent the average, with the error bars plotting the standard deviation of 15 plants in three groups of five. The letters above the bars indicate different homogeneous groups with statistically significant differences (Fisher's LSD Test,  $P < 0.05$ ). Asterisks indicate statistically significant differences from the mock treatment ( $P < 0.05$  one asterisk,  $P < 0.01$  two) using the Student's t test (one tail).

## References

- Argueso, C.T., Ferreira, F.J., Epple, P., To, J.P., Hutchison, C.E., Schaller, G.E., Dangl, J.L., and Kieber, J.J. (2012). Two-component elements mediate interactions between cytokinin and salicylic acid in plant immunity. *PLoS Genet* **8**, e1002448.
- Argyros, R.D., Mathews, D.E., Chiang, Y.H., Palmer, C.M., Thibault, D.M., Etheridge, N., Argyros, D.A., Mason, M.G., Kieber, J.J., and Schaller, G.E. (2008). Type B response regulators of Arabidopsis play key roles in cytokinin signaling and plant development. *Plant Cell* **20**, 2102-2116.
- Autran, D., Jonak, C., Belcram, K., Beemster, G.T., Kronenberger, J., Grandjean, O., Inze, D., and Traas, J. (2002). Cell numbers and leaf development in Arabidopsis: a functional analysis of the STRUWWELPETER gene. *EMBO J* **21**, 6036-6049.
- Backstrom, S., Elfving, N., Nilsson, R., Wingsle, G., and Bjorklund, S. (2007). Purification of a plant mediator from Arabidopsis thaliana identifies PFT1 as the Med25 subunit. *Mol Cell* **26**, 717-729.
- Benjamini, Y., and Hochberg, B. (1995). Controlling the False Discovery Rate: A Practical and Powerful Approach to Multiple Testing. *Journal of the Royal Statistical Society. Series B* **57**, 289-300.
- Boube, M., Joulia, L., Cribbs, D.L., and Bourbon, H.M. (2002). Evidence for a mediator of RNA polymerase II transcriptional regulation conserved from yeast to man. *Cell* **110**, 143-151.
- Bourbon, H.M., Aguilera, A., Ansari, A.Z., Asturias, F.J., Berk, A.J., Bjorklund, S., Blackwell, T.K., Borggreffe, T., Carey, M., Carlson, M., Conaway, J.W., Conaway, R.C., Emmons, S.W., Fondell, J.D., Freedman, L.P., Fukasawa, T., Gustafsson, C.M., Han, M., He, X., Herman, P.K., Hinnebusch, A.G., Holmberg, S., Holstege, F.C., Jaehning, J.A., Kim, Y.J., Kuras, L., Leutz, A., Lis, J.T., Meisterernest, M., Naar, A.M., Nasmyth, K., Parvin, J.D., Ptashne, M., Reinberg, D., Ronne, H., Sadowski, I., Sakurai, H., Sipiczki, M., Sternberg, P.W., Stillman, D.J., Strich, R., Struhl, K., Svejstrup, J.Q., Tuck, S., Winston, F., Roeder, R.G., and Kornberg, R.D. (2004). A unified nomenclature for protein subunits of mediator complexes linking transcriptional regulators to RNA polymerase II. *Mol Cell* **14**, 553-557.
- Browse, J. (2009). Jasmonate Passes Muster: A Receptor and Targets for the Defense Hormone. *Annual Review of Plant Biology* **60**, 183-205.
- Cai, G., Imasaki, T., Takagi, Y., and Asturias, F.J. (2009). Mediator structural conservation and implications for the regulation mechanism. *Structure* **17**, 559-567.
- Canet, J.V., Dobón, A., Ibáñez, F., Perales, L., and Tornero, P. (2010a). Resistance and biomass in Arabidopsis: a new model for Salicylic Acid perception. *Plant Biotech J* **8**, 126-141.
- Canet, J.V., Dobón, A., Roig, A., and Tornero, P. (2010b). Structure-Function Analysis of npr1 Alleles in Arabidopsis Reveals a Role for its Paralogs in the Perception of Salicylic Acid. *Plant, Cell & Environ* **33**, 1911-1922.
- Cao, H., Bowling, S.A., Gordon, A.S., and Dong, X. (1994). Characterization of an Arabidopsis Mutant That Is Nonresponsive to Inducers of Systemic Acquired Resistance. *Plant Cell* **6**, 1583-1592.
- Cao, H., Glazebrook, J., Clarke, J.D., Volko, S., and Dong, X. (1997). The Arabidopsis NPR1 gene that controls systemic acquired resistance encodes a novel protein containing ankyrin repeats. *Cell* **88**, 57-63.

- Cao, H., Li, X., and Dong, X.** (1998). Generation of broad-spectrum disease resistance by overexpression of an essential regulatory gene in systemic acquired resistance. *Proc Natl Acad Sci U S A* **95**, 6531-6536.
- Cerdan, P.D., and Chory, J.** (2003). Regulation of flowering time by light quality. *Nature* **423**, 881-885.
- Curtis, M.D., and Grossniklaus, U.** (2003). A gateway cloning vector set for high-throughput functional analysis of genes in planta. *Plant Physiol* **133**, 462-469.
- Chadick, J.Z., and Asturias, F.J.** (2005). Structure of eukaryotic Mediator complexes. *Trends Biochem Sci* **30**, 264-271.
- Choi, J., Huh, S.U., Kojima, M., Sakakibara, H., Paek, K.H., and Hwang, I.** (2010). The cytokinin-activated transcription factor ARR2 promotes plant immunity via TGA3/NPR1-dependent salicylic acid signaling in Arabidopsis. *Dev Cell* **19**, 284-295.
- Chrivia, J.C., Kwok, R.P., Lamb, N., Hagiwara, M., Montminy, M.R., and Goodman, R.H.** (1993). Phosphorylated CREB binds specifically to the nuclear protein CBP. *Nature* **365**, 855-859.
- de Hoon, M.J., Imoto, S., Nolan, J., and Miyano, S.** (2004). Open source clustering software. *Bioinformatics* **20**, 1453-1454.
- Debener, T., Lehnackers, H., Arnold, M., and Dangl, J.L.** (1991). Identification and molecular mapping of a single *Arabidopsis thaliana* locus determining resistance to a phytopathogenic *Pseudomonas syringae* isolate. *Plant J* **1**, 289-302.
- Defraia, C.T., Schmelz, E.A., and Mou, Z.** (2008). A rapid biosensor-based method for quantification of free and glucose-conjugated salicylic acid. *Plant Methods* **4**, 28.
- Delaney, T.P., Friedrich, L., and Ryals, J.A.** (1995). Arabidopsis signal transduction mutant defective in chemically and biologically induced disease resistance. *Proc Natl Acad Sci U S A* **92**, 6602-6606.
- Deng, W.-L., Preston, G., Collmer, A., Chang, C.-J., and Huang, H.-C.** (1998). Characterization of the *hrpC* and *hrpRS* operons of *Pseudomonas syringae* pathovars syringae, tomato, and glycinea and analysis of the ability of *hrpF*, *hrpG*, *hrcC*, *hrpT* and *hrpV* mutants to elicit the hypersensitive response and disease in plants. *J. Bacteriol.* **180**, 4523-4531.
- Després, C., DeLong, C., Glaze, S., Liu, E., and Fobert, P.R.** (2000). The Arabidopsis NPR1/NIM1 protein enhances the DNA binding activity of a subgroup of the TGA family of bZIP transcription factors. *Plant Cell* **12**, 279-290.
- Dhawan, R., Luo, H., Foerster, A.M., Abuqamar, S., Du, H.N., Briggs, S.D., Mittelsten Scheid, O., and Mengiste, T.** (2009). HISTONE MONOUBIQUITINATION1 interacts with a subunit of the mediator complex and regulates defense against necrotrophic fungal pathogens in Arabidopsis. *Plant Cell* **21**, 1000-1019.
- Dobón, A., Canet, J.V., Perales, L., and Tornero, P.** (2011). Quantitative genetic analysis of salicylic acid perception in Arabidopsis. *Planta* **234**, 671-684.
- Dong, X.** (2004). NPR1, all things considered. *Curr Opin Plant Biol* **7**, 547-552.
- Durrant, W.E., Wang, S., and Dong, X.** (2007). Arabidopsis SNI1 and RAD51D regulate both gene transcription and DNA recombination during the defense response. *Proc Natl Acad Sci U S A* **104**, 4223-4227.
- Elfving, N., Davoine, C., Benloch, R., Blomberg, J., Brannstrom, K., Muller, D., Nilsson, A., Ulfstedt, M., Ronne, H., Wingsle, G., Nilsson, O., and**

- Bjorklund, S.** (2011). The *Arabidopsis thaliana* Med25 mediator subunit integrates environmental cues to control plant development. *Proc Natl Acad Sci U S A* **108**, 8245-8250.
- Eulgem, T., Rushton, P.J., Robatzek, S., and Somssich, I.E.** (2000). The WRKY superfamily of plant transcription factors. *Trends in Plant Science* **5**, 199-206.
- Falk, A., Feys, B.J., Frost, L.N., Jones, J.D., Daniels, M.J., and Parker, J.E.** (1999). EDS1, an essential component of R gene-mediated disease resistance in *Arabidopsis* has homology to eukaryotic lipases. *Proc Natl Acad Sci U S A* **96**, 3292 - 3297.
- Flanagan, P.M., Kelleher, R.J., 3rd, Sayre, M.H., Tschochner, H., and Kornberg, R.D.** (1991). A mediator required for activation of RNA polymerase II transcription in vitro. *Nature* **350**, 436-438.
- Frye, C.A., Tang, D., and Innes, R.W.** (2001). Negative regulation of defense responses in plants by a conserved MAPKK kinase. *Proc. Natl. Acad. Sci. U S A* **98**, 373-378.
- Fu, Z.Q., Yan, S., Saleh, A., Wang, W., Ruble, J., Oka, N., Mohan, R., Spoel, S.H., Tada, Y., Zheng, N., and Dong, X.** (2012). NPR3 and NPR4 are receptors for the immune signal salicylic acid in plants. *Nature*.
- Garcion, C., Lohmann, A., Lamodièrè, E., Catinot, J., Buchala, A., Doermann, P., and Metraux, J.-P.** (2008). Characterization and Biological Function of the ISOCHORISMATE SYNTHASE2 Gene of *Arabidopsis*. *Plant Physiol.* **147**, 1279-1287.
- Glazebrook, J., Rogers, E.E., and Ausubel, F.M.** (1996). Isolation of *Arabidopsis* mutants with enhanced disease susceptibility by direct screening. *Genetics* **143**, 973-982.
- Grant, M.R., Godiard, L., Straube, E., Ashfield, T., Lewald, J., Sattler, A., Innes, R.W., and Dangl, J.L.** (1995). Structure of the *Arabidopsis RPM1* gene enabling dual specificity disease resistance. *Science* **269**, 843-846.
- Grantham, R.** (1974). Amino acid difference formula to help explain protein evolution. *Science* **185**, 862-864.
- Guo, L., Han, A., Bates, D.L., Cao, J., and Chen, L.** (2007). Crystal structure of a conserved N-terminal domain of histone deacetylase 4 reveals functional insights into glutamine-rich domains. *Proc Natl Acad Sci U S A* **104**, 4297-4302.
- Hruz, T., Laule, O., Szabo, G., Wessendorp, F., Bleuler, S., Oertle, L., Widmayer, P., Gruissem, W., and Zimmermann, P.** (2008). Genevestigator V3: a reference expression database for the meta-analysis of transcriptomes. *Advances in Bioinformatics*, 420747
- Huang, W.E., Wang, H., Zheng, H., Huang, L., Singer, A.C., Thompson, I., and Whiteley, A.S.** (2005). Chromosomally located gene fusions constructed in *Acinetobacter* sp. ADP1 for the detection of salicylate. *Environ Microbiol.* **7**, 1339-1348.
- Issemann, I., and Green, S.** (1990). Activation of a member of the steroid hormone receptor superfamily by peroxisome proliferators. *Nature* **347**, 645-650.
- Jakoby, M., Weisshaar, B., Droge-Laser, W., Vicente-Carbajosa, J., Tiedemann, J., Kroj, T., and Parcy, F.** (2002). bZIP transcription factors in *Arabidopsis*. *Trends Plant Sci.* **7**, 106-111.
- Kachroo, A., Lapchyk, L., Fukushige, H., Hildebrand, D., Klessig, D., and Kachroo, P.** (2003). Plastidial Fatty Acid Signaling Modulates Salicylic Acid-



- and Jasmonic Acid-Mediated Defense Pathways in the Arabidopsis ssi2 Mutant. *Plant Cell* **15**, 2952-2965.
- Karimi, M., Inze, D., and Depicker, A.** (2002). GATEWAY vectors for Agrobacterium-mediated plant transformation. *Trends Plant Sci* **7**, 193-195.
- Kelleher, R.J., 3rd, Flanagan, P.M., and Kornberg, R.D.** (1990). A novel mediator between activator proteins and the RNA polymerase II transcription apparatus. *Cell* **61**, 1209-1215.
- Kiba, T., Aoki, K., Sakakibara, H., and Mizuno, T.** (2004). Arabidopsis response regulator, ARR22, ectopic expression of which results in phenotypes similar to the wol cytokinin-receptor mutant. *Plant Cell Physiol* **45**, 1063-1077.
- Kiba, T., Naitou, T., Koizumi, N., Yamashino, T., Sakakibara, H., and Mizuno, T.** (2005). Combinatorial microarray analysis revealing arabidopsis genes implicated in cytokinin responses through the His->Asp Phosphorelay circuitry. *Plant Cell Physiol* **46**, 339-355.
- Kidd, B.N., Edgar, C.I., Kumar, K.K., Aitken, E.A., Schenk, P.M., Manners, J.M., and Kazan, K.** (2009). The mediator complex subunit PFT1 is a key regulator of jasmonate-dependent defense in Arabidopsis. *Plant Cell* **21**, 2237-2252.
- Kidd, B.N., Cahill, D.M., Manners, J.M., Schenk, P.M., and Kazan, K.** (2011). Diverse roles of the Mediator complex in plants. *Semin Cell Dev Biol* **22**, 741-748.
- Kinkema, M., Fan, W., and Dong, X.** (2000). Nuclear localization of NPR1 is required for activation of PR gene expression. *Plant Cell* **12**, 2339-2350.
- Kubista, M., Akerman, B., and Norden, B.** (1987). Characterization of interaction between DNA and 4',6-diamidino-2-phenylindole by optical spectroscopy. *Biochemistry* **26**, 4545-4553.
- Lawton, K., Weymann, K., Friedrich, L., Vernooij, B., Uknes, S., and Ryals, J.** (1995). Systemic acquired resistance in Arabidopsis requires salicylic acid but not ethylene. *Mol Plant Microbe Interact.* **8**, 863-870.
- Lawton, K.A., Friedrich, L., Hunt, M., Weymann, K., Delaney, T., Kessmann, H., Staub, T., and Ryals, J.** (1996). Benzothiadiazole induces disease resistance in Arabidopsis by activation of the systemic acquired resistance signal transduction pathway. *Plant J* **10**, 71-82.
- Lohse, M., Nunes-Nesi, A., Kruger, P., Nagel, A., Hannemann, J., Giorgi, F.M., Childs, L., Osorio, S., Walther, D., Selbig, J., Sreenivasulu, N., Stitt, M., Fernie, A.R., and Usadel, B.** (2010). Robin: an intuitive wizard application for R-based expression microarray quality assessment and analysis. *Plant Physiol* **153**, 642-651.
- Lu, M., Tang, X., and Zhou, J.M.** (2001). Arabidopsis NHO1 Is Required for General Resistance against Pseudomonas Bacteria. *Plant Cell* **13**, 437-447.
- Macho, A.P., Guevara, C.M., Tornero, P., Ruiz-Albert, J., and Beuzon, C.R.** (2010). The Pseudomonas syringae effector protein HopZ1a suppresses effector-triggered immunity. *New Phytol* **187**, 1018-1033.
- Maier, F., Zwicker, S., Huckelhoven, A., Meissner, M., Funk, J., Pfitzner, A.J., and Pfitzner, U.M.** (2011). NONEXPRESSOR OF PATHOGENESIS-RELATED PROTEINS1 (NPR1) and some NPR1-related proteins are sensitive to salicylic acid. *Mol Plant Pathol* **12**, 73-91.
- Maldonado, A.M., Doerner, P., Dixon, R.A., Lamb, C.J., and Cameron, R.K.** (2002). A putative lipid transfer protein involved in systemic resistance signalling in Arabidopsis. *Nature* **419**, 399-403.

- Martinez-Zapater, J.M., and Salinas, J.** (1998). *Arabidopsis* Protocols. (Humana Press).
- Mathur, S., Vyas, S., Kapoor, S., and Tyagi, A.K.** (2011). The Mediator Complex in Plants: Structure, Phylogeny, and Expression Profiling of Representative Genes in a Dicot (*Arabidopsis*) and a Monocot (Rice) during Reproduction and Abiotic Stress. *Plant Physiol* **157**, 1609-1627.
- Mindrinos, M., Katagiri, F., Yu, G.-L., and Ausubel, F.M.** (1994). The *A. thaliana* disease resistance gene *RPS2* encodes a protein containing a nucleotide-binding site and leucine-rich repeats. *Cell* **78**, 1089-1099.
- Mittal, S., and Davis, K.R.** (1995). Role of the phytotoxin Coronatine in the infection of *Arabidopsis thaliana* by *Pseudomonas syringae* pv. tomato. *Mol Plant Microbe Interact* **8**, 165-171.
- Mylin, L.M., Gerardot, C.J., Hopper, J.E., and Dickson, R.C.** (1991). Sequence conservation in the *Saccharomyces* and *Kluveromyces* GAL11 transcription activators suggests functional domains. *Nucleic Acids Res* **19**, 5345-5350.
- Nandi, A., Welti, R., and Shah, J.** (2004). The *Arabidopsis thaliana* Dihydroxyacetone Phosphate Reductase Gene SUPPRESSOR OF FATTY ACID DESATURASE DEFICIENCY1 Is Required for Glycerolipid Metabolism and for the Activation of Systemic Acquired Resistance. *Plant Cell* **16**, 465-477.
- Radhakrishnan, I., Perez-Alvarado, G.C., Parker, D., Dyson, H.J., Montminy, M.R., and Wright, P.E.** (1997). Solution structure of the KIX domain of CBP bound to the transactivation domain of CREB: a model for activator:coactivator interactions. *Cell* **91**, 741-752.
- Ritter, C., and Dangl, J.L.** (1995). The *avrRpm1* gene of *Pseudomonas syringae* pv. *maculicola* is required for virulence on *Arabidopsis*. *Mol Plant Microbe Interact* **8**, 444-453.
- Ritter, C., and Dangl, J.L.** (1996). Interference between two specific pathogen recognition events mediated by distinct plant disease resistance genes. *Plant Cell* **8**, 251-257.
- Rivas-San Vicente, M., and Plasencia, J.** (2011). Salicylic acid beyond defence: its role in plant growth and development. *J Exp Bot* **62**, 3321-3338.
- Robert-Seilaniantz, A., Grant, M., and Jones, J.D.** (2011). Hormone crosstalk in plant disease and defense: more than just jasmonate-salicylate antagonism. *Annu Rev Phytopathol* **49**, 317-343.
- Saldanha, A.J.** (2004). Java Treeview--extensible visualization of microarray data. *Bioinformatics* **20**, 3246-3248.
- Sasaki, E., Takahashi, C., Asami, T., and Shimada, Y.** (2011). AtCAST, a tool for exploring gene expression similarities among DNA microarray experiments using networks. *Plant Cell Physiol* **52**, 169-180.
- Shah, J., Tsui, F., and Klessig, D.F.** (1997). Characterization of a salicylic acid-insensitive mutant (*sai1*) of *Arabidopsis thaliana* identified in a selective screen utilizing the SA-inducible expression of the *tms2* gene. *Mol Plant Microbe Interact* **10**, 69-78.
- Shahi, P., Gulshan, K., Naar, A.M., and Moye-Rowley, W.S.** (2010). Differential roles of transcriptional mediator subunits in regulation of multidrug resistance gene expression in *Saccharomyces cerevisiae*. *Mol Biol Cell* **21**, 2469-2482.
- Song, J., Durrant, W.E., Wang, S., Yan, S., Tan, E.H., and Dong, X.** (2011). DNA repair proteins are directly involved in regulation of gene expression during plant immune response. *Cell Host Microbe* **9**, 115-124.

- Spoel, S.H., Koornneef, A., Claessens, S.M., Korzelius, J.P., Van Pelt, J.A., Mueller, M.J., Buchala, A.J., Metraux, J.P., Brown, R., Kazan, K., Van Loon, L.C., Dong, X., and Pieterse, C.M.** (2003). NPR1 modulates cross-talk between salicylate- and jasmonate-dependent defense pathways through a novel function in the cytosol. *Plant Cell* **15**, 760-770.
- Suzuki, Y., Nogi, Y., Abe, A., and Fukasawa, T.** (1988). GAL11 protein, an auxiliary transcription activator for genes encoding galactose-metabolizing enzymes in *Saccharomyces cerevisiae*. *Mol Cell Biol* **8**, 4991-4999.
- Swarbreck, D., Wilks, C., Lamesch, P., Berardini, T.Z., Garcia-Hernandez, M., Foerster, H., Li, D., Meyer, T., Muller, R., Ploetz, L., Radenbaugh, A., Singh, S., Swing, V., Tissier, C., Zhang, P., and Huala, E.** (2008). The Arabidopsis Information Resource (TAIR): gene structure and function annotation. *Nucl. Acids Res.* **36**, D1009-1014.
- Taatjes, D.J.** (2010). The human Mediator complex: a versatile, genome-wide regulator of transcription. *Trends Biochem Sci* **35**, 315-322.
- Tada, Y., Spoel, S.H., Pajerowska-Mukhtar, K., Mou, Z., Song, J., Wang, C., Zuo, J., and Dong, X.** (2008). Plant immunity requires conformational charges of NPR1 via S-nitrosylation and thioredoxins. *Science*. **321**, 952-956. .
- Talcott, B., and Moore, M.S.** (1999). Getting across the nuclear pore complex. *Trends Cell Biol* **9**, 312-318.
- Taubert, S., Van Gilst, M.R., Hansen, M., and Yamamoto, K.R.** (2006). A Mediator subunit, MDT-15, integrates regulation of fatty acid metabolism by NHR-49-dependent and -independent pathways in *C. elegans*. *Genes Dev* **20**, 1137-1149.
- Taubert, S., Hansen, M., Van Gilst, M.R., Cooper, S.B., and Yamamoto, K.R.** (2008). The Mediator subunit MDT-15 confers metabolic adaptation to ingested material. *PLoS Genet* **4**, e1000021.
- Terriente-Felix, A., Lopez-Varea, A., and de Celis, J.F.** (2010). Identification of genes affecting wing patterning through a loss-of-function mutagenesis screen and characterization of med15 function during wing development. *Genetics* **185**, 671-684.
- Thakur, J.K., Arthanari, H., Yang, F., Pan, S.J., Fan, X., Breger, J., Frueh, D.P., Gulshan, K., Li, D.K., Mylonakis, E., Struhl, K., Moye-Rowley, W.S., Cormack, B.P., Wagner, G., and Naar, A.M.** (2008). A nuclear receptor-like pathway regulating multidrug resistance in fungi. *Nature* **452**, 604-609.
- Thakur, J.K., Arthanari, H., Yang, F., Chau, K.H., Wagner, G., and Naar, A.M.** (2009). Mediator subunit Gal11p/MED15 is required for fatty acid-dependent gene activation by yeast transcription factor Oaf1p. *J Biol Chem* **284**, 4422-4428.
- Ton, J., and Mauch-Mani, B.** (2004). Beta-amino-butyric acid-induced resistance against necrotrophic pathogens is based on ABA-dependent priming for callose. *Plant J* **38**, 119-130.
- Tornero, P., and Dangl, J.L.** (2001). A high throughput method for quantifying growth of phytopathogenic bacteria in *Arabidopsis thaliana*. *Plant J* **28**, 475-481.
- Usadel, B., Nagel, A., Thimm, O., Redestig, H., Blaesing, O.E., Palacios-Rojas, N., Selbig, J., Hannemann, J., Piques, M.C., Steinhauser, D., Scheible, W.R., Gibon, Y., Morcuende, R., Weicht, D., Meyer, S., and Stitt, M.** (2005). Extension of the visualization tool MapMan to allow statistical analysis of arrays, display of corresponding genes, and comparison with known responses. *Plant Physiol.* **138**, 1195-1204.

- Vanacker, H., Lu, H., Rate, D.N., and Greenberg, J.T.** (2001). A role for salicylic acid and NPR1 in regulating cell growth in Arabidopsis. *Plant J.* **28**, 209-216.
- Vandesompele, J., De Preter, K., Pattyn, F., Poppe, B., Van Roy, N., De Paepe, A., and Speleman, F.** (2002). Accurate normalization of real-time quantitative RT-PCR data by geometric averaging of multiple internal control genes. *Genome Biol* **3**, RESEARCH0034.
- Vlot, A.C., Dempsey, D.M.A., and Klessig, D.F.** (2009). Salicylic Acid, a Multifaceted Hormone to Combat Disease. *Ann Rev Phytopathology* **47**, 177-206.
- Wang, D., Weaver, N.D., Kesarwani, M., and Dong, X.** (2005). Induction of protein secretory pathway is required for systemic acquired resistance. *Science.* **308**, 1036-1040.
- Wang, S., Durrant, W.E., Song, J., Spivey, N.W., and Dong, X.** (2010). Arabidopsis BRCA2 and RAD51 proteins are specifically involved in defense gene transcription during plant immune responses. *Proc Natl Acad Sci U S A* **107**, 22716-22721.
- Weigel, R.R., Bauscher, C., Pfitzner, A.J., and Pfitzner, U.M.** (2001). NIMIN-1, NIMIN-2 and NIMIN-3, members of a novel family of proteins from Arabidopsis that interact with NPR1/NIM1, a key regulator of systemic acquired resistance in plants. *Plant Mol Biol* **46**, 143-160.
- Wiermer, M., Feys, B.J., and Parker, J.E.** (2005). Plant immunity: the EDS1 regulatory node. *Curr Opin Plant Biol.* **8**, 383-389.
- Wu, Y., Zhang, D., Chu, Jee Y., Boyle, P., Wang, Y., Brindle, Ian D., De Luca, V., and Després, C.** (2012). The Arabidopsis NPR1 Protein Is a Receptor for the Plant Defense Hormone Salicylic Acid. *Cell Reports*.
- Zhang, Y., Fan, W., Kinkema, M., Li, X., and Dong, X.** (1999). Interaction of NPR1 with basic leucine zipper protein transcription factors that bind sequences required for salicylic acid induction of the PR-1 gene. *Proc Natl Acad Sci U S A* **96**, 6523-6528.

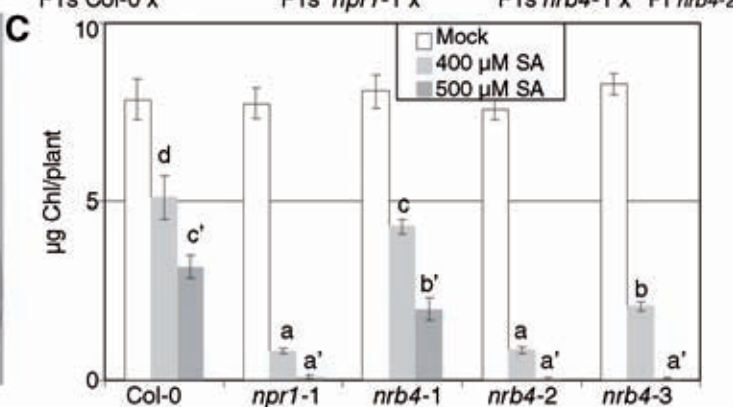
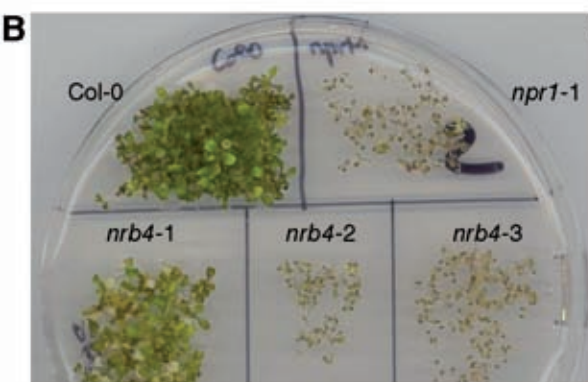
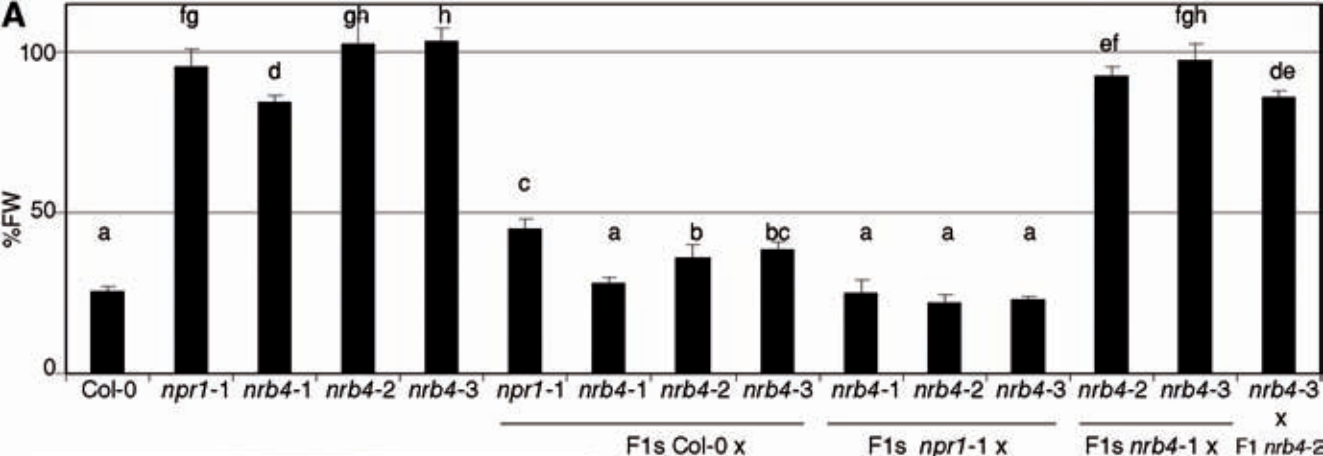


**Figure 1. SA related phenotypes of *nrb4* plants.** **A** Plants were treated with either mock or 350  $\mu$ M BTH four times over three weeks, their weights recorded, and the ratio between the BTH and mock treated plants calculated (15 plants in three groups of five). The ratio is expressed as percentage of fresh weight (%FW). **B** Plants were grown on MS plates supplied with 0, 400 and 500  $\mu$ M SA, the picture shows the 500  $\mu$ M SA plate at day 14. **C** The chlorophyll content of plants growing in the plates described in B was measured as an indication of the response to SA (30 plants in three groups of 10). The experiments were repeated three times with similar results, and the data represent the average, with the error bars plotting the standard deviation. The letters above the bars indicate different homogeneous groups with statistically significant differences (Fisher's LSD Test,  $P < 0.05$ ). In panel C the differences were evaluated between genotypes grown at either 400  $\mu$ M SA or 500  $\mu$ M SA (marked with the symbol prime).

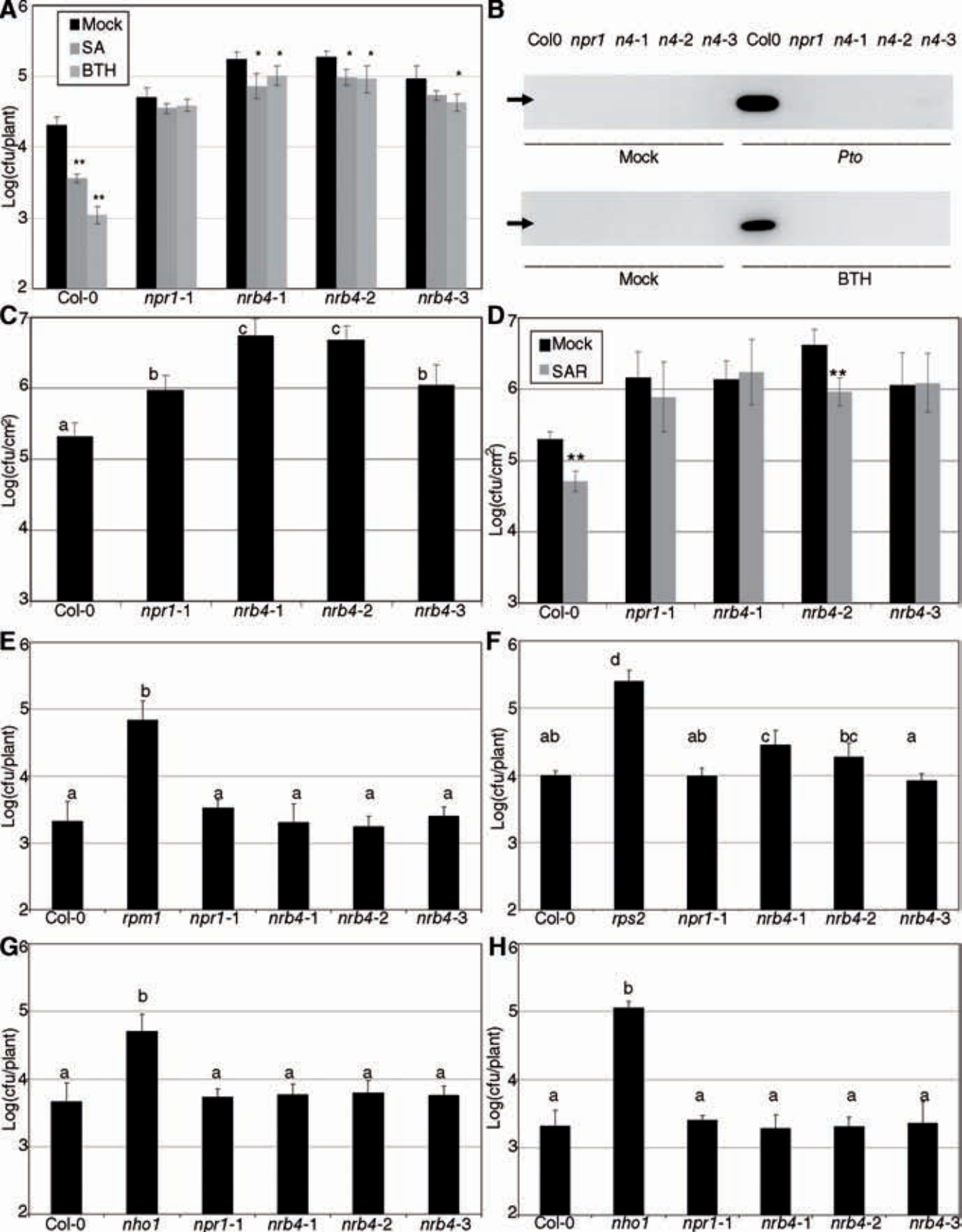


**Figure 2. Pathogenic phenotypes of *nrb4*.** **A** 17-day-old plants were treated with either 500  $\mu$ M SA, 350  $\mu$ M BTH or a mock solution. One day later the plants were inoculated with *Pseudomonas syringae* pv. *tomato* isolate DC3000 (*Pto*) at an OD<sub>600</sub> of 0.1. Three days after inoculation, the growth of *Pto* was evaluated as Logarithm of colony forming units (cfu) per plant. **B** PR1 Western blot of the indicated genotypes three days after mock or a *Pto* inoculation (top), and one day after mock or 350  $\mu$ M BTH treatment (bottom). The genotypes -abbreviated- are the same as in A. The arrow indicates the position of PR1 (14 kDa). **C** 32-day-old plants were treated with *Pto* as in A. In these plants, only a sample of the surface area was measured, so the units are Log(cfu/cm<sup>2</sup>). **D** Three leaves of 30-day-old plants were hand infiltrated with either *Pto*(*avrRpm1*) or a mock solution. Two days later *Pto* was inoculated and its growth in systemic leaves measured as in C. SAR stands for Systemic Acquired Resistance. **E** *Pto*(*avrRpm1*) was inoculated in *nrb4* as in A. *rpm1* is included as a control. **F** Inoculations with *Pto*(*avrRpt2*), with *rps2* added as a control. **G** *Pseudomonas syringae* pv. *phaseolicola* isolate NPS3121 was inoculated as in A, with *nho1* used as a control. **H** Inoculations with *Pseudomonas syringae* pv. *tabaci* was inoculated as in A, with *nho1* used as a control. The experiments were repeated three times with similar results, and the data represent the average, with the error bars plotting the standard deviation of 15 plants in three groups of five. The letters above the bars indicate different homogeneous groups with statistically significant differences (Fisher's LSD Test, P < 0.05). Asterisks indicate statistically significant differences from the mock treatment (P < 0.05 one asterisk, P < 0.01 two) using the Student's t test (one tail).

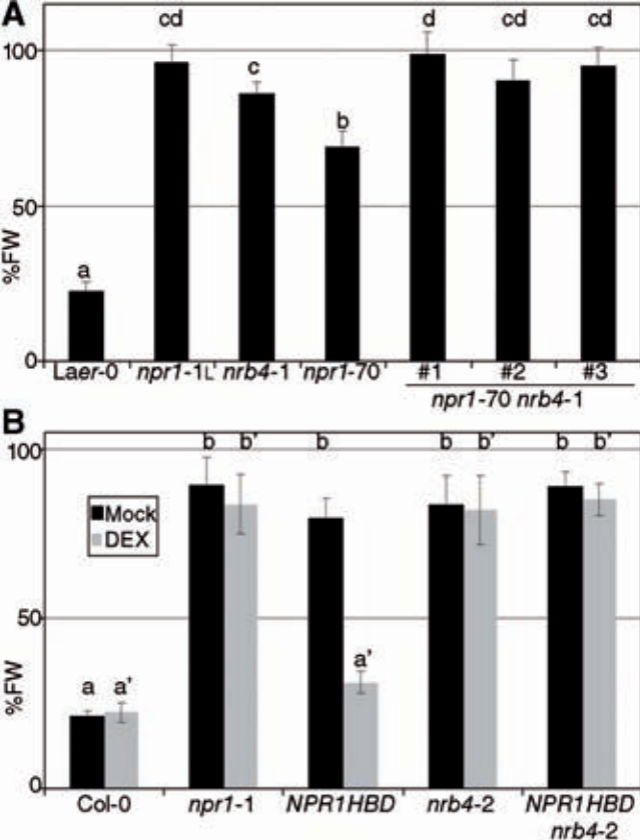


**Figure 3. Epistasis of *NRB4* with *NPR1*.**

**A** Three double mutants *nrb4-1 npr1-70* were tested as in Figure 1A. **B** *35S::NPR1-HBD* (*NPR1HBD*) in an *nrb4-2* background was tested with and without dexamethasone (DEX) for its response to BTH. The experiments were repeated three times with similar results, and the data represent the average, with the error bars plotting the standard deviation of 15 plants in three groups of five. The letters above the bars indicate different homogeneous groups with statistically significant differences (Fisher's LSD Test,  $P < 0.05$ ).

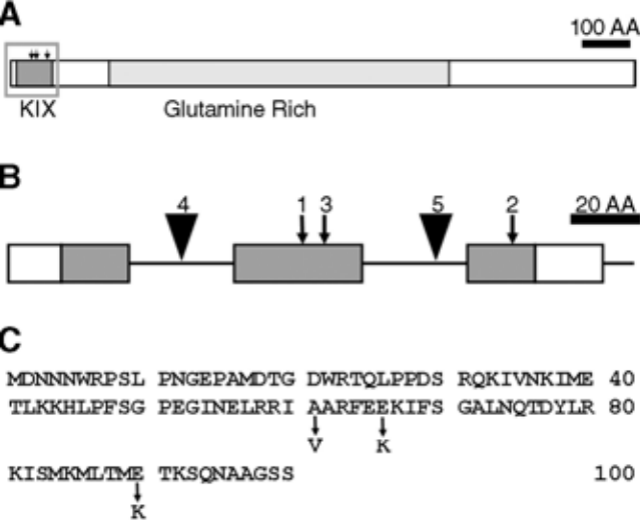


**Figure 4.-Predicted structure of NRB4.** **A** Drawing of the predicted NRB4 protein, showing the conserved KIX domain and the region rich in glutamine. **B** Magnification of the KIX domain, showing the introns (horizontal lines), the point mutations (arrows) and the T-DNAs insertions (triangles) found in *NRB4* (At1g15780). The number above the mutation indicates the number of allele. The region shown corresponds to the grey rectangle in A. **C** Sequence of the first 100 AA of NRB4, indicating the point mutations.



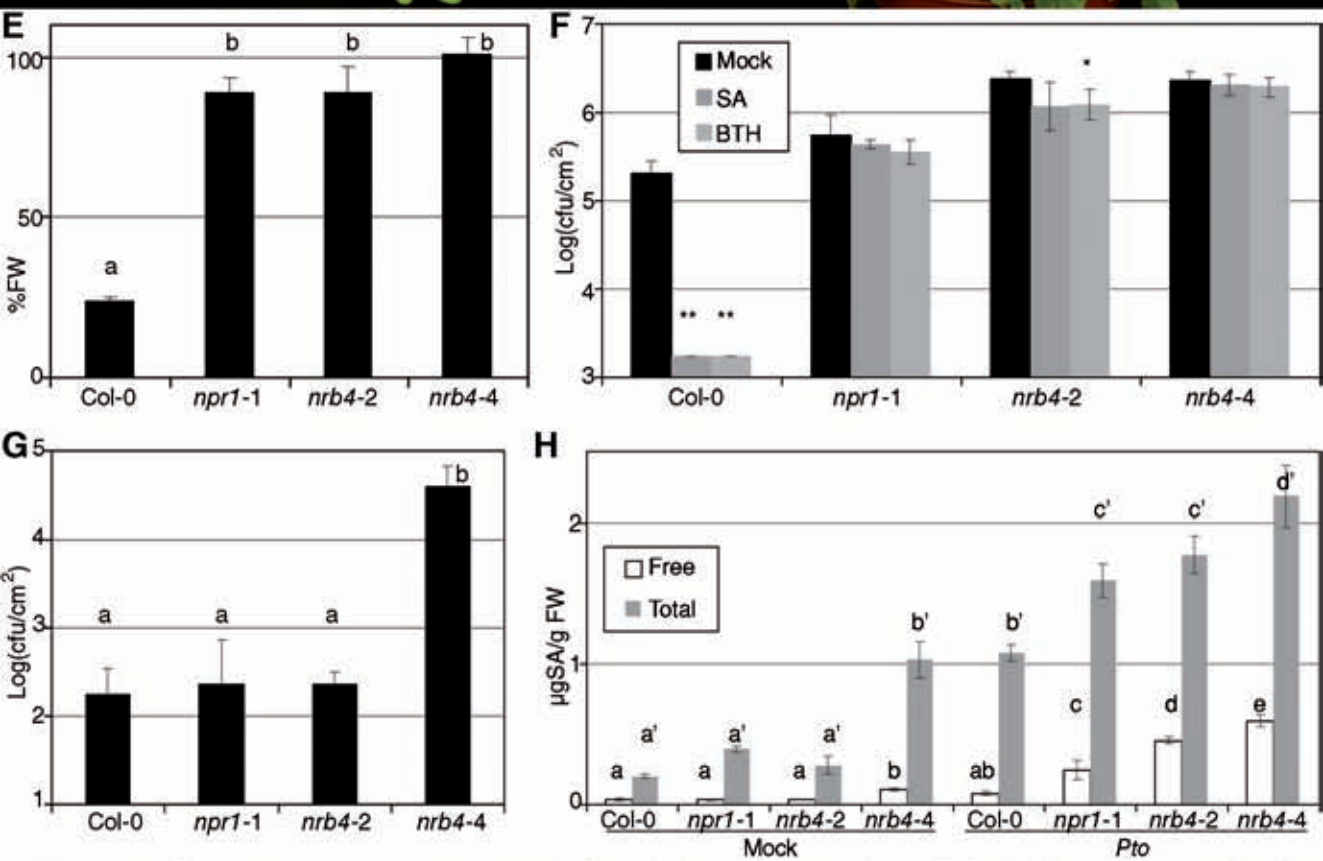
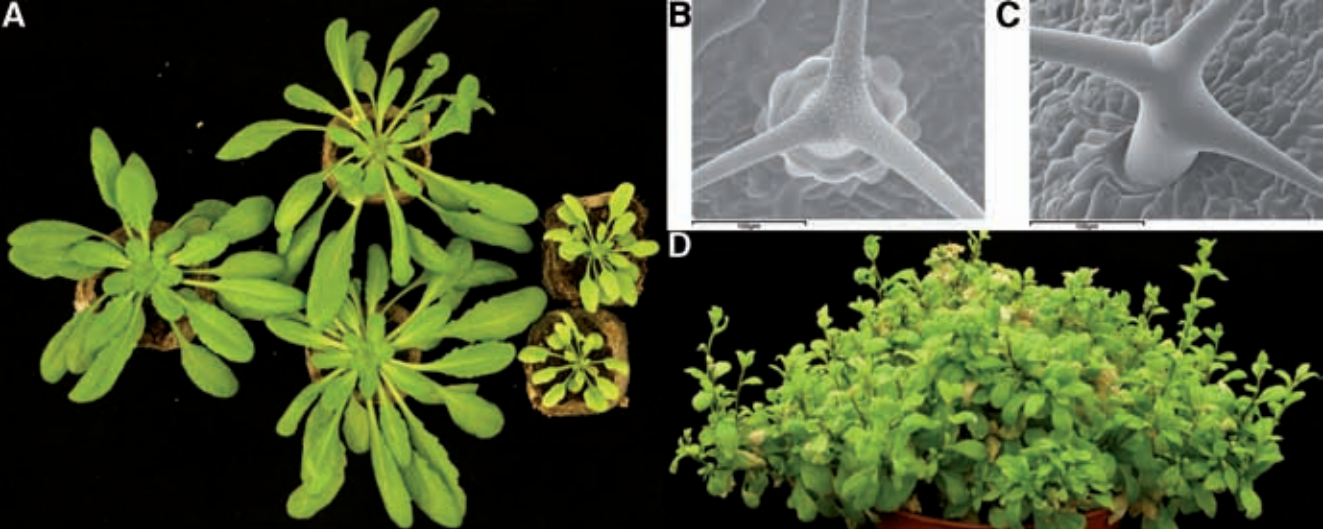


**Figure 5. -*nrb4-4* is a null allele.** **A** From left to right, wild type plant, *NRB4/nrb4-4* plants, and *nrb4-4* homozygous plants. Picture taken after six weeks in short day conditions. **B** Cryo-SEM pictures of wild type trichomes. The leaves sampled were approximately 7 mm and plants were five weeks old. **C** Cryo-SEM of *nrb4-4* trichomes, although plants were seven weeks old in order to sample leaves of roughly the same size. The length of the bar (bottom of the picture) is 100 µm. **D** Picture of *nrb4-4* plants taken after 18 weeks (seven in short day, eleven in long day). **E** Plants were tested as in Figure 1A, but with one more week of growth and two more treatments. **F** Response of *nrb4-4* plants to SA and BTH in growth curves. The inoculations were done as in Figure 2C, with the particularity that *nrb4-4* plants were seven weeks old. **G** *Pseudomonas syringae* pv. *maculicola* CR299 was inoculated and its growth measured as F. **H** The amount of SA (both free and total) was measured three days after a mock or a *Pto* inoculation. The experiments were repeated three times with similar results, and the data represent the average, with the error bars plotting the standard deviation of 15 plants in three groups of five, except in the case of H, where three samples of 100 mg were taken. The letters above the bars indicate different homogeneous groups with statistically significant differences (Fisher's LSD Test,  $P < 0.05$ ). The differences in free SA and total SA (marked with the symbol prime) were evaluated between genotypes. Asterisks indicate statistically significant differences from the mock treatment ( $P < 0.05$  one asterisk,  $P < 0.01$  two) using the Student's t test (one tail).

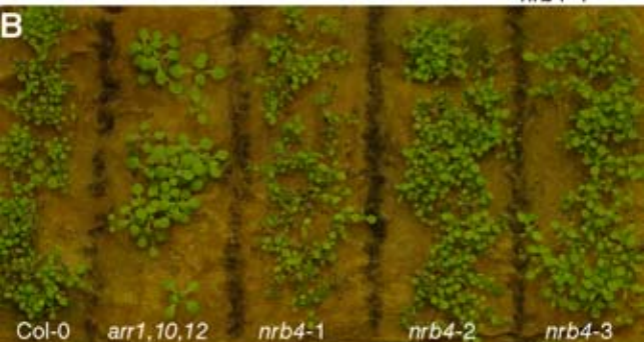
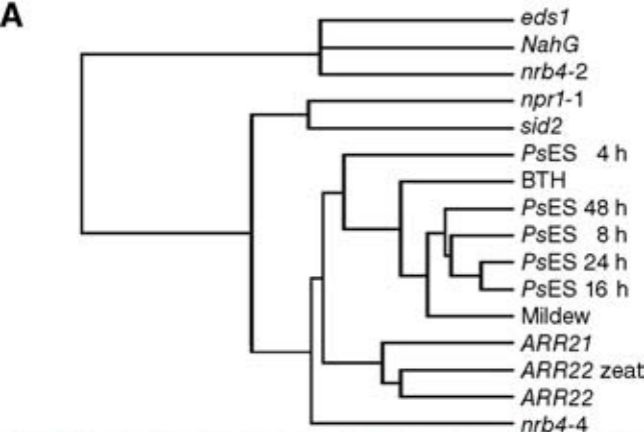


**Figure 6.-Molecular footprint of *nrb4*.**

The transcriptomes of *nrb4-2*, *nrb4-4*, and Col-0 plants were determined, and then compared with different transcriptomic experiments by means of hierarchical clustering with Cluster 3.0 (de Hoon et al., 2004), and visualization as a dendrogram with JavaTreeView (Saldanha, 2004). The references of the experiments used are specified in the Methods section, and the parameters used were the default settings. **B**

Growth response to cytokinins. Seeds of the indicated genotypes were grown in rock wool imbided with 5  $\mu$ M trans-zeatin. This picture was taken after 21 days' growth. *arr1,10,12* stands for the triple mutant *arr1 arr10 arr12*, used as a control for lack of response to cytokinins.

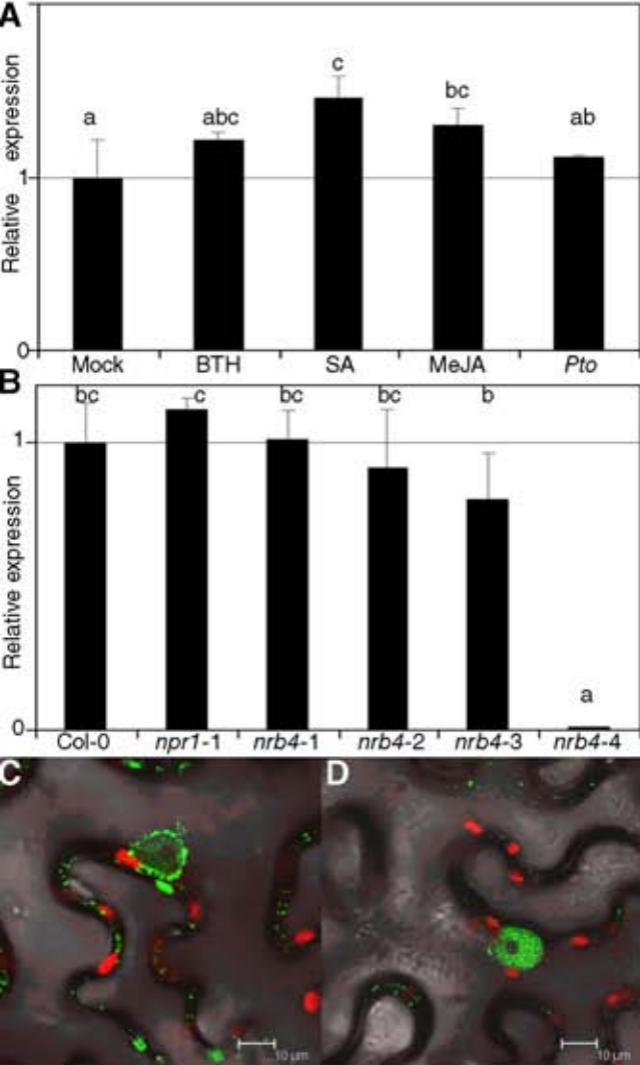


**Figure 7.- Expression of *NRB4* and cellular localization.** **A** *NRB4* expression was measured one day after treatment with mock, 350  $\mu$ M BTH, 500  $\mu$ M SA, and 100  $\mu$ M Methyl jasmonate (MeJA), or three days after a *Pto* inoculation (RNA extracted and RT-qPCR from three independent samples of 100 mg each). The levels of expression are normalized to three reference genes and to the level of Col-0. **B** RNA was extracted from three-week-old plants (five weeks for *nrb4-4*), and transcript levels for *NRB4* were measured by RT-qPCR as in A. **C** *Agrobacterium tumefaciens* with the construct *35S:NRB4-GFP* was infiltrated into leaves of *Nicotiana benthamiana*, and the expression was detected with a confocal microscopy four days later. **D** Similar to C with the construct *35S:GFP-NRB4*. The experiments were repeated three times with similar results, and the data represent the average, with the error bars plotting the standard deviation of 15 plants in three groups of five. The letters above the bars indicate different homogeneous groups with statistically significant differences (Fisher's LSD Test,  $P < 0.05$ ).

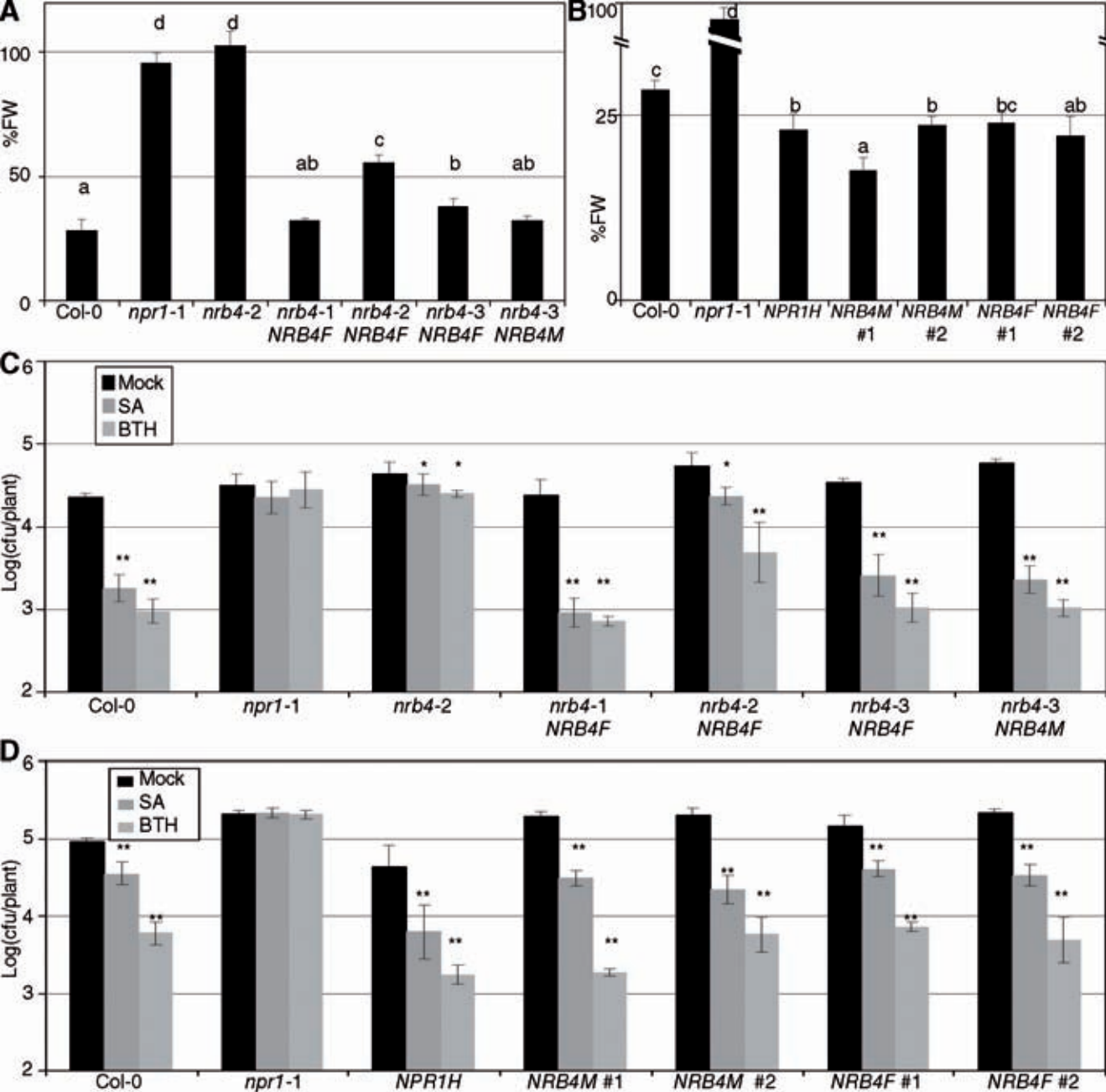
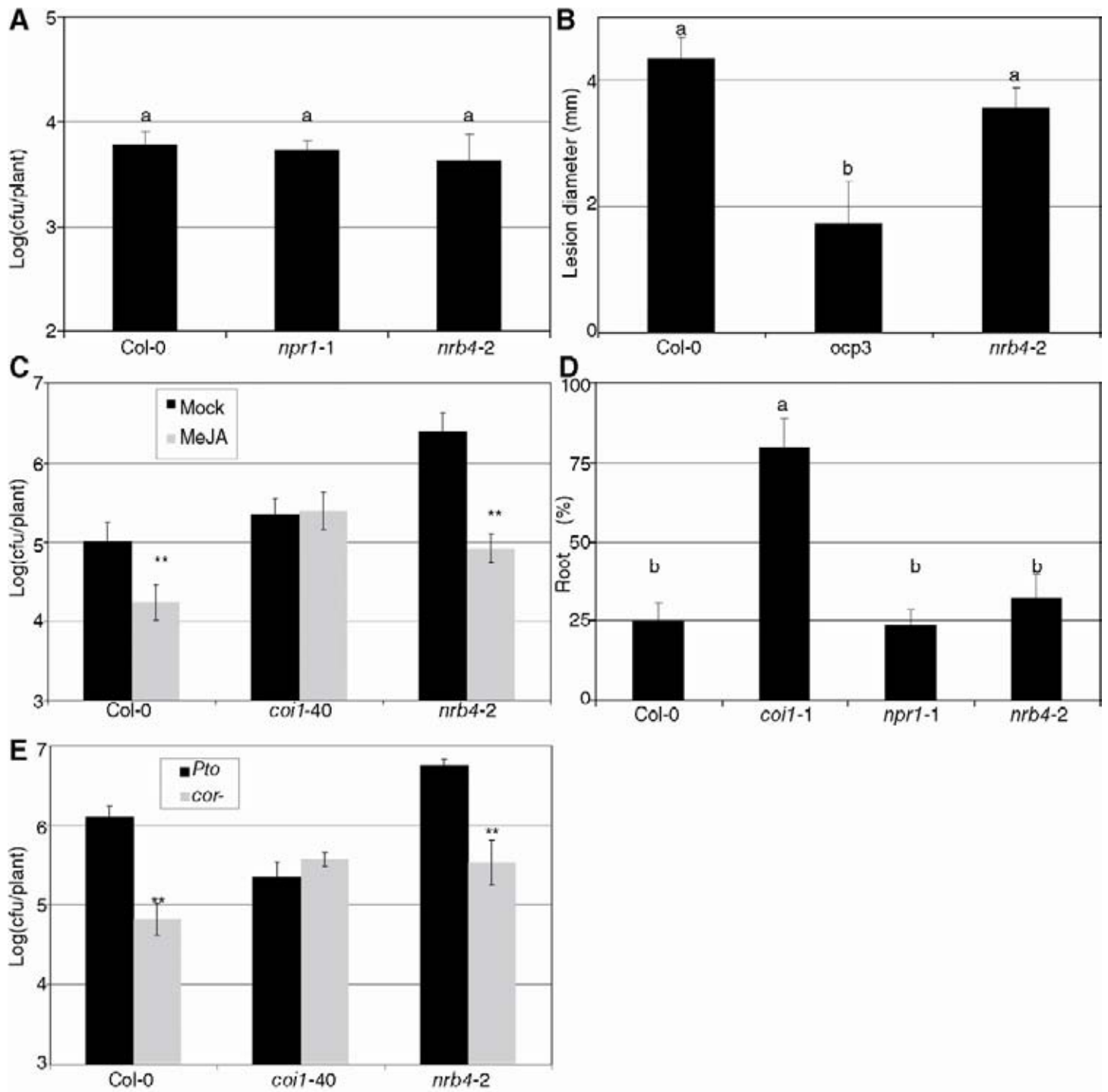
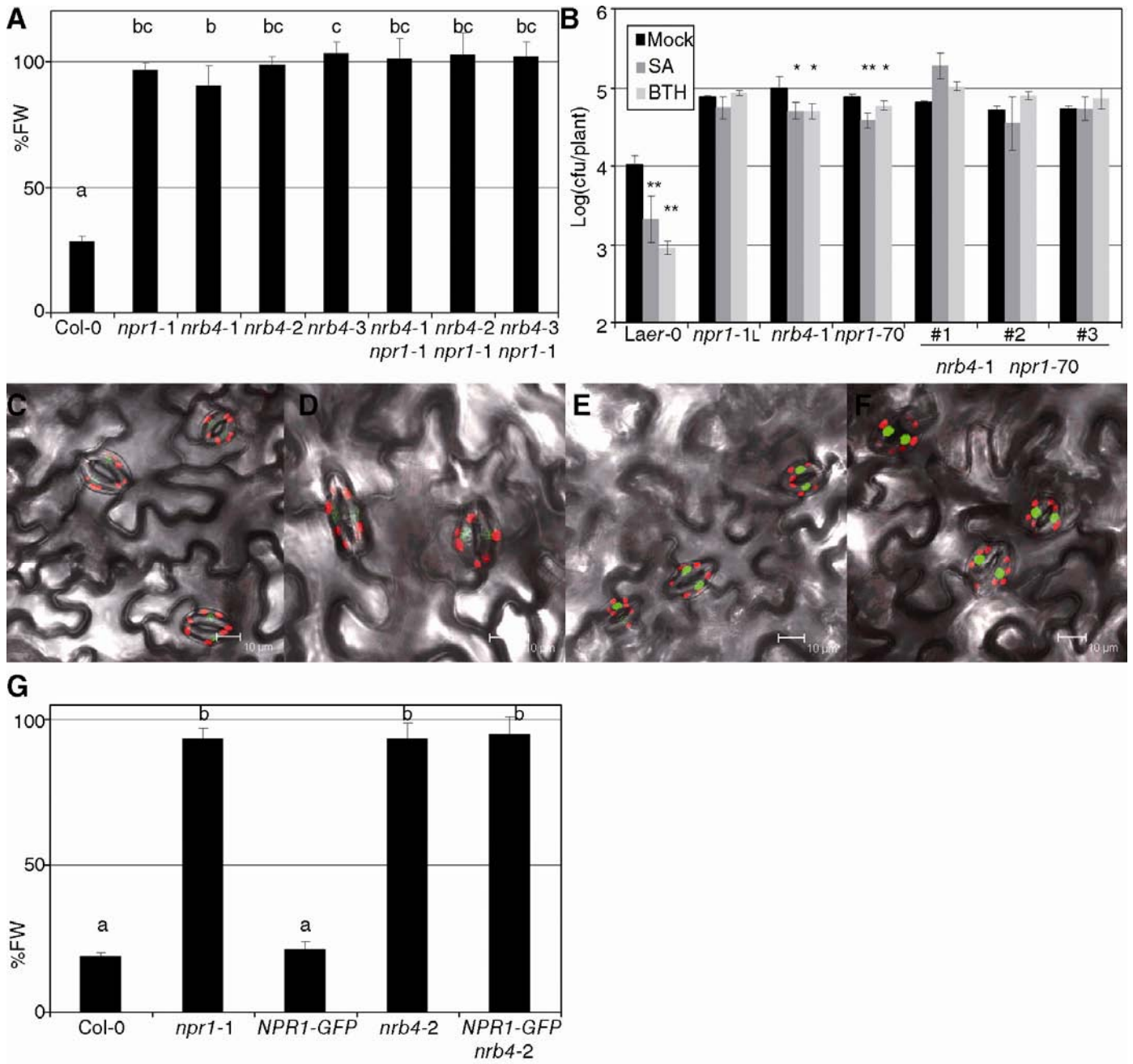


**Figure 8.-Phenotypes of transgenic lines.** **A** Transgenic plants homozygous for the construct *35S::NRB4-GFP (NRB4F)* or for the equivalent construct with only the first 670 AA (*NRB4M*), were obtained in the mutant alleles. The panel shows the response to BTH in fresh weight of the mentioned lines tested as in Figure 1A. **B** The constructs described in A were transformed into Col-0, and their response to BTH in fresh weight recorded. The number indicates an independent line. **C** Response of the transgenic lines described in A to SA and BTH in growth curves, as described in Figure 2A. **D** Response of the transgenic lines described in B to SA and BTH in growth curves, as described in Figure 2A. The experiments were repeated three times with similar results, and the data represent the average, with the error bars plotting the standard deviation of 15 plants in three groups of five. The letters above the bars indicate different homogeneous groups with statistically significant differences (Fisher's LSD Test,  $P < 0.05$ ). Asterisks indicate statistically significant differences from the mock treatment ( $P < 0.05$  one asterisk,  $P < 0.01$  two) using the Student's t test (one tail).



**Supplemental Figure 1. Additional phenotypes of *nrb4* in defense.** **A** Responses to *Pto* (*hrpC*-), a strain that lacks virulence in Arabidopsis (Deng et al., 1998). 18-day-old plants were inoculated at an OD<sub>600</sub> of 0.1. Three days after inoculation, the growth of *Pto* was evaluated as Logarithm of colony forming units (cfu) per plant. **B** Inoculations with *Plectosphaerella cucumerina*. *P. cucumerina* was provided by Brigitte Mauch-Mani (University of Neuchatel, Switzerland), and used as described (Ton and Mauch-Mani, 2004). **C** Response to Methyl Jasmonate (MeJA) induced resistance. MeJA was applied by spray at 100  $\mu$ M in 0.1% DMSO and 0.02% Silwet L-77 one day before *Pto* inoculation. **D** Responses to JA-Ile in the length of roots. Plants were grown in Johnson's media (Johnson et al., 1957) with 1 mM KH<sub>2</sub>PO<sub>4</sub>, with or without 50  $\mu$ M MeJA (Duchefa). The length of the roots was measured with ImageJ software (MIH, Bethesda, MD, USA). **E** Responses to coronatine. *Pto*(*cfa*<sup>-</sup>) a strain that lacks coronatine (Mittal and Davis, 1995) was inoculated, along *Pto*, as indicated in A. The experiments were repeated three times with similar results, and the data represent the average, with the error bars plotting the standard deviation of 15 plants in three groups of five. The letters above the bars indicate different homogeneous groups with statistically significant differences (Fisher's LSD Test, P < 0.05). Asterisks indicate statistically significant differences from the mock treatment (P < 0.05 one asterisk, P < 0.01 two) using the Student's t test (one tail).

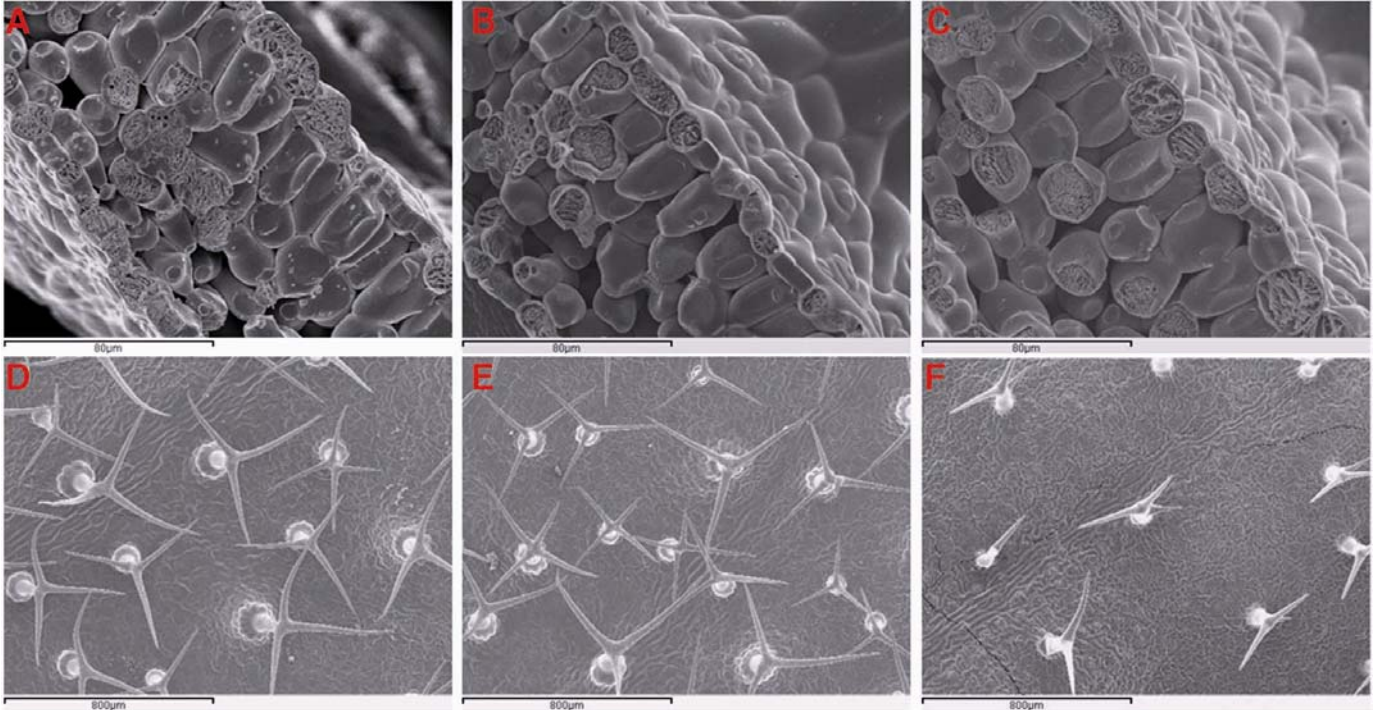


**Supplemental Figure 2. Epistasis of *NRB4* with *NPRI*.** **A** Three double mutants *nrb4 npr1-1* and their controls were treated with either mock or 350  $\mu$ M BTH four times over three weeks, their weights recorded, and the ratio between the BTH and mock treated plants calculated (15 plants in three groups of five). The ratio is expressed as percentage of fresh weight (%FW). **B** Three double mutants *nrb4-1 npr1-70* were tested for its response to SA and BTH upon *Pto* inoculation. **C** Confocal image of Arabidopsis *35S:NPRI-GFP* in an *npr1-1* background in mock conditions. **D** Same transgenic in an *nrb4-2 npr1-1* background in mock conditions. **E**. The same line as in C, one day after 350  $\mu$ M BTH treatment. **F** The same line as in D, one day after 350  $\mu$ M BTH treatment. **G** The lines described above were tested for its response to BTH. The overexpression of *NPRI*, even if it is detected in the nucleus (F), did not complement the mutation *nrb4-2*. The experiments were repeated three times with similar results, and the data represent the average, with the error bars plotting the standard deviation of 15 plants in three groups of five. The letters above the bars indicate different homogeneous groups with statistically significant differences (Fisher's LSD Test,  $P < 0.05$ ). Asterisks indicate statistically significant differences from the mock treatment ( $P < 0.05$  one asterisk,  $P < 0.01$  two) using the Student's t test (one tail).

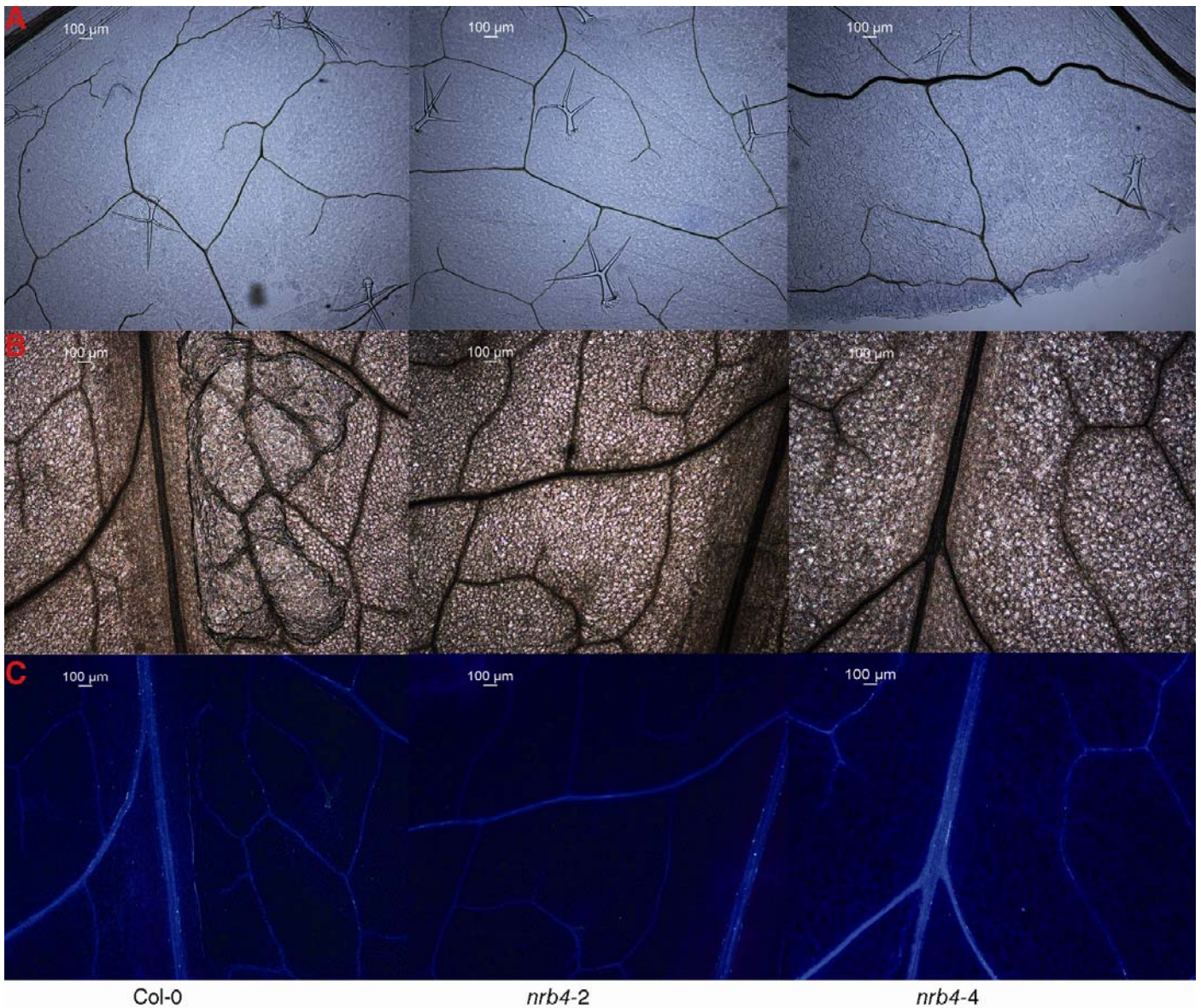




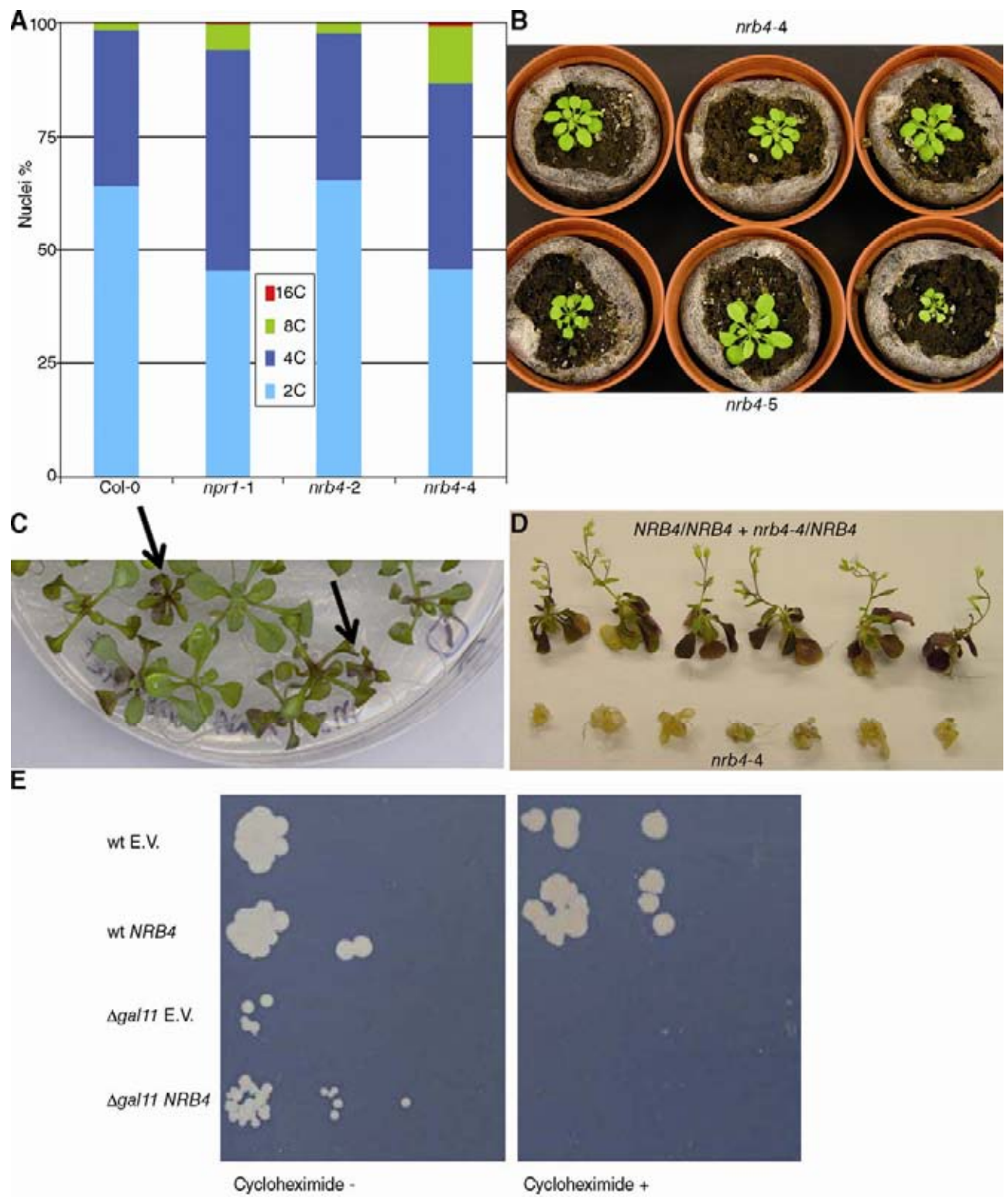
**Supplemental Figure 3. Additional pictures of *nrb4-4*.** **A** Wild type plant, growing seven weeks in short day and six weeks in long day with no treatment or inoculation. **B** *nrb4-4* plant of the same age, growing in the same conditions. **C** *nrb4-4* plant growing seven weeks in short day and eleven weeks in long day, as in A. **D** Detail of the plant in C, note the absence of flowers. **E** *nrb4-4* plant with flowers. **F** Detail of the plant in E. As a reference, the pots have a diameter of 6 cm.



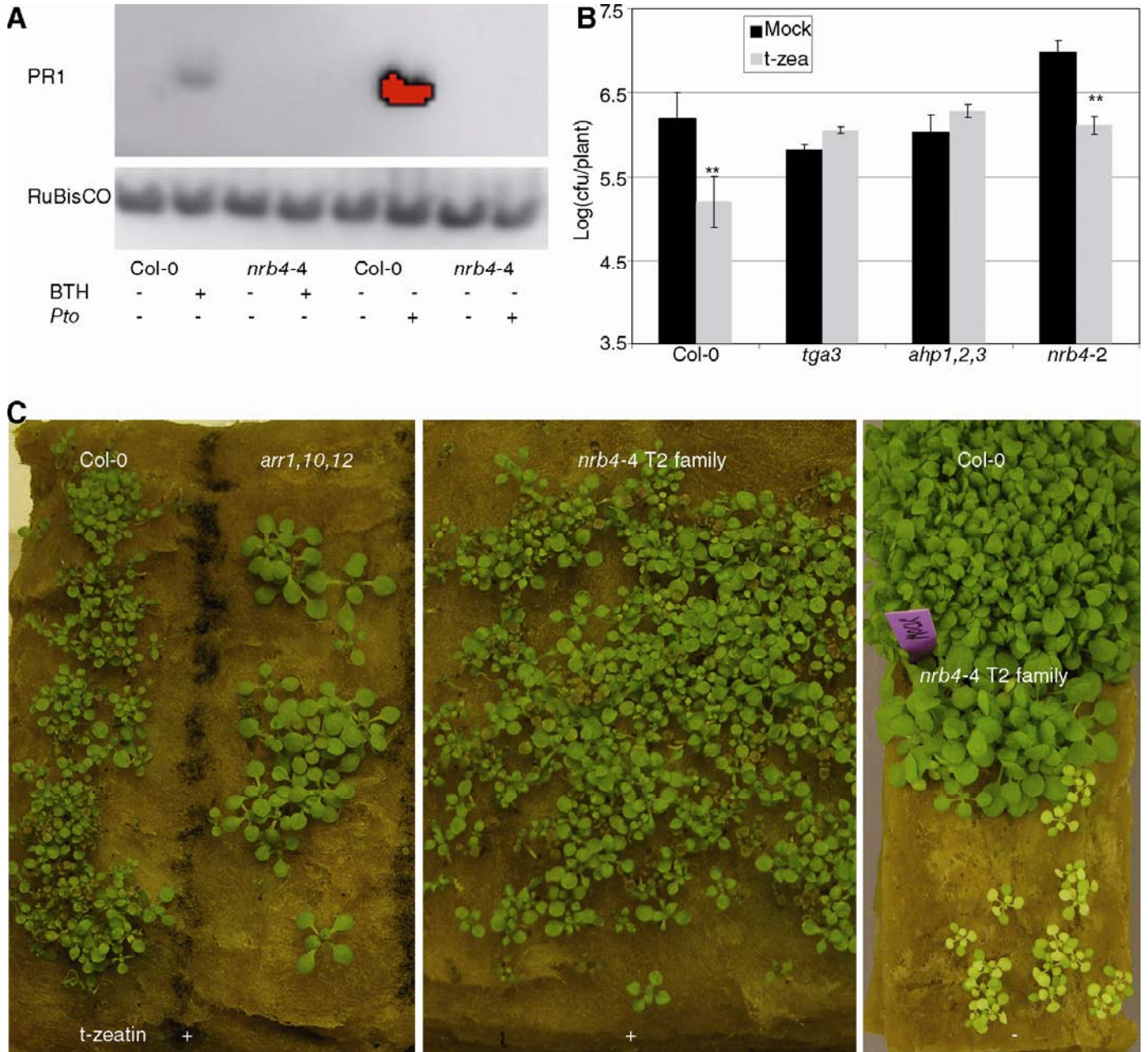
**Supplemental Figure 4. Additional pictures of Cryo-SEM.** **A** Section of Col-0. **B** Section of *nrb4-2*. **C** Section of *nrb4-4*. **D** Surface of a leaf from Col-0. **E** Idem from *nrb4-2*. **F** Idem from *nrb4-4*. The length of the bar in A, B, and C is 80  $\mu\text{m}$ , and in D, E, and F is 800  $\mu\text{m}$ . The leaves were five weeks old for Col-0 and *nrb4-2* and seven weeks for *nrb4-4*.



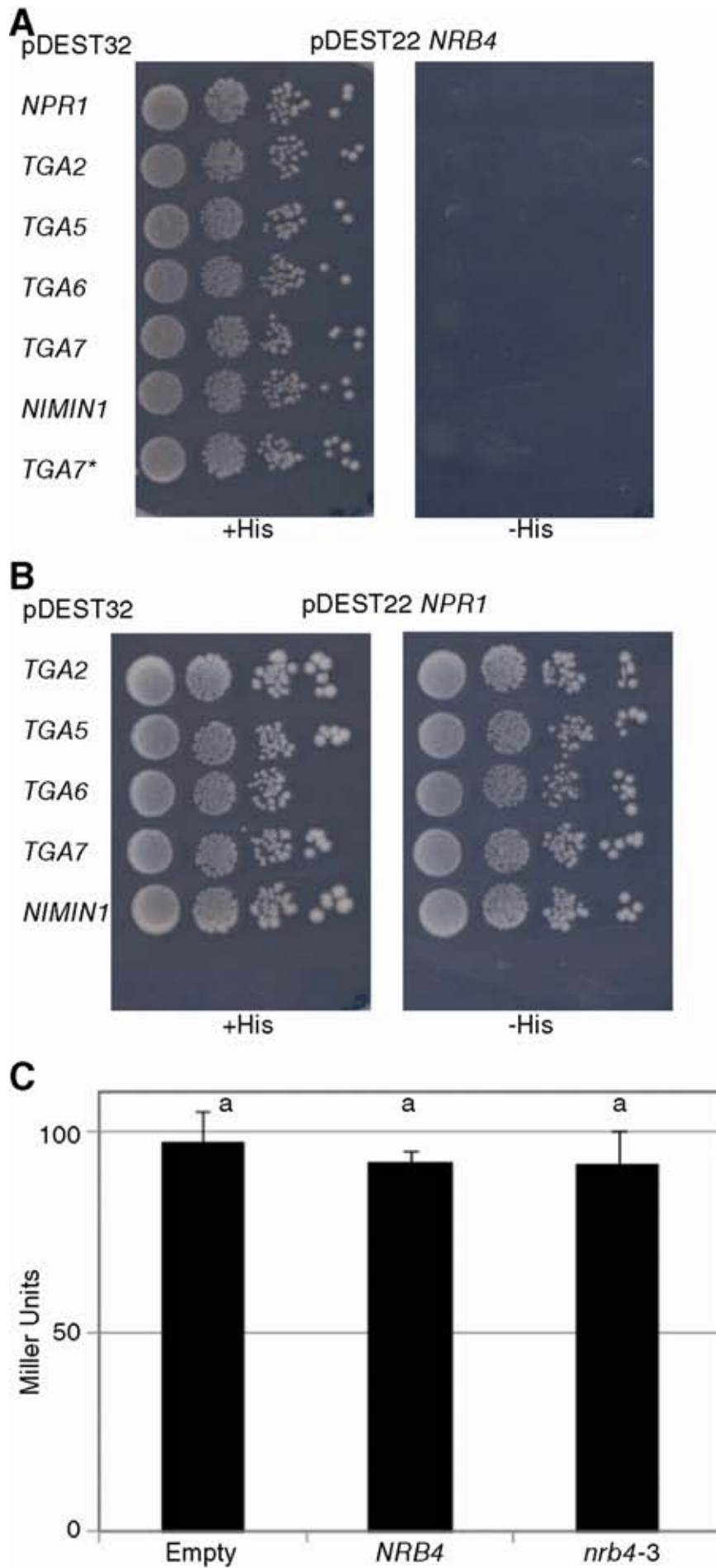
**Supplemental Figure 5. Stainings of *nrb4*.** **A** Trypan blue stains, unveiling cell death and membrane damage in Col-0, *nrb4-2*, and *nrb4-4*. **B** Aniline blue stains under visible light. **C** The same Aniline blue stains under ultraviolet light, which detects callose depositions. Trypan Blue and Aniline Blue staining were performed as described (Tornero et al., 2002; Conrath et al., 1989, respectively). No differences among genotypes were observed with these stains.



**Supplemental Figure 6. Characterization of *nrb4* null alleles.** **A** DNA content. Nuclei from the indicated genotypes were extracted, stained with DAPI, and the relative amount of DNA measured with a CyFlow Ploidy Analyzer (Partec GmbH, Münster Germany) following the manufacturer's instructions. At least 5000 nuclei were counted in each measurement, and the same result was obtained in three independent experiments. **B** Phenotypes of *nrb4-5* in comparison to *nrb4-4*. **C** Phenotypes of a T2 segregating family of *nb4-4/NRB4* in MS plates. The arrows point to *nrb4-4* homozygous plants (confirmed by PCR) Picture taken at two weeks of growing. **D** Plants selected in C were transferred to MS plates with 500  $\mu$ M SA, and the picture was taken two weeks after the transfer. **E** Lack of complementation in yeast. Empty vector (E.V.) pAG423 (Alberti et al., 2007) and *NRB4* cloned in pAG423 were introduced in wild type (wt) and  *$\Delta gal11$* . The different strains were grown in liquid and then plated in SD His- plates with or without cycloheximide (0.2 $\mu$ g/ml). The wt and  *$\Delta gal11$*  strains were obtained from EUROSCARF (Ref. Y00000 and Y01742, respectively).

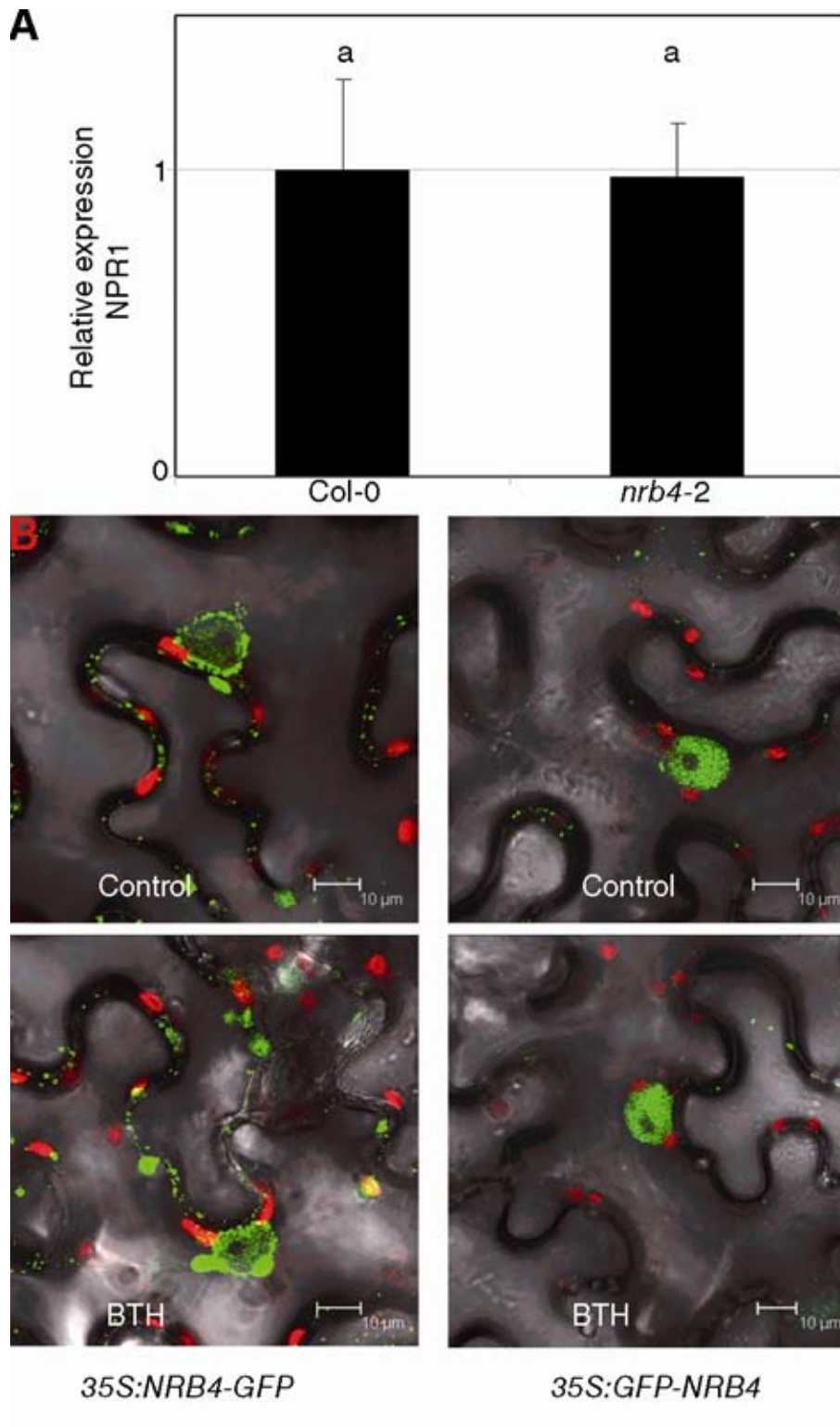


**Supplemental Figure 7. Phenotypes from the transcriptomic analysis.** **A** PR1 immunoblot of Col-0 and *nrb4-4* three days after mock or a *Pto* inoculation and one day after mock or 350  $\mu$ M BTH. The same blot was probed with anti-RuBisCO for loading and transfer control. The red color indicates saturation of the signal. **B** Resistance induced by cytokinins. Trans-zeatin (t-zea) 1  $\mu$ M or a mock solution was applied one day previous to the inoculation with *Pto*. *tga3* (Choi et al., 2010) and *ahp1 ahp2 ahp3* (Hutchison et al., 2006, abbreviated as *ahp1,2,3*) were included as controls. **C** *nrb4-4* did not have a specific phenotype with cytokinins. The controls Col-0 and *arr1 arr10 arr12* growing in 5  $\mu$ M trans-zeatin (left) are the same as in Figure 6B. A T2 family, segregating for *nrb4-4* (middle) did not produce plants with a different perception to cytokinins. Col-0 and the same T2 family of *nrb4-4* plants growing in control conditions (right). In the case of *nrb4-4*, the space shown at the bottom of the picture was cleared of wild type plants, to check if the *nrb4-4* homozygous plants can grow in this media. The experiments were repeated three times with similar results, and the data represent the average, with the error bars plotting the standard deviation of 15 plants in three groups of five. Asterisks indicate statistically significant differences from the mock treatment ( $P < 0.05$  one asterisk,  $P < 0.01$  two) using the Student's t test (one tail).

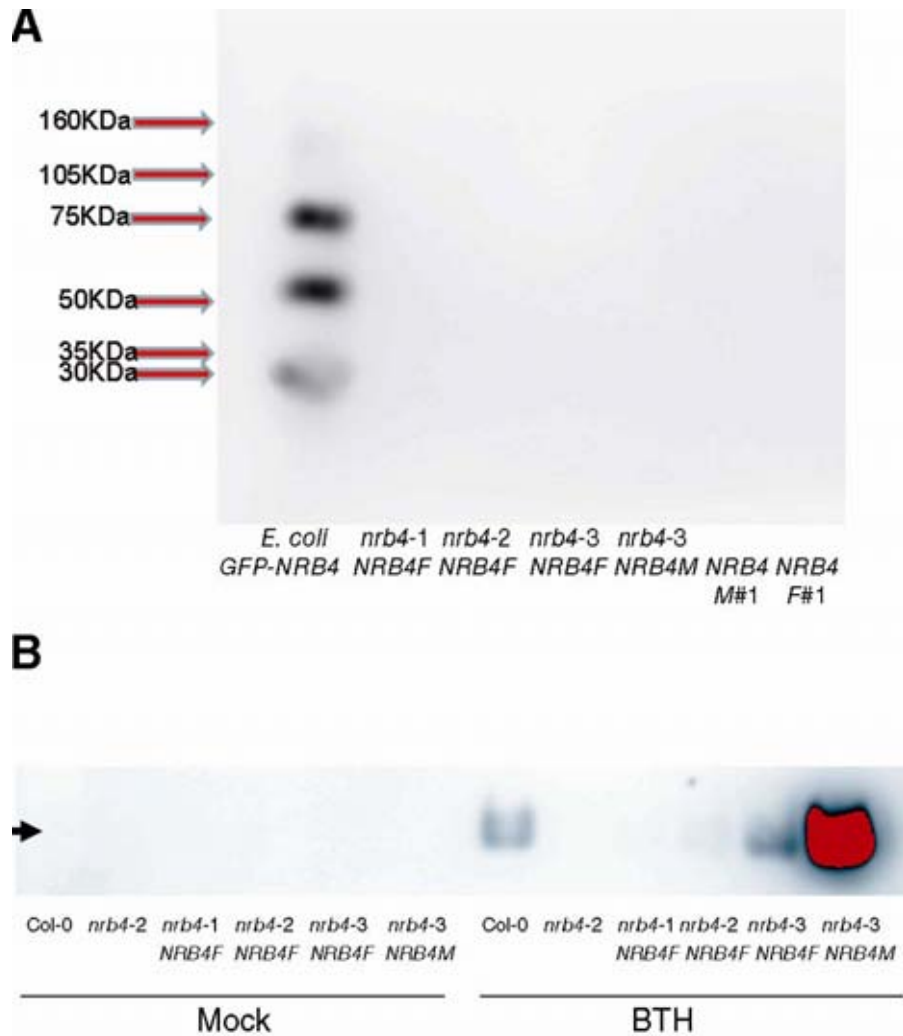




**Supplemental Figure 8. Yeast n-hybrid interactions. A** Interactions between *NRB4* and proteins that have a role in SA perception. The yeasts that had *NRB4* and any of these proteins were able to grow in His<sup>+</sup> plates, but not in His<sup>-</sup> plates. Therefore, there was not detectable interaction. TGA7\* stands for an additional control with an empty pDEST22, since TGA7 was able to autoactivate the system with no 3AT (the His<sup>-</sup> plates contained 5 mM 3AT). **B** As a control, interactions between *NPR1* and the rest of proteins that have a role in SA perception. **C** *NRB4* did not alter the interaction between *NPR1* and TGA2. *NRB4* was cloned in a third vector, and introduced in the first yeast of B. There was no statistical difference between introducing *NRB4*, respect *nrb4-3*, or to the empty vector. All the plates were Lys<sup>-</sup>, Trp<sup>-</sup>, Leu<sup>-</sup>, and 100 μM SA. Similar experiments with no SA produced the same results. Similarly, bimolecular fluorescence complementation between *NRB4* and *NPR1* or *TGA2* did not produce a positive result in *Nicotiana benthamiana*. The pictures were taken 3-5 days after growing at 28°C. *NRB4* was cloned in three different versions for detection of interactions in the yeast two hybrid system: a short version, from 1 to 112 aa, included the KIX domain; an intermediate version, from 1 to 670 aa, spanned half of the coding sequence; and a full version. The full version when fused to the GAL4 BD was autoactivated, even with mutated versions of *NRB4* that recreated the EMS mutations herein described. The three versions of the wild type protein fused with the GAL4 AD were tested for interaction in yeast with genes described in SA response. The experiment shown in this figure corresponds to the full version of *NRB4*. The experiments were repeated three times with similar results, and the data represent the average, with the error bars plotting the standard deviation of three colonies. The letters above the bars indicate different homogeneous groups with statistically significant differences (Fisher's LSD Test, P < 0.05).



**Supplemental Figure 9. Expression of *NPR1* and *NBR4*.** **A** *NPR1* was detectable in *nrb4-2* at normal levels. The levels of expression of *NPR1*, measured by RT-qPCR, are normalized to three reference genes and to the level of Col-0. The RNA was extracted from three-week-old plants, from three independent samples of 100 mg each. **B** The nuclear localization did not change with the application of 350  $\mu$ M BTH. *35S:NRB4-GFP* (left) and *35S:GFP-NRB4* (right) were infiltrated in *N. benthamiana*. Then, a mock or a 350  $\mu$ M BTH was applied one day before these pictures were taken. The controls correspond to the Figure 7C and D, respectively. The experiments were repeated three times with similar results, and the data represent the average, with the error bars plotting the standard deviation of three independent RT-qPCRs. The letters above the bars indicate different homogeneous groups with statistically significant differences (Fisher's LSD Test,  $P < 0.05$ ).



**Supplemental Figure 10. Characterization of *NRB4* complementation.** **A** In the stable transgenic lines, GFP was not detectable by immunoblot. A immunoblot with antibody raised against GFP (Roche, Madrid, Spain) was performed in different extracts. The first line of the immunoblot is a *GFP-NRB4* fusion expressed in *E. coli*, which shows partial processing. The rest of lines correspond to plant extracts from the same lines described in Figure 8. The arrows point the position of the weight markers. **B** The complemented *nrb4* alleles express PR1 upon BTH application. The lines described in Figure 8 were treated with BTH and PR1 detected as in Figure 2B. There is a low expression of PR-1 in the lines that contain *35S:NRB4-GFP* (*NRB4F*) in *nrb4-1* and *nrb4-2*, a expression similar to Col-0 in the *35S:NRB4* in *nrb4-3*, and a very strong expression in the lines that overexpress the first 670 AA of NRB4 plus GFP (*NRB4M*) in *nrb4-3*. The red color indicates saturation of signal.

**Supplemental Table 1. Evaluation of segregations.**

<b>Population</b>	<b>Observed</b>			<b>Expected</b>		$\chi^2$	<b>d.f.</b>	<b>p</b>
	<b>wt</b>	<b>mut</b>	<b>Total</b>	<b>(3/4)</b>	<b>(1/4)</b>			
F2 Col-0 x <i>nrb4-1</i>	297	108	405	303.75	101.25	0.600	1	0.44
F2 Col-0 x <i>nrb4-2</i>	248	87	335	251.25	83.75	0.168	1	0.68
F2 Col-0 x <i>nrb4-3</i>	345	104	449	336.75	112.25	0.808	1	0.37
				<b>(1/2)</b>	<b>(1/2)</b>			
F1 <i>nrb4-4</i> het x <i>nrb4-1</i>	25	23	48	24	24	0.083	1	0.77
F1 <i>nrb4-4</i> het x <i>nrb4-2</i>	26	30	56	28	28	0.286	1	0.59
F1 <i>nrb4-4</i> het x <i>nrb4-3</i>	28	30	58	29	29	0.069	1	0.79
				<b>(3/4)</b>	<b>(1/4)</b>			
F1 <i>nrb4-5</i> het x <i>nrb4-4</i> het	40	11	51	38.25	12.75	0.320	1	0.57

Segregations observed in the indicated populations. The phenotypic classes were evaluated with the  $\chi^2$  statistics. The p value gives the probability that any deviation from expected results is due to chance only. Since in all the cases the p value is bigger than the standard value of 0.05, the segregations fit the proposed model.

**Supplemental Table 2. Evaluation of phenotypes in T-DNA insertion lines.**

<b>AGI</b>	<b>NASC</b>	<b>T-DNA</b>	<b>Status</b>	<b>Position</b>	<b>Phenotype (% wt)</b>
	Col-0				100
	<i>npr1-1</i>		Homoz		0
AT1G07950	N656591	SALK_065283C	Homoz	Exon	100
AT1G11760	N665553	SALK_023845C	Homoz	5'	100
AT1G11760	N678300	SALK_028490C	Homoz	5'	100
AT1G15780	N835429	SAIL_792_F02	Heteroz	Intron, <i>nrb4-4</i>	75
AT1G15780		GABI_955_E02	Heteroz	Intron, <i>nrb4-5</i>	75
AT1G16430	N870082	SAIL_9_E04	Heteroz	Exon	100
AT1G23230	N659417	SALK_060062C	Homoz	Exon	100
AT1G23230	N671536	SALK_074015C	Homoz	Exon	100
AT1G25540	N679089	SALK_129555C	Homoz	Exon	100
AT1G25540	N677751	SALK_059316C	Homoz	Exon	100
AT1G26665		No info			
AT1G29940	N876306	SAIL_726_H01	Heteroz	Exon	100
AT1G31360	N661000	SALK_087178C	Homoz	Exon	100
AT1G44910	N521070	SALK_021070	Heteroz	Exon	100
AT1G54250	N679260	SALK_151800C	Homoz	Exon	100
AT1G55080	N529118	SALK_029118	Heteroz	Exon	100
AT1G55325	N861503	SAIL_1169_H11	Homoz	Exon	100
AT1G60850	N655705	SALK_088247	Homoz	Exon	100
AT2G03070	N682656	SALK_092406C	Homoz	Exon	100
AT2G22370	N677657	SALK_027178C	Homoz	Intron	100
AT2G28230		No info			
AT2G29540	N507414	SALK_007414	Heteroz	Exon	100
AT2G38250	N667374	SALK_133090C	Homoz	5'	100
AT2G48110	N671698	SALK_092499C	Homoz	5'	100
AT2G48110	N667838	SALK_015532C	Homoz	Exon	100
AT3G01435		No info			
AT3G04740	N521711	SALK_021711	Heteroz	Exon	100
AT3G09180	N512449	SALK_012449	Heteroz	Exon	100
AT3G10690	N506294	SALK_006294	Heteroz	3'	100
AT3G21350	N662531	SALK_055723C	Homoz	5'	100
AT3G21350	N656864	SALK_110696C	Homoz	5'	100
AT3G23590	N667150	SALK_119561C	Homoz	Exon	100
AT3G23590	N661810	SALK_022477C	Homoz	Exon	100
AT3G25940	N562311	SALK_062311	Heteroz	3'	100
AT3G52860	N685672	SALK_037570C	Homoz	5'	100
AT3G57660	N673273	SALK_116823C	Homoz	3'	100
AT3G57660	N673356	SALK_122465C	Homoz	3'	100
AT3G59600		No info			

AT4G00450	N678935	SALK_108241C	Homoz	Exon	100
AT4G04780		No info			
AT4G04920	N548091	SALK_048091	Heteroz	Intron	100
AT4G09070	N553156	SALK_053156	Heteroz	3'	100
AT4G25210	N599954	SALK_099954	Heteroz	Exon	100
AT4G25210	N607213	SALK_107213	Heteroz	5'	100
AT4G25630	N682661	SALK_093373C	Homoz	Exon	100
AT5G02850	N622082	SALK_122082	Heteroz	Exon	100
AT5G02850	N683125	SALK_007367C	Homoz	5'	100
AT5G03220	N678464	SALK_049958C	Homoz	5'	100
AT5G03500	N676132	SALK_088220C	Homoz	Intron	100
AT5G12230	N657910	SALK_037435C	Homoz	5'	100
AT5G12230	N658182	SALK_034955C	Homoz	Intron	100
AT5G19480		No info			
AT5G19910	N682219	SALK_035522C	Homoz	Exon	100
AT5G20170	N663678	SALK_111977C	Homoz	Exon	100
AT5G28540	N675173	SALK_054493C	Homoz	3'	100
AT5G28540	N675862	SALK_079156C	Homoz	5'	100
AT5G41010	N549327	SALK_049327	Heteroz	Intron	100
AT5G41910	N663226	SALK_087920C	Homoz	5'	100
AT5G41910	N678994	SALK_115673C	Homoz	5'	100
AT5G42020	N659850	SALK_047956C	Homoz	Exon	100
AT5G42060	N669407	SALK_014079C	Homoz	5'	100
AT5G63480	N654793	SALK_095631C	Homoz	Intron	100
AT5G64680	N685462	SALK_023879	Homoz	5'	100
AT5G67240	N542641	SALK_042641	Heteroz	Exon	100

Phenotypes observed in the indicated populations, either homozygous or heterozygous T-DNA insertions in Arabidopsis genes with homology with Mediator genes. The phenotypic classes were evaluated visually, as described by Canet et al., 2010.

**Supplemental Table 3. Lack of homologs in Arabidopsis for several nuclear receptors.**

<b>Name</b>	<b>Organism</b>	<b>AA</b>	<b>Max. E value</b>	<b>Identities</b>	<b>Positives</b>
Pdr1p	Yeast	1068	7.7	37/143	58/143
PDR3p	Yeast	976	2.3	27/99	47/99
Oaf1p	Yeast	1047	0.38	24/90	46/90
PPAR $\alpha$	H. sapiens	468	2.3	13/42	24/42
NHR-49	C. elegans	501	0.41	18/62	29/62

The mentioned proteins were used to search in the Arabidopsis genome with BLASTP (TAIR10, [www.arabidopsis.org](http://www.arabidopsis.org)), with the default settings. The column “AA” indicates the number of aa of the original protein. The “Max. E value” indicates the maximal E value obtained with BLASTP, while the “Identities” and “Positives” columns indicate the ratio of aa either identical or similar in the best stretch of homology.



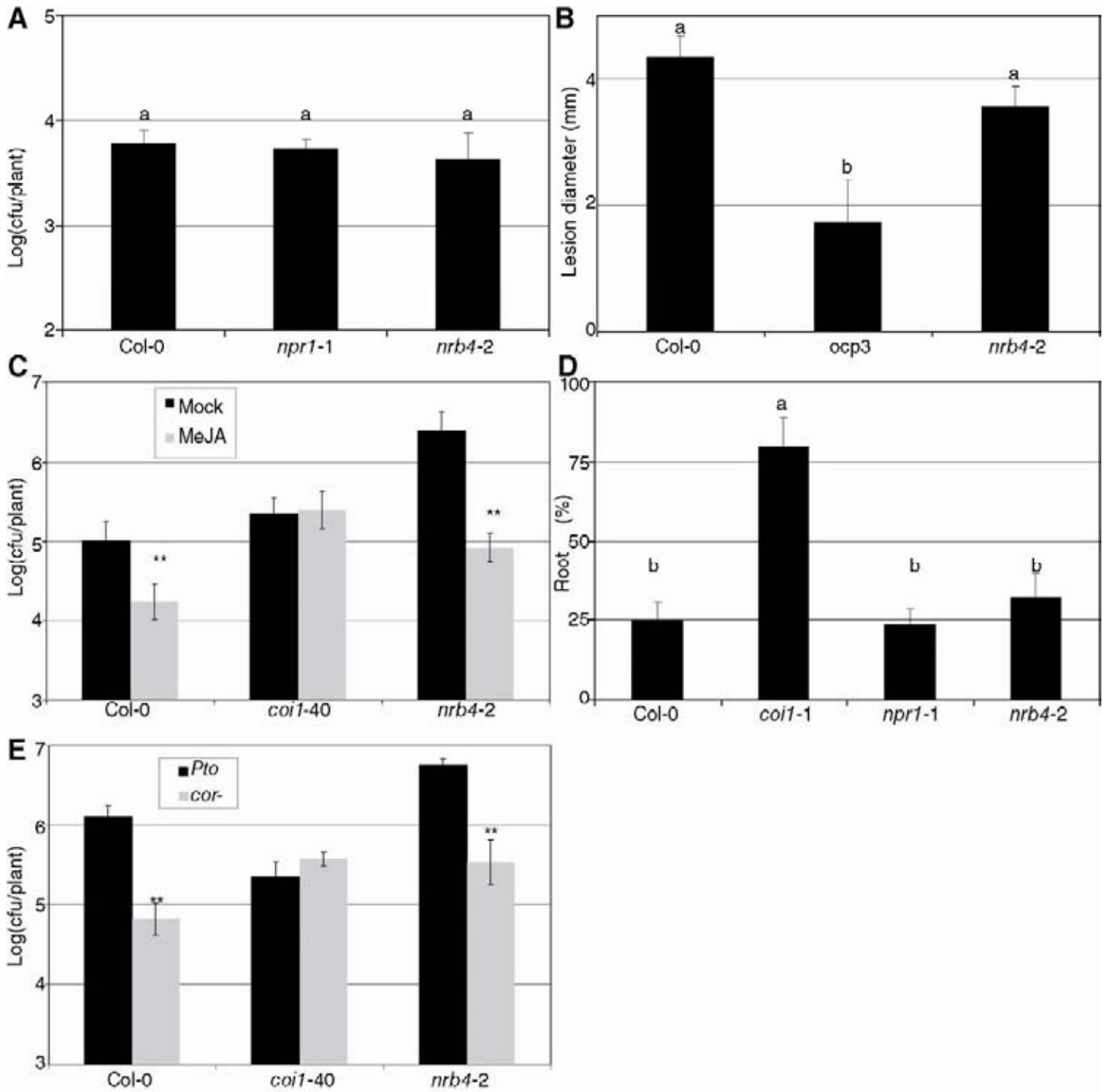
**Supplemental Table 4. Primers used**

<b>Name</b>	<b>Sequence</b>	<b>Objective</b>
5249817-NlaIII-F	TGAGCAGCAAGAAAGATGATG	nrb4 mapping
5249817-NlaIII-R	CTTAGCAGAGGTACGAGGATCA	nrb4 mapping
5346165-DdeI-F	CACCAAACACCACACTTCTCA	nrb4 mapping
5346165-DdeI-R	CATATCTTCAAATCTTTGAGTTGG	nrb4 mapping
5377218-NlaIII-F	CTGGATTTTGGTTCGAGTTAGC	nrb4 mapping
5377218-NlaIII-R	GTGGCAATAGAGGCACAAGT	nrb4 mapping
5393430-CauI-F	GAAGAGTGGTTGCAAGCGTA	nrb4 mapping
5393430-CauI-R	TTTTTGCAGATCCACGTTT	nrb4 mapping
5406030-NlaIII-F	AGTTGGTTCGGAGCTTTTCTCT	nrb4 mapping
5406030-NlaIII-R	GATTCTCCACACCACCCACT	nrb4 mapping
5425793-SecI-F	AGAACGAGCTCGAACACGAA	nrb4 mapping
5425793-SecI-R	CTGAAACATTGAATCCCATTTG	nrb4 mapping
5440252-MseI-F	TGCTTTCATAATCGTTGTGTT	nrb4 mapping
5440252-MseI-R	CACACCAAACAAGCTTCTGTC	nrb4 mapping
5455705-HinfI-F	GAATCTTGATGCTTGCTTGG	nrb4 mapping
5455705-HinfI-R	CCATGTCCGGGAAACTTATC	nrb4 mapping
5494532-RsaI-F	GTTGATCGGAAAGGAAAAGTAAAA	nrb4 mapping
5494532-RsaI-R	AAAAACGGATAACCAAACATGG	nrb4 mapping
F10B6.1-F	ATTATATTGTTCAACATCAACTGCACAT	nrb4 mapping
F10B6.1-R	TTTATCTCTTAAACAAGTTCGTAAACCAAC	nrb4 mapping
T16N11.1-F	AATAGATTAGAAATGAACAGGAGAATTGACT	nrb4 mapping
T16N11.1-R	TGGCATTTTAAATAACATCCTCACC	nrb4 mapping
15780.1	TAACAAAAAATCCCAATCACGTGTG	NRB4 sequencing
15780.2	AACAATTGGAGGCCTTCTCTTCC	NRB4 sequencing
15780.3	AAATATTGCACGCCAACAAGCA	NRB4 sequencing
15780.4	AAGGCGTTCAATAGGCAGCTCA	NRB4 sequencing
15780.5	TATGCACAGGCCGAGGAAGC	NRB4 sequencing
15780.6	GCATCTGCGGATTTGTTTGG	NRB4 sequencing
15780.7	CAAGCCTCTGGTATCCATCAGC	NRB4 sequencing
15780.8	TCTGTTGGATGCCTGAGCTATTTG	NRB4 sequencing
15780.9	AATCTATGGATGTGCCATTATTAGCG	NRB4 sequencing
15780.10	TGCGCAGAATGGAAACACTAAA	NRB4 sequencing
15780.11	TTCCGGTGGGATTGGCTATT	NRB4 sequencing
15780.12	GAATGAAATCTACCAGAGAGTTGCA	NRB4 sequencing
15780.13	TGGTTTGGGACAGCAACGG	NRB4 sequencing
NRB4FP2-attb1	GGGGACAAGTTTGTACAAAAAAGCAGGCTTCGAAG GAGATAGAACCATGGATAATAACAATTGGAGGCCT	NRB4 Cloning in pDONR221, C-terminal
NRB4RP1-attb2	GGGGACCACTTTGTACAAGAAAGCTGGGTCTATGG ATGTGCCATTATTAGC	NRB4S Cloning in pDONR221
NRB4RP2-attb2	GGGGACCACTTTGTACAAGAAAGCTGGGTAAGCCA CCTTATCTTTTAATGC	NRB4M Cloning in pDONR221
NRB4RP3-attb2	GGGGACCACTTTGTACAAGAAAGCTGGGTGGGAAG CTGCTACATATTTCTC	NRB4F Cloning in pDONR221
NRB4FP4-attb1	GGGGACAAGTTTGTACAAAAAAGCAGGCTTCATGG ATAATAACAATTGGAGG	NRB4 Cloning in pDONR221, N-terminal

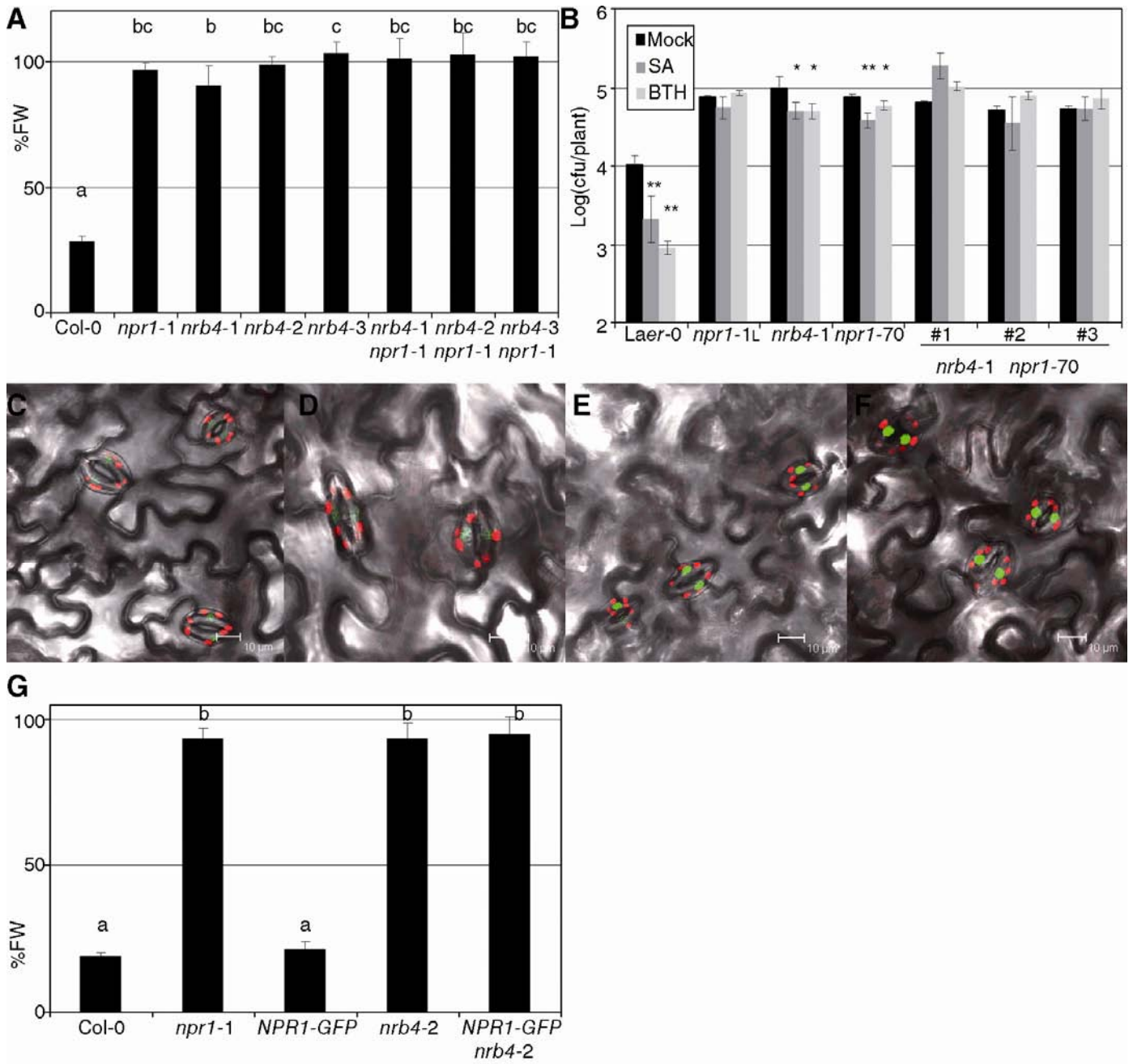
qRT NPR1.1	GAAGAATCGTTTCCCGAGTTCC	NPR1 RT-qPCR
qRT NPR1.2	CATCACCGGGTGTAAGATAGCA	NPR1 RT-qPCR
qRT NRB4.3	TTGCCACCTGATTCTCGTCA	NRB4 RT-qPCR
qRT NRB4.4	CTCTGGTCCGGAAAATGGAA	NRB4 RT-qPCR

## **Supplemental References**

- Alberti, S., Gitler, A.D., and Lindquist, S.** (2007). A suite of Gateway cloning vectors for high-throughput genetic analysis in *Saccharomyces cerevisiae*. *Yeast* **24**, 913-919.
- Canet, J.V., Dobón, A., Roig, A., and Tornero, P.** (2010). Structure-Function Analysis of *npr1* Alleles in *Arabidopsis* Reveals a Role for its Paralogs in the Perception of Salicylic Acid. *Plant, Cell & Environ* **33**, 1911-1922.
- Conrath, U., Domard, A., and Kauss, H.** (1989). Chitosan-elicited synthesis of callose and of coumarin derivatives in parsley cell suspension cultures. *Plant Cell Reports* **8**, 152-155.
- Choi, J., Huh, S.U., Kojima, M., Sakakibara, H., Paek, K.H., and Hwang, I.** (2010). The cytokinin-activated transcription factor ARR2 promotes plant immunity via TGA3/NPR1-dependent salicylic acid signaling in *Arabidopsis*. *Dev Cell* **19**, 284-295.
- Deng, W.-L., Preston, G., Collmer, A., Chang, C.-J., and Huang, H.-C.** (1998). Characterization of the *hrpC* and *hrpRS* operons of *Pseudomonas syringae* pathovars *syringae*, *tomato*, and *glycinea* and analysis of the ability of *hrpF*, *hrpG*, *hrcC*, *hrpT* and *hrpV* mutants to elicit the hypersensitive response and disease in plants. *J. Bacteriol.* **180**, 4523-4531.
- Hutchison, C.E., Li, J., Argueso, C., Gonzalez, M., Lee, E., Lewis, M.W., Maxwell, B.B., Perdue, T.D., Schaller, G.E., Alonso, J.M., Ecker, J.R., and Kieber, J.J.** (2006). The *Arabidopsis* histidine phosphotransfer proteins are redundant positive regulators of cytokinin signaling. *Plant Cell* **18**, 3073-3087.
- Johnson, C.M., Stout, P.R., Broyer, T.C., and Carlton, A.B.** (1957). Comparative chlorine requirements of different plant species. *Plant and Soil* **8**, 337-353.
- Mittal, S., and Davis, K.R.** (1995). Role of the phytotoxin Coronatine in the infection of *Arabidopsis thaliana* by *Pseudomonas syringae* pv. *tomato*. *Mol Plant Microbe Interact* **8**, 165-171.
- Ton, J., and Mauch-Mani, B.** (2004). Beta-amino-butyric acid-induced resistance against necrotrophic pathogens is based on ABA-dependent priming for callose. *Plant J* **38**, 119-130.
- Tornero, P., Merritt, P., Sadanandom, A., Shirasu, K., Innes, R.W., and Dangl, J.L.** (2002). RAR1 and NDR1 contribute quantitatively to disease resistance in *Arabidopsis*, and their relative contributions are dependent on the R gene assayed. *Plant Cell* **14**, 1005-1015.



**Supplemental Figure 1. Additional phenotypes of *nrb4* in defense.** **A** Responses to *Pto* (*hrpC*-), a strain that lacks virulence in Arabidopsis (Deng et al., 1998). 18-day-old plants were inoculated at an OD<sub>600</sub> of 0.1. Three days after inoculation, the growth of *Pto* was evaluated as Logarithm of colony forming units (cfu) per plant. **B** Inoculations with *Plectosphaerella cucumerina*. *P. cucumerina* was provided by Brigitte Mauch-Mani (University of Neuchatel, Switzerland), and used as described (Ton and Mauch-Mani, 2004). **C** Response to Methyl Jasmonate (MeJA) induced resistance. MeJA was applied by spray at 100  $\mu$ M in 0.1% DMSO and 0.02% Silwet L-77 one day before *Pto* inoculation. **D** Responses to JA-Ile in the length of roots. Plants were grown in Johnson's media (Johnson et al., 1957) with 1 mM KH<sub>2</sub>PO<sub>4</sub>, with or without 50  $\mu$ M MeJA (Duchefa). The length of the roots was measured with ImageJ software (MIH, Bethesda, MD, USA). **E** Responses to coronatine. *Pto*(*cfa*<sup>-</sup>) a strain that lacks coronatine (Mittal and Davis, 1995) was inoculated, along *Pto*, as indicated in A. The experiments were repeated three times with similar results, and the data represent the average, with the error bars plotting the standard deviation of 15 plants in three groups of five. The letters above the bars indicate different homogeneous groups with statistically significant differences (Fisher's LSD Test, P < 0.05). Asterisks indicate statistically significant differences from the mock treatment (P < 0.05 one asterisk, P < 0.01 two) using the Student's t test (one tail).

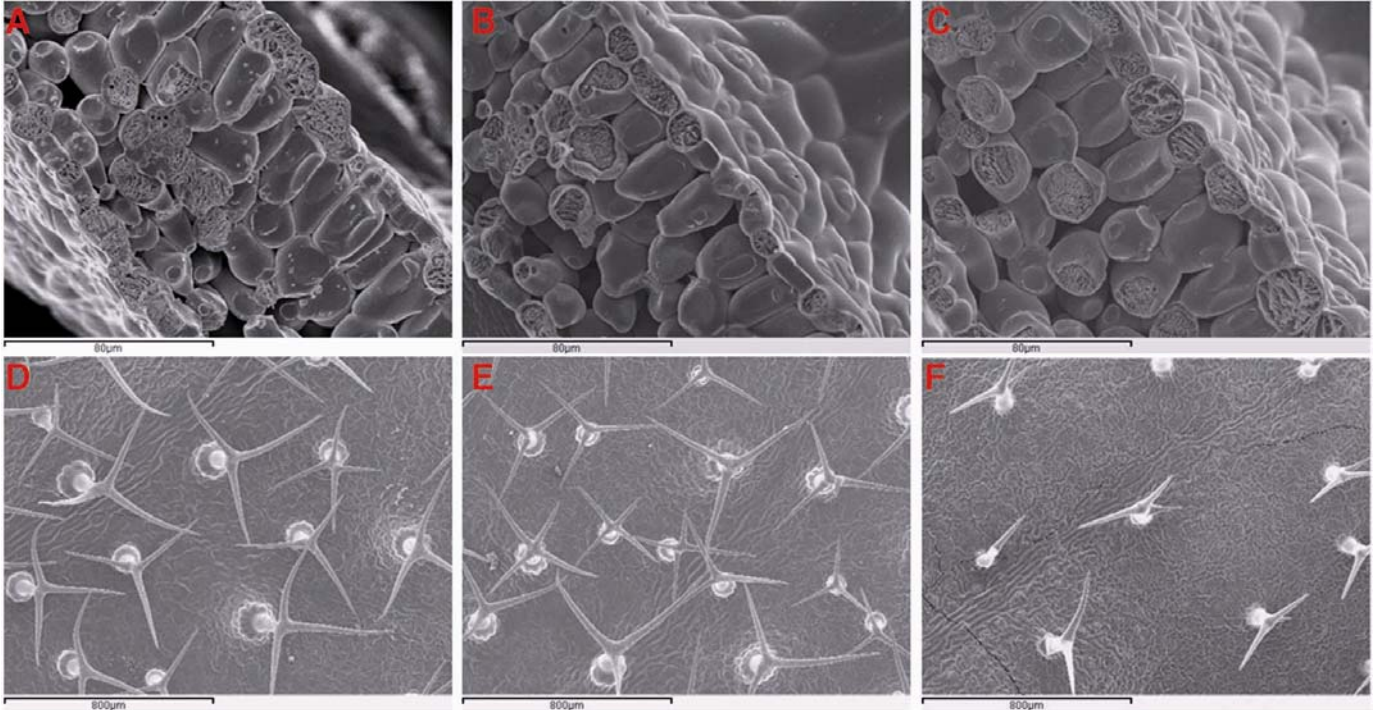


**Supplemental Figure 2. Epistasis of *NRB4* with *NPRI*.** **A** Three double mutants *nrb4 npr1-1* and their controls were treated with either mock or 350  $\mu$ M BTH four times over three weeks, their weights recorded, and the ratio between the BTH and mock treated plants calculated (15 plants in three groups of five). The ratio is expressed as percentage of fresh weight (%FW). **B** Three double mutants *nrb4-1 npr1-70* were tested for its response to SA and BTH upon *Pto* inoculation. **C** Confocal image of Arabidopsis *35S:NPRI-GFP* in an *npr1-1* background in mock conditions. **D** Same transgenic in an *nrb4-2 npr1-1* background in mock conditions. **E**. The same line as in C, one day after 350  $\mu$ M BTH treatment. **F** The same line as in D, one day after 350  $\mu$ M BTH treatment. **G** The lines described above were tested for its response to BTH. The overexpression of *NPRI*, even if it is detected in the nucleus (F), did not complement the mutation *nrb4-2*. The experiments were repeated three times with similar results, and the data represent the average, with the error bars plotting the standard deviation of 15 plants in three groups of five. The letters above the bars indicate different homogeneous groups with statistically significant differences (Fisher's LSD Test,  $P < 0.05$ ). Asterisks indicate statistically significant differences from the mock treatment ( $P < 0.05$  one asterisk,  $P < 0.01$  two) using the Student's t test (one tail).

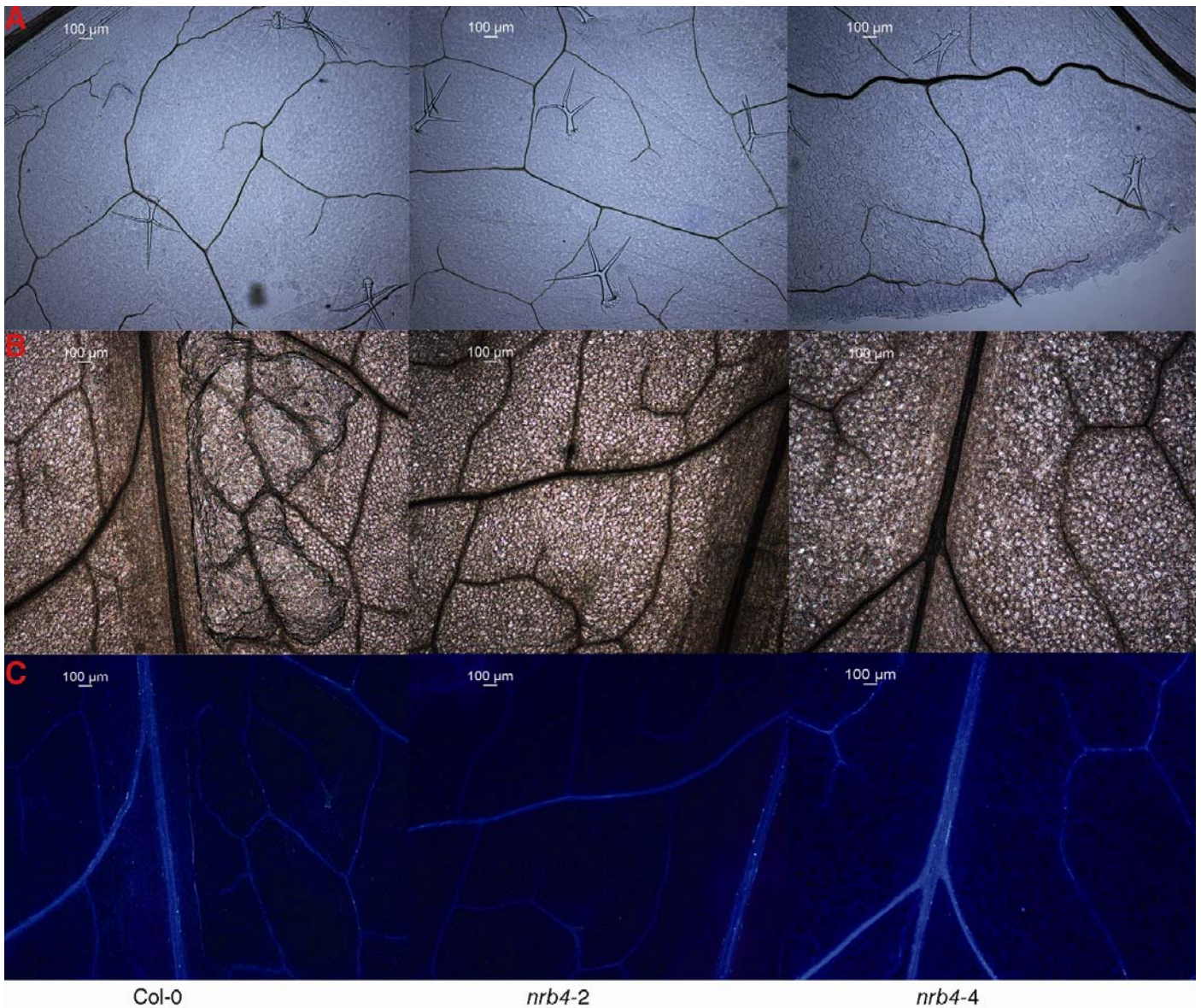


**Supplemental Figure 3. Additional pictures of *nrb4-4*.** **A** Wild type plant, growing seven weeks in short day and six weeks in long day with no treatment or inoculation. **B** *nrb4-4* plant of the same age, growing in the same conditions. **C** *nrb4-4* plant growing seven weeks in short day and eleven weeks in long day, as in A. **D** Detail of the plant in C, note the absence of flowers. **E** *nrb4-4* plant with flowers. **F** Detail of the plant in E. As a reference, the pots have a diameter of 6 cm.

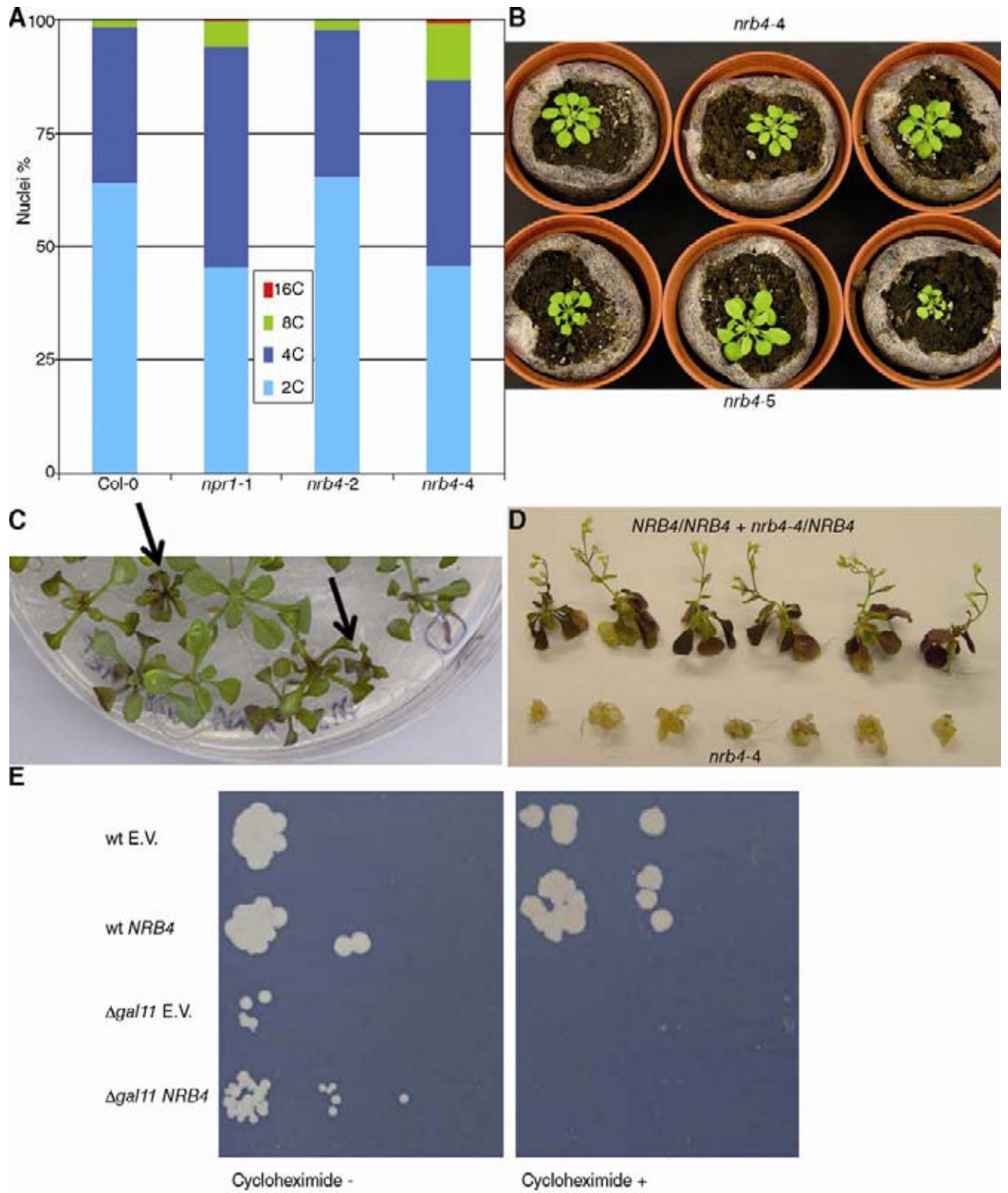




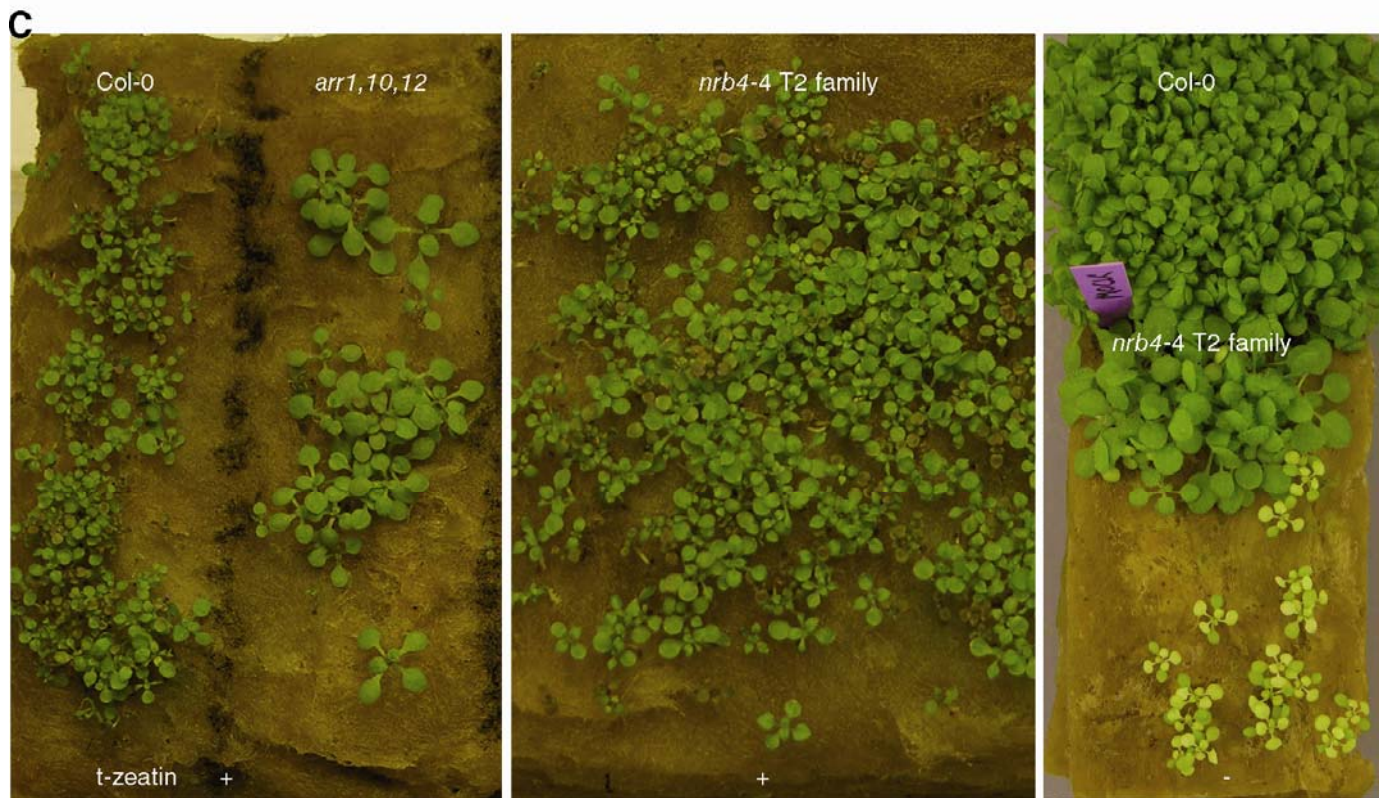
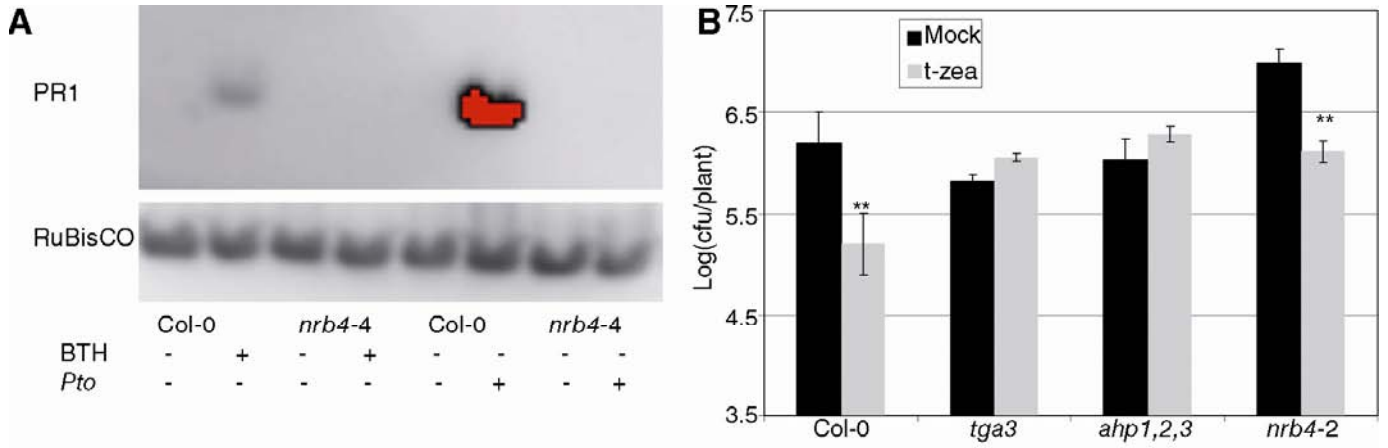
**Supplemental Figure 4. Additional pictures of Cryo-SEM.** **A** Section of Col-0. **B** Section of *nrb4-2*. **C** Section of *nrb4-4*. **D** Surface of a leaf from Col-0. **E** Idem from *nrb4-2*. **F** Idem from *nrb4-4*. The length of the bar in A, B, and C is 80 μm, and in D, E, and F is 800 μm. The leaves were five weeks old for Col-0 and *nrb4-2* and seven weeks for *nrb4-4*.



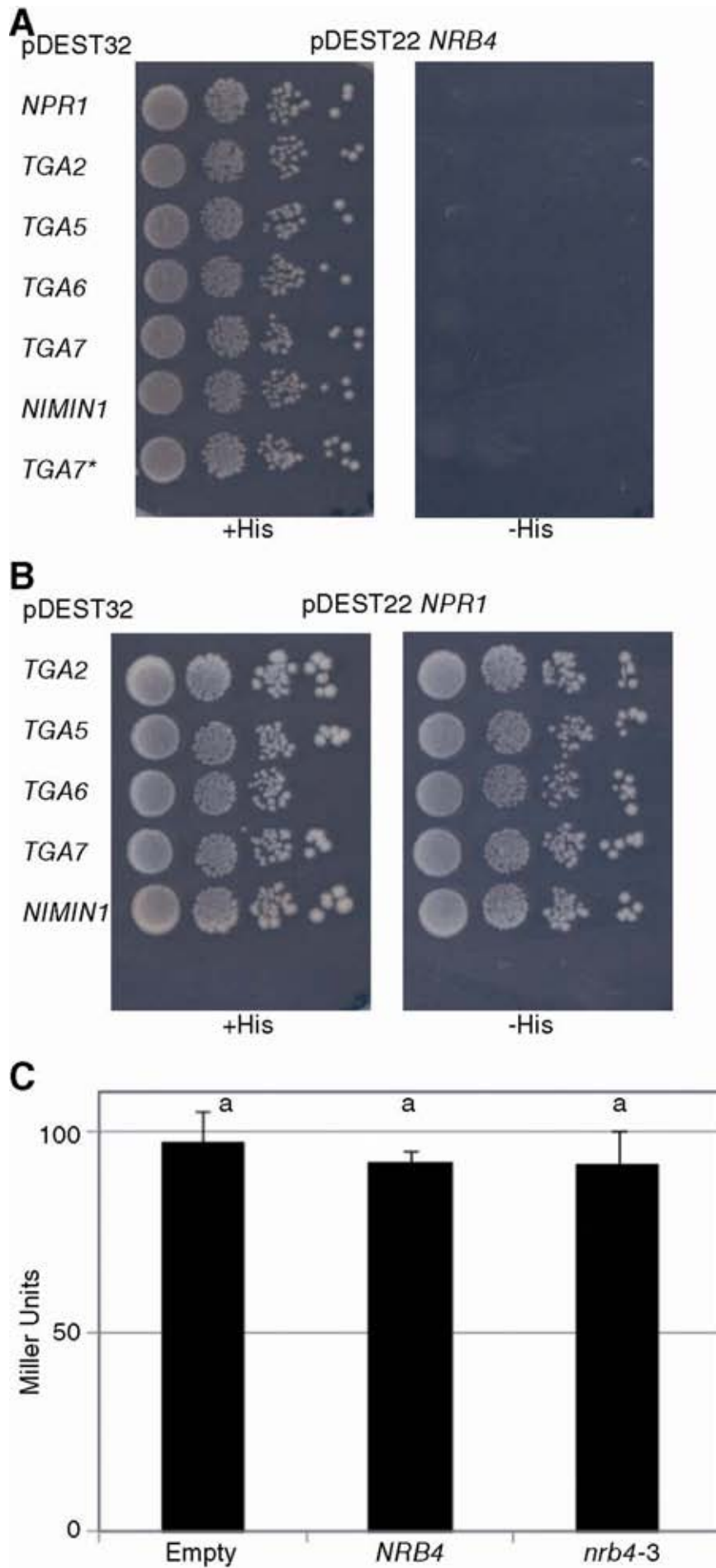
**Supplemental Figure 5. Stainings of *nrb4*.** **A** Trypan blue stains, unveiling cell death and membrane damage in Col-0, *nrb4-2*, and *nrb4-4*. **B** Aniline blue stains under visible light. **C** The same Aniline blue stains under ultraviolet light, which detects callose depositions. Trypan Blue and Aniline Blue staining were performed as described (Tornero et al., 2002; Conrath et al., 1989, respectively). No differences among genotypes were observed with these stains.



**Supplemental Figure 6. Characterization of *nrb4* null alleles.** **A** DNA content. Nuclei from the indicated genotypes were extracted, stained with DAPI, and the relative amount of DNA measured with a CyFlow Ploidy Analyzer (Partec GmbH, Münster Germany) following the manufacturer's instructions. At least 5000 nuclei were counted in each measurement, and the same result was obtained in three independent experiments. **B** Phenotypes of *nrb4-5* in comparison to *nrb4-4*. **C** Phenotypes of a T2 segregating family of *nb4-4/NRB4* in MS plates. The arrows point to *nrb4-4* homozygous plants (confirmed by PCR) Picture taken at two weeks of growing. **D** Plants selected in C were transferred to MS plates with 500  $\mu$ M SA, and the picture was taken two weeks after the transfer. **E** Lack of complementation in yeast. Empty vector (E.V.) pAG423 (Alberti et al., 2007) and *NRB4* cloned in pAG423 were introduced in wild type (wt) and  *$\Delta gal11$* . The different strains were grown in liquid and then plated in SD His- plates with or without cycloheximide (0.2 $\mu$ g/ml). The wt and  *$\Delta gal11$*  strains were obtained from EUROSCARF (Ref. Y00000 and Y01742, respectively).

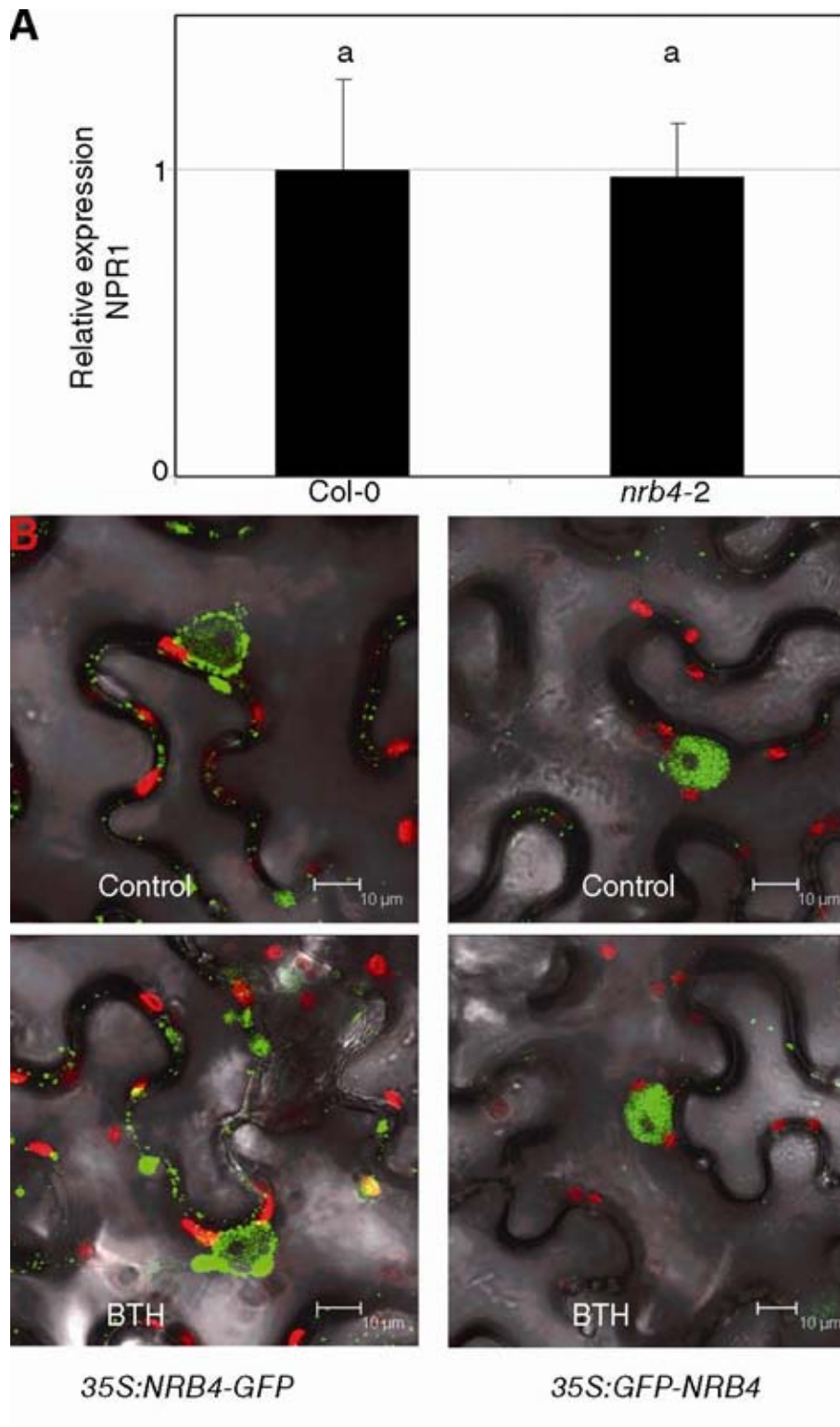


**Supplemental Figure 7. Phenotypes from the transcriptomic analysis.** **A** PR1 immunoblot of Col-0 and *nrb4-4* three days after mock or a *Pto* inoculation and one day after mock or 350  $\mu$ M BTH. The same blot was probed with anti-RuBisCO for loading and transfer control. The red color indicates saturation of the signal. **B** Resistance induced by cytokinins. Trans-zeatin (t-zea) 1  $\mu$ M or a mock solution was applied one day previous to the inoculation with *Pto*. *tga3* (Choi et al., 2010) and *ahp1 ahp2 ahp3* (Hutchison et al., 2006, abbreviated as *ahp1,2,3*) were included as controls. **C** *nrb4-4* did not have a specific phenotype with cytokinins. The controls Col-0 and *arr1 arr10 arr12* growing in 5  $\mu$ M trans-zeatin (left) are the same as in Figure 6B. A T2 family, segregating for *nrb4-4* (middle) did not produce plants with a different perception to cytokinins. Col-0 and the same T2 family of *nrb4-4* plants growing in control conditions (right). In the case of *nrb4-4*, the space shown at the bottom of the picture was cleared of wild type plants, to check if the *nrb4-4* homozygous plants can grow in this media. The experiments were repeated three times with similar results, and the data represent the average, with the error bars plotting the standard deviation of 15 plants in three groups of five. Asterisks indicate statistically significant differences from the mock treatment ( $P < 0.05$  one asterisk,  $P < 0.01$  two) using the Student's t test (one tail).

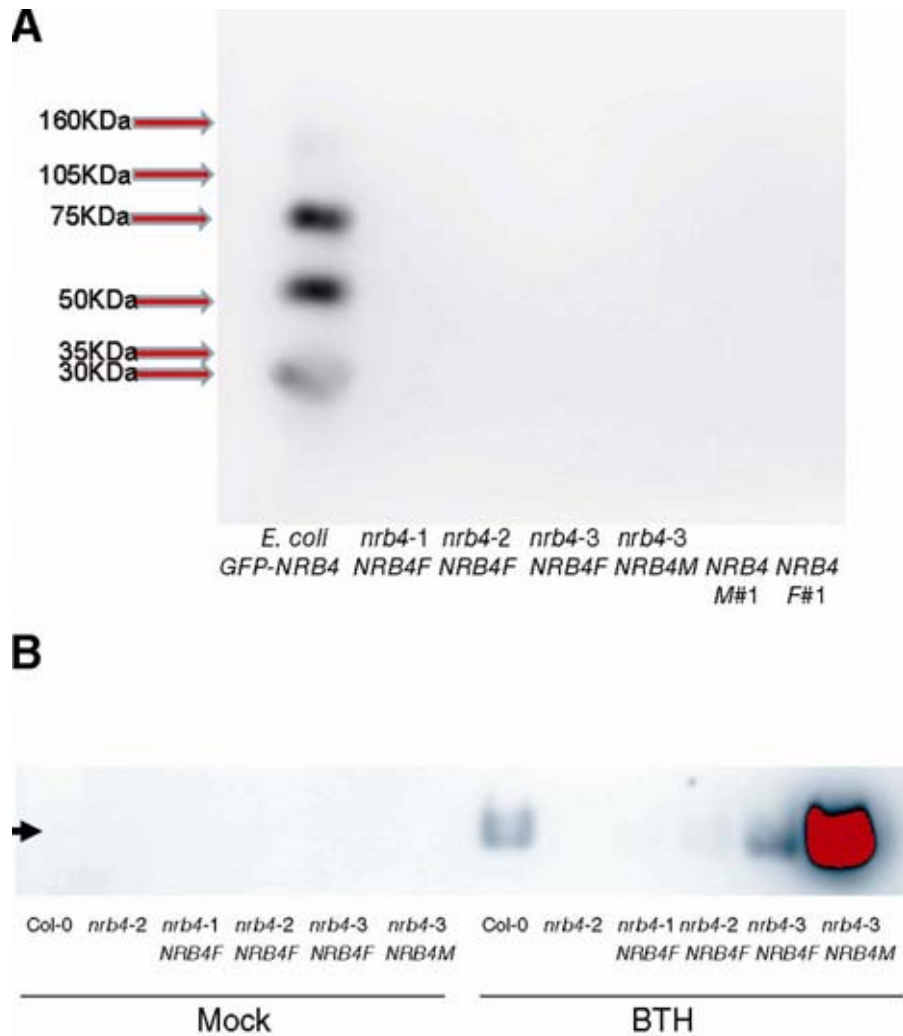


**Supplemental Figure 8. Yeast n-hybrid interactions. A** Interactions between *NRB4* and proteins that have a role in SA perception. The yeasts that had *NRB4* and any of these proteins were able to grow in His<sup>+</sup> plates, but not in His<sup>-</sup> plates. Therefore, there was not detectable interaction. TGA7\* stands for an additional control with an empty pDEST22, since TGA7 was able to autoactivate the system with no 3AT (the His<sup>-</sup> plates contained 5 mM 3AT). **B** As a control, interactions between *NPR1* and the rest of proteins that have a role in SA perception. **C** *NRB4* did not alter the interaction between *NPR1* and *TGA2*. *NRB4* was cloned in a third vector, and introduced in the first yeast of B. There was no statistical difference between introducing *NRB4*, respect *nrb4-3*, or to the empty vector. All the plates were Lys<sup>-</sup>, Trp<sup>-</sup>, Leu<sup>-</sup>, and 100 μM SA. Similar experiments with no SA produced the same results. Similarly, bimolecular fluorescence complementation between *NRB4* and *NPR1* or *TGA2* did not produce a positive result in *Nicotiana benthamiana*. The pictures were taken 3-5 days after growing at 28°C. *NRB4* was cloned in three different versions for detection of interactions in the yeast two hybrid system: a short version, from 1 to 112 aa, included the KIX domain; an intermediate version, from 1 to 670 aa, spanned half of the coding sequence; and a full version. The full version when fused to the GAL4 BD was autoactivated, even with mutated versions of *NRB4* that recreated the EMS mutations herein described. The three versions of the wild type protein fused with the GAL4 AD were tested for interaction in yeast with genes described in SA response. The experiment shown in this figure corresponds to the full version of *NRB4*. The experiments were repeated three times with similar results, and the data represent the average, with the error bars plotting the standard deviation of three colonies. The letters above the bars indicate different homogeneous groups with statistically significant differences (Fisher's LSD Test, P < 0.05).





**Supplemental Figure 9. Expression of *NPR1* and *NBR4*.** **A** *NPR1* was detectable in *nrb4-2* at normal levels. The levels of expression of *NPR1*, measured by RT-qPCR, are normalized to three reference genes and to the level of Col-0. The RNA was extracted from three-week-old plants, from three independent samples of 100 mg each. **B** The nuclear localization did not change with the application of 350  $\mu$ M BTH. *35S:NRB4-GFP* (left) and *35S:GFP-NRB4* (right) were infiltrated in *N. benthamiana*. Then, a mock or a 350  $\mu$ M BTH was applied one day before these pictures were taken. The controls correspond to the Figure 7C and D, respectively. The experiments were repeated three times with similar results, and the data represent the average, with the error bars plotting the standard deviation of three independent RT-qPCRs. The letters above the bars indicate different homogeneous groups with statistically significant differences (Fisher's LSD Test,  $P < 0.05$ ).



**Supplemental Figure 10. Characterization of *NRB4* complementation.** **A** In the stable transgenic lines, GFP was not detectable by immunoblot. A immunoblot with antibody raised against GFP (Roche, Madrid, Spain) was performed in different extracts. The first line of the immunoblot is a *GFP-NRB4* fusion expressed in *E. coli*, which shows partial processing. The rest of lines correspond to plant extracts from the same lines described in Figure 8. The arrows point the position of the weight markers. **B** The complemented *nrb4* alleles express PR1 upon BTH application. The lines described in Figure 8 were treated with BTH and PR1 detected as in Figure 2B. There is a low expression of PR-1 in the lines that contain *35S:NRB4-GFP* (*NRB4F*) in *nrb4-1* and *nrb4-2*, a expression similar to Col-0 in the *35S:NRB4* in *nrb4-3*, and a very strong expression in the lines that overexpress the first 670 AA of NRB4 plus GFP (*NRB4M*) in *nrb4-3*. The red color indicates saturation of signal.

**Supplemental Table 1. Evaluation of segregations.**

<b>Population</b>	<b>Observed</b>			<b>Expected</b>		$\chi^2$	<b>d.f.</b>	<b>p</b>
	<b>wt</b>	<b>mut</b>	<b>Total</b>	<b>(3/4)</b>	<b>(1/4)</b>			
F2 Col-0 x <i>nrb4-1</i>	297	108	405	303.75	101.25	0.600	1	0.44
F2 Col-0 x <i>nrb4-2</i>	248	87	335	251.25	83.75	0.168	1	0.68
F2 Col-0 x <i>nrb4-3</i>	345	104	449	336.75	112.25	0.808	1	0.37
				<b>(1/2)</b>	<b>(1/2)</b>			
F1 <i>nrb4-4</i> het x <i>nrb4-1</i>	25	23	48	24	24	0.083	1	0.77
F1 <i>nrb4-4</i> het x <i>nrb4-2</i>	26	30	56	28	28	0.286	1	0.59
F1 <i>nrb4-4</i> het x <i>nrb4-3</i>	28	30	58	29	29	0.069	1	0.79
				<b>(3/4)</b>	<b>(1/4)</b>			
F1 <i>nrb4-5</i> het x <i>nrb4-4</i> het	40	11	51	38.25	12.75	0.320	1	0.57

Segregations observed in the indicated populations. The phenotypic classes were evaluated with the  $\chi^2$  statistics. The p value gives the probability that any deviation from expected results is due to chance only. Since in all the cases the p value is bigger than the standard value of 0.05, the segregations fit the proposed model.

**Supplemental Table 2. Evaluation of phenotypes in T-DNA insertion lines.**

<b>AGI</b>	<b>NASC</b>	<b>T-DNA</b>	<b>Status</b>	<b>Position</b>	<b>Phenotype (% wt)</b>
	Col-0				100
	<i>npr1-1</i>		Homoz		0
AT1G07950	N656591	SALK_065283C	Homoz	Exon	100
AT1G11760	N665553	SALK_023845C	Homoz	5'	100
AT1G11760	N678300	SALK_028490C	Homoz	5'	100
AT1G15780	N835429	SAIL_792_F02	Heteroz	Intron, <i>nrb4-4</i>	75
AT1G15780		GABI_955_E02	Heteroz	Intron, <i>nrb4-5</i>	75
AT1G16430	N870082	SAIL_9_E04	Heteroz	Exon	100
AT1G23230	N659417	SALK_060062C	Homoz	Exon	100
AT1G23230	N671536	SALK_074015C	Homoz	Exon	100
AT1G25540	N679089	SALK_129555C	Homoz	Exon	100
AT1G25540	N677751	SALK_059316C	Homoz	Exon	100
AT1G26665		No info			
AT1G29940	N876306	SAIL_726_H01	Heteroz	Exon	100
AT1G31360	N661000	SALK_087178C	Homoz	Exon	100
AT1G44910	N521070	SALK_021070	Heteroz	Exon	100
AT1G54250	N679260	SALK_151800C	Homoz	Exon	100
AT1G55080	N529118	SALK_029118	Heteroz	Exon	100
AT1G55325	N861503	SAIL_1169_H11	Homoz	Exon	100
AT1G60850	N655705	SALK_088247	Homoz	Exon	100
AT2G03070	N682656	SALK_092406C	Homoz	Exon	100
AT2G22370	N677657	SALK_027178C	Homoz	Intron	100
AT2G28230		No info			
AT2G29540	N507414	SALK_007414	Heteroz	Exon	100
AT2G38250	N667374	SALK_133090C	Homoz	5'	100
AT2G48110	N671698	SALK_092499C	Homoz	5'	100
AT2G48110	N667838	SALK_015532C	Homoz	Exon	100
AT3G01435		No info			
AT3G04740	N521711	SALK_021711	Heteroz	Exon	100
AT3G09180	N512449	SALK_012449	Heteroz	Exon	100
AT3G10690	N506294	SALK_006294	Heteroz	3'	100
AT3G21350	N662531	SALK_055723C	Homoz	5'	100
AT3G21350	N656864	SALK_110696C	Homoz	5'	100
AT3G23590	N667150	SALK_119561C	Homoz	Exon	100
AT3G23590	N661810	SALK_022477C	Homoz	Exon	100
AT3G25940	N562311	SALK_062311	Heteroz	3'	100
AT3G52860	N685672	SALK_037570C	Homoz	5'	100
AT3G57660	N673273	SALK_116823C	Homoz	3'	100
AT3G57660	N673356	SALK_122465C	Homoz	3'	100
AT3G59600		No info			

AT4G00450	N678935	SALK_108241C	Homoz	Exon	100
AT4G04780		No info			
AT4G04920	N548091	SALK_048091	Heteroz	Intron	100
AT4G09070	N553156	SALK_053156	Heteroz	3'	100
AT4G25210	N599954	SALK_099954	Heteroz	Exon	100
AT4G25210	N607213	SALK_107213	Heteroz	5'	100
AT4G25630	N682661	SALK_093373C	Homoz	Exon	100
AT5G02850	N622082	SALK_122082	Heteroz	Exon	100
AT5G02850	N683125	SALK_007367C	Homoz	5'	100
AT5G03220	N678464	SALK_049958C	Homoz	5'	100
AT5G03500	N676132	SALK_088220C	Homoz	Intron	100
AT5G12230	N657910	SALK_037435C	Homoz	5'	100
AT5G12230	N658182	SALK_034955C	Homoz	Intron	100
AT5G19480		No info			
AT5G19910	N682219	SALK_035522C	Homoz	Exon	100
AT5G20170	N663678	SALK_111977C	Homoz	Exon	100
AT5G28540	N675173	SALK_054493C	Homoz	3'	100
AT5G28540	N675862	SALK_079156C	Homoz	5'	100
AT5G41010	N549327	SALK_049327	Heteroz	Intron	100
AT5G41910	N663226	SALK_087920C	Homoz	5'	100
AT5G41910	N678994	SALK_115673C	Homoz	5'	100
AT5G42020	N659850	SALK_047956C	Homoz	Exon	100
AT5G42060	N669407	SALK_014079C	Homoz	5'	100
AT5G63480	N654793	SALK_095631C	Homoz	Intron	100
AT5G64680	N685462	SALK_023879	Homoz	5'	100
AT5G67240	N542641	SALK_042641	Heteroz	Exon	100

Phenotypes observed in the indicated populations, either homozygous or heterozygous T-DNA insertions in Arabidopsis genes with homology with Mediator genes. The phenotypic classes were evaluated visually, as described by Canet et al., 2010.

**Supplemental Table 3. Lack of homologs in Arabidopsis for several nuclear receptors.**

<b>Name</b>	<b>Organism</b>	<b>AA</b>	<b>Max. E value</b>	<b>Identities</b>	<b>Positives</b>
Pdr1p	Yeast	1068	7.7	37/143	58/143
PDR3p	Yeast	976	2.3	27/99	47/99
Oaf1p	Yeast	1047	0.38	24/90	46/90
PPAR $\alpha$	H. sapiens	468	2.3	13/42	24/42
NHR-49	C. elegans	501	0.41	18/62	29/62

The mentioned proteins were used to search in the Arabidopsis genome with BLASTP (TAIR10, [www.arabidopsis.org](http://www.arabidopsis.org)), with the default settings. The column “AA” indicates the number of aa of the original protein. The “Max. E value” indicates the maximal E value obtained with BLASTP, while the “Identities” and “Positives” columns indicate the ratio of aa either identical or similar in the best stretch of homology.

**Supplemental Table 4. Primers used**

<b>Name</b>	<b>Sequence</b>	<b>Objective</b>
5249817-NlaIII-F	TGAGCAGCAAGAAAGATGATG	nrb4 mapping
5249817-NlaIII-R	CTTAGCAGAGGTACGAGGATCA	nrb4 mapping
5346165-DdeI-F	CACCAAACACCACACTTCTCA	nrb4 mapping
5346165-DdeI-R	CATATCTTCAAATCTTTGAGTTGG	nrb4 mapping
5377218-NlaIII-F	CTGGATTTTGGTTCGAGTTAGC	nrb4 mapping
5377218-NlaIII-R	GTGGCAATAGAGGCACAAGT	nrb4 mapping
5393430-CauI-F	GAAGAGTGGTTGCAAGCGTA	nrb4 mapping
5393430-CauI-R	TTTTTGCAGTCCACGTTT	nrb4 mapping
5406030-NlaIII-F	AGTTGGTTCGGAGCTTTTCTCT	nrb4 mapping
5406030-NlaIII-R	GATTCTCCACACCACCCACT	nrb4 mapping
5425793-SecI-F	AGAACGAGCTCGAACACGAA	nrb4 mapping
5425793-SecI-R	CTGAAACATTGAATCCCATTG	nrb4 mapping
5440252-MseI-F	TGCTTTCATAATCGTTGTGTT	nrb4 mapping
5440252-MseI-R	CACACCAAACAAGCTTCTGTC	nrb4 mapping
5455705-HinfI-F	GAATCTTGATGCTTGCTTGG	nrb4 mapping
5455705-HinfI-R	CCATGTCCGGGAAACTTATC	nrb4 mapping
5494532-RsaI-F	GTTGATCGGAAAGGAAAAGTAAAA	nrb4 mapping
5494532-RsaI-R	AAAAACGGATAACCAAACATGG	nrb4 mapping
F10B6.1-F	ATTATATTGTTCAACATCAACTGCACAT	nrb4 mapping
F10B6.1-R	TTTATCTCTTAAACAAGTTCGTAAACCAAC	nrb4 mapping
T16N11.1-F	AATAGATTAGAAATGAACAGGAGAATTGACT	nrb4 mapping
T16N11.1-R	TGGCATTTTAAATAACATCCTCACC	nrb4 mapping
15780.1	TAACAAAAAATCCCAATCACGTGTG	NRB4 sequencing
15780.2	AACAATTGGAGGCCTTCTCTTCC	NRB4 sequencing
15780.3	AAATATTGCACGCCAACAAGCA	NRB4 sequencing
15780.4	AAGGCGTTCAATAGGCAGCTCA	NRB4 sequencing
15780.5	TATGCACAGGCCGAGGAAGC	NRB4 sequencing
15780.6	GCATCTGCGGATTTGTTTGG	NRB4 sequencing
15780.7	CAAGCCTCTGGTATCCATCAGC	NRB4 sequencing
15780.8	TCTGTTGGATGCCTGAGCTATTTG	NRB4 sequencing
15780.9	AATCTATGGATGTGCCATTATTAGCG	NRB4 sequencing
15780.10	TGCGCAGAATGGAAACACTAAA	NRB4 sequencing
15780.11	TTCCGGTGGGATTGGCTATT	NRB4 sequencing
15780.12	GAATGAAATCTACCAGAGAGTTGCA	NRB4 sequencing
15780.13	TGGTTTGGGACAGCAACGG	NRB4 sequencing
NRB4FP2-attb1	GGGGACAAGTTTGTACAAAAAAGCAGGCTTCGAAG GAGATAGAACCATGGATAATAACAATTGGAGGCCT	NRB4 Cloning in pDONR221, C-terminal
NRB4RP1-attb2	GGGGACCACTTTGTACAAGAAAGCTGGGTCTATGG ATGTGCCATTATTAGC	NRB4S Cloning in pDONR221
NRB4RP2-attb2	GGGGACCACTTTGTACAAGAAAGCTGGGTAAGCCA CCTTATCTTTTAATGC	NRB4M Cloning in pDONR221
NRB4RP3-attb2	GGGGACCACTTTGTACAAGAAAGCTGGGTGGGAAG CTGCTACATATTTCTC	NRB4F Cloning in pDONR221
NRB4FP4-attb1	GGGGACAAGTTTGTACAAAAAAGCAGGCTTCATGG ATAATAACAATTGGAGG	NRB4 Cloning in pDONR221, N-terminal



qRT NPR1.1	GAAGAATCGTTTCCCGAGTTCC	NPR1 RT-qPCR
qRT NPR1.2	CATCACCGGGTGTAAGATAGCA	NPR1 RT-qPCR
qRT NRB4.3	TTGCCACCTGATTCTCGTCA	NRB4 RT-qPCR
qRT NRB4.4	CTCTGGTCCGGAAAATGGAA	NRB4 RT-qPCR

## **Supplemental References**

- Alberti, S., Gitler, A.D., and Lindquist, S.** (2007). A suite of Gateway cloning vectors for high-throughput genetic analysis in *Saccharomyces cerevisiae*. *Yeast* **24**, 913-919.
- Canet, J.V., Dobón, A., Roig, A., and Tornero, P.** (2010). Structure-Function Analysis of *npr1* Alleles in *Arabidopsis* Reveals a Role for its Paralogs in the Perception of Salicylic Acid. *Plant, Cell & Environ* **33**, 1911-1922.
- Conrath, U., Domard, A., and Kauss, H.** (1989). Chitosan-elicited synthesis of callose and of coumarin derivatives in parsley cell suspension cultures. *Plant Cell Reports* **8**, 152-155.
- Choi, J., Huh, S.U., Kojima, M., Sakakibara, H., Paek, K.H., and Hwang, I.** (2010). The cytokinin-activated transcription factor ARR2 promotes plant immunity via TGA3/NPR1-dependent salicylic acid signaling in *Arabidopsis*. *Dev Cell* **19**, 284-295.
- Deng, W.-L., Preston, G., Collmer, A., Chang, C.-J., and Huang, H.-C.** (1998). Characterization of the *hrpC* and *hrpRS* operons of *Pseudomonas syringae* pathovars *syringae*, *tomato*, and *glycinea* and analysis of the ability of *hrpF*, *hrpG*, *hrcC*, *hrpT* and *hrpV* mutants to elicit the hypersensitive response and disease in plants. *J. Bacteriol.* **180**, 4523-4531.
- Hutchison, C.E., Li, J., Argueso, C., Gonzalez, M., Lee, E., Lewis, M.W., Maxwell, B.B., Perdue, T.D., Schaller, G.E., Alonso, J.M., Ecker, J.R., and Kieber, J.J.** (2006). The *Arabidopsis* histidine phosphotransfer proteins are redundant positive regulators of cytokinin signaling. *Plant Cell* **18**, 3073-3087.
- Johnson, C.M., Stout, P.R., Broyer, T.C., and Carlton, A.B.** (1957). Comparative chlorine requirements of different plant species. *Plant and Soil* **8**, 337-353.
- Mittal, S., and Davis, K.R.** (1995). Role of the phytotoxin Coronatine in the infection of *Arabidopsis thaliana* by *Pseudomonas syringae* pv. *tomato*. *Mol Plant Microbe Interact* **8**, 165-171.
- Ton, J., and Mauch-Mani, B.** (2004). Beta-amino-butyric acid-induced resistance against necrotrophic pathogens is based on ABA-dependent priming for callose. *Plant J* **38**, 119-130.
- Tornero, P., Merritt, P., Sadanandom, A., Shirasu, K., Innes, R.W., and Dangl, J.L.** (2002). RAR1 and NDR1 contribute quantitatively to disease resistance in *Arabidopsis*, and their relative contributions are dependent on the R gene assayed. *Plant Cell* **14**, 1005-1015.